

การแตกของเซลล์จุลินทรีย์โดยใช้ฟลูออไรด์เบดสามเฟสแบบใช้ใบกวน



นางสาว นริศรา สุขสมัย

สถาบันวิทยบริการ

จุฬาลงกรณ์มหาวิทยาลัย

วิทยานิพนธ์นี้เป็นส่วนหนึ่งของการศึกษาตามหลักสูตรปริญญาวิทยาศาสตรมหาบัณฑิต

สาขาวิชาวิศวกรรมเคมี ภาควิชาวิศวกรรมเคมี  
คณะวิศวกรรมศาสตร์ จุฬาลงกรณ์มหาวิทยาลัย

ปีการศึกษา 2543

ISBN xxx-xxx-xxx-x

ลิขสิทธิ์ของจุฬาลงกรณ์มหาวิทยาลัย

MICROORGANISM CELL DISRUPTION USING A THREE-PHASE  
FLUIDIZED BED WITH AGITATOR



Miss Narisara Suksamai

สถาบันวิทยบริการ  
จุฬาลงกรณ์มหาวิทยาลัย  
A Thesis Submitted in Partial Fulfillment of the Requirements  
for the Degree of Master of Engineering in Chemical Engineering

Department of Chemical Engineering

Faculty of Engineering

Chulalongkorn University

Academic Year 2000

ISBN xxx-xxx-xxx-x

Thesis Title                    Microorganism Cell Disruption using A Three-Phase  
Fluidized Bed with Agitator  
By                                    Narisara Suksamai  
Field of Study                    Chemical Engineering  
Thesis Advisor                 Associate Professor Tawatchai Charinpanitkul, Dr.Eng.

---

Accepted by the Faculty of Engineering, Chulalongkorn University in Partial  
Fulfillment of the Requirements for the Master's Degree

..... Dean of Faculty of Engineering  
(Professor Somsak Panyakeow, Dr.Eng.)

THESIS COMMITTEE

.....Chairman  
(Associate Professor Chirakarn Muangnapoh, Dr.Ing.)

.....Thesis Advisor  
(Associate Professor Tawatchai Charinpanitkul, Dr.Eng)

.....Member  
(Professor Wiwut Tanthapanichakoon, Ph.D..)

.....Member  
(Assistant Professor Seeroong Prichanont, Ph.D.)

นริศรา สุขสมัย: การแตกของเซลล์จุลินทรีย์โดยใช้ฟลูอิดิซ์เบดสามเฟสแบบใช้ใบกวนร่วม  
(Microorganism cells disruption using a three-phase fluidized bed with agitation)

อ. ที่ปรึกษา: อ. รศ. ดร. ธวัชชัย ชรินพาณิชกุล, 163 หน้า. ISBN XXX-XXX-XXX-X

งานวิจัยนี้เป็นการประยุกต์ใช้ฟลูอิดิซ์เบดสามเฟสแบบใช้ใบกวนร่วมในการทำให้เซลล์ยีสต์สายพันธุ์ *Saccharomyces cerevisiae* แตกแล้วปลดปล่อยโปรตีนภายในเซลล์ซึ่งมีประโยชน์ในเชิงอุตสาหกรรม ระบบสามเฟสนี้ประกอบด้วยสารละลายยีสต์, อากาศ, และลูกแก้วซึ่งใช้เป็นของเหลว, ก๊าซ, และ ของแข็งในระบบตามลำดับ เราได้ทำการศึกษาปัจจัยในการดำเนินการที่มีผลต่อการแตกของเซลล์ซึ่งได้แก่ ความเร็วรอบใบกวน, การใส่ดราฟทิฟไว้ภายในคอลัมน์, ความเร็วของอากาศ, ความเร็วของของเหลวและขนาดของลูกแก้วที่มีผลต่อการแตกของเซลล์ยีสต์ และใช้ศึกษาประสิทธิภาพของการทำให้เซลล์แตกวัดจากการกระจายขนาดของเซลล์ยีสต์, โปรตีนที่ปลดปล่อยออกมา, และการศึกษาลักษณะของเซลล์โดยอาศัยกล้องจุลทรรศน์

ผลการทดลองแสดงให้เห็นว่าสำหรับระบบที่ไม่ใช้ลูกแก้วนั้น การเพิ่มความเร็วรอบของใบกวนในช่วง 500 ถึง 3000 รอบไม่มีผลต่อการแตกของเซลล์ทั้งระบบที่มีการให้อากาศและไม่มีการให้อากาศ แต่สำหรับระบบที่มีการใช้ลูกแก้วอัตราการแตกของเซลล์จะเพิ่มขึ้นตามการเพิ่มความเร็วรอบของใบกวน สำหรับการติดตั้งดราฟทิฟจะไม่มีต่อการแตกของเซลล์อย่างมีนัยสำคัญเมื่อเปรียบเทียบกับกรณีที่ไม่ใส่ดราฟทิฟ ในการให้อากาศเข้าไปในระบบนั้นไม่มีต่อการแตกของเซลล์ทั้งในกรณีที่มีและไม่มีการปั่นกวน แต่การเพิ่มความเร็วของอากาศระหว่าง 10 ถึง 40 เซนติเมตรต่อนาที่กลับจะทำให้อัตราการแตกของเซลล์ลดลงแต่จะช่วยให้การถ่ายเทความร้อนได้ดีขึ้น สำหรับการหมุนวนสารละลายยีสต์โดยใช้ปั๊มด้วยความเร็ว 10 ถึง 30 เซนติเมตรต่อนาที่ไม่มีผลทำให้เซลล์ยีสต์ลดการแตก แต่การเพิ่มความเร็วในการหมุนวนกลับจะลดอัตราการแตกของเซลล์ลง สำหรับการใช้ลูกแก้วที่มีเส้นผ่านศูนย์กลาง 1000 ไมครอนจะให้ประสิทธิภาพในการทำให้เซลล์แตกสูงกว่ากรณีใช้ลูกแก้วขนาด 2000 ไมครอน และการทดลองทำให้เซลล์แตกภายในระบบที่ไม่มีดราฟทิฟที่ความเร็วรอบต่ำพบว่าไม่สามารถทำให้เซลล์ยีสต์แตกได้แม้ว่าจะมีการทำให้เกิดการสัมผัสกันโดยตรงระหว่างยีสต์กับลูกแก้ว

สถาบันวิทยบริการ  
จุฬาลงกรณ์มหาวิทยาลัย

ภาควิชา.....ลายมือชื่อ.....  
สาขาวิชา.....ลายมือชื่ออาจารย์ที่ปรึกษา.....  
ปีการศึกษา.....

# #4070309621: MAJOR CHEMICAL ENGINEERING

KEY WORD: CELL DISRUPTION/ BAKER'S YEAST/ FLUIDIZED BED

NARISARA SUKSAMAI: MICROORGANISM CELLS DISRUPTION USING A  
THREE-PHASE FLUIDIZED BED WITH AGITATION.

THESIS ADVISOR: ASSOC. PROF. TAWATCHAI CHARINPANITKUL, Dr. Eng., 163 pp.  
ISBN XXX-XXX-XXX-X

In this study, for the disruption of baker's yeast cells (*Saccharomyces cerevisiae*) to recover useful intracellular protein, a three-phase fluidized bed with agitator has been utilized as a new type cell disrupter. The three-phase system consists of yeast suspension, air bubble and glass beads employed as liquid phase, gas phase and solid phase, respectively. The operating parameters for the yeast cell disruption, which are impeller speed, the existing of draft tube in the fluidized bed column, superficial gas velocity, and superficial liquid velocity as well as bead size have been investigated extensively. The efficiency of disruption is evaluated by the yeast cell size distribution, and measuring total crude soluble protein released as well as using microscopic observation.

The results show that in the case of presence of glass beads, an increase in the impeller speed between in the range of 500 rpm and 3000 rpm does not affect on yeast cells disruption whether the gas bubbles are introduced into the system or not. On the other hands, with the presence of glass beads, the rate constant of yeast cells disruption increases with the increasing the impeller speed. The existing of the coaxial draft tube does not affect the yeast cell disruption compared with the single-phase mixing without the draft tube. Introduction of the gas bubbles into the bubble column also does not affect on yeast cells disruption whether the agitation is employed or not. Increasing the superficial gas velocity between 10 to 40 cm/min decreases the rate constant of yeast cell disruption but contributes the better heat transfer. The circulation of yeast suspension using centrifugal pump at the feed rate between 10 and 30 cm/min provides insignificant effect on the yeast cell disruption. Increasing the superficial liquid velocity decreases the rate constant of yeast cell disruption in the three-phase fluidized bed system. Glass beads with a diameter of 1000  $\mu\text{m}$  contribute to the higher efficiency of yeast cell disruption compared with those of 2000  $\mu\text{m}$ . The yeast cell rupture becomes less efficient at low impeller speed (25 rpm) although the direct contact between glass beads and impeller blades is employed.

Department.....Student's signature.....

Field of study.....Advisor's signature.....

Academic year.....

## ACKNOWLEDGEMENT

The author wishes to express her gratitude to her thesis advisor, Associate Professor Tawatchai Charinpanitkul, for his encouraging guidance, and suggestions throughout this study. His comments and suggestions not merely provide valuable knowledge but widen his perspective in practical applications as well.

The author wishes to express gratitude to Associate Professor Chirakarn Muangnapoh and Biochemical Engineering Laboratory for support the analytical equipment to this work.

The author wishes to express gratitude to Professor Wiwut Tanthapanichakoon and Assistance Professor Seeroong Prichanont as well as Dr. Welai Luewisuthichart for their stimulating comments and participation as the thesis committee.

The author sincerely thanks with appreciation to Mr. Pudjakom Choungchaisukasam for his enormous number of suggestions and assistance.

This research has obtained financial support from Senior Research Scholar Award (Prof. Wiwut Tanthapanichakoon) of Thailand Research Fund and Graduate School of Chulalongkorn University. Some laboratory equipment has been supported by the ASAHI Glass Foundation.

Furthermore, special thanks to credit all friends in Particle Technology and Material Processing Laboratory members who have supported and given her very helpful advice as well as cheering her up to continue this study.

Finally, the author is beholden to her mother as the rainmaker for her encouragement, understanding, inspiration and very useful help.

# CONTENTS

	PAGE
ABSTRACT IN THAI.....	IV
ABSTRACT IN ENGLISH.....	V
ACKNOWLEDGEMENT.....	VI
CONTENTS.....	VII
LIST OF TABLES.....	X
LIST OF FIGURES.....	XI
NOMENCLATURES.....	XIX
CHAPTERS	
1 INTRODUCTION.....	1
1.1 Background of Work.....	1
1.2 The Objective of Work.....	4
1.3 The Scope of Work.....	4
1.4 The Benefits of Work.....	4
2 LITERATURE REVIEWS.....	5
3 CELL DISRUPTION.....	13
3.1 Cell Wall Structure of <i>Saccharomyces cerevisiae</i> .....	13
3.2 Classification of Disruption Techniques.....	14
3.2.1 Non-mechanical Disruption.....	16
3.2.1.1 Physical Method.....	16
3.2.1.2 Chemical Method.....	17
3.2.1.3 Enzymatic Method.....	19
3.2.2 Mechanical Disruption.....	21
3.3 Disruption Measurement.....	34



	PAGE
4	Gas-Liquid-Solid Fluidization..... 37
4.1	The Phenomena of Gas-Liquid-Solid Fluidization..... 39
4.2	The Hydrodynamic of Gas-Liquid-Solid Fluidization..... 39
4.3	Agitation in Three-Phase Fluidized Bed..... 45
4.3.1	Classification of Impellers..... 45
4.3.2	Flow Patterns in Agitated Column..... 47
4.3.3	Draft Tube..... 48
4.4	Design Parameters for Gas-Liquid-Solid Fluidization..... 50
4.5	Advantages and Disadvantages of Fluidized Beds..... 56
5	EXPERIMENTS ..... 58
5.1	Fluidized Bed Unit..... 58
5.2	Yeast Suspension Preparation..... 62
5.3	Preliminary Experiments..... 66
5.3.1	Study of Influence of Temperature on Yeast Cell Disruption..... 66
5.3.2	Study of Influence of Yeast Suspension Circulation through of using Centrifugal Pump on Yeast Cell Disruption..... 67
5.4	Disruption Experiments..... 69
5.4.1	Experimental Conditions..... 69
5.4.2	Experimental Procedure..... 72
5.5	Measurement of Cell Size Distribution..... 73
5.6	Measurement of Crude Soluble Protein Released..... 74
5.7	Microscope Observation..... 77
6	RESULTS AND DISCUSSIONS..... 78
6.1	Influence of Preliminary Parameters..... 79
6.2	Influence of Agitation on Yeast Cell Disruption..... 85
6.3	Influence of Superficial Gas Velocity on Yeast Cell Disruption..... 100
6.4	Influence of Superficial Liquid Velocity on Yeast Cell Disruption..... 109
6.5	Influence of Agitation and Superficial Gas Velocity on Yeast Cell Disruption..... 114



	PAGE
6.6 Influence of Superficial Gas Velocity on the Yeast Cell Disruption in Three-Phase Fluidized Bed System.....	123
6.7 Influence of Superficial Liquid Velocity on the Yeast Cell Disruption in Three-Phase Fluidized Bed System.....	126
6.8 Influence of Bead Size on the Yeast Cell Disruption in Three-Phase Fluidized Bed System.....	130
6.9 Influence of Low Impeller Speed in Three-Phase Fluidized Bed System without Draft tube on the yeast cell disruption.....	134
7. CONCLUSIONS AND RECOMMENDATIONS.....	138
7.1 Conclusions.....	138
7.2 Recommendations for Further Study.....	140
REFERENCES.....	141
APPENDIX	
A EXPERIMENTAL DATAS OF PROTEIN ANALYSIS BY KJELDAHL METHOD MEASURED BY TECATOR KJELTEC .....	145
B CALCULATIONS.....	151
C CALIBRATION CURVES.....	158
BIOGRAPY.....	163

## LIST OF TABLES

	PAGE	
Table 1-1	Some examples of intracellular microbial enzymes produced commercially.....	2
Table 4-1	Examples of applications of three-phase fluidized bed processes	38
Table 5-1	The details of fluidized bed system .....	59
Table 5-2	Size listing of yeast cell distribution .....	63
Table 5-3	The result of density measurement using Pycnometer .....	65
Table 5-4	The result of viscosity measurement using Viscometer .....	65
Table 5-5	The operating condition of three-phase fluidized bed system for the study of effect of impeller speed, superficial gas velocity, superficial liquid velocity, and size of glass beads on the yeast cell disruption.....	71

## LIST OF FIGURES

		PAGE
Figure 3-1	Two-layer structure of yeast cell wall including the cell membrane	13
Figure 3-2	Classification of cell disruption techniques.....	15
Figure 3-3	Typical process flow diagram of mechanically cells disintegration	21
Figure 3-4	Simplified drawing of the Netzsch agitator mill system.....	25
Figure 3-5	Simplified drawing of the Netzsch model LM-20 mill.....	25
Figure 3-6	Some design of agitator disks.....	26
Figure 3-7	Centric and eccentric arrangement of agitator disks on the drive shaft.....	26
Figure 3-8	Different types of bead separators.....	28
Figure 3-9	Schematic view of high-pressure homogenizer.....	30
Figure 3-10	Details of valve seats of the high-pressure homogenizer.....	33
Figure 3-11	Disruption of <i>Saccharomyces cerevisiae</i> with a high-pressure homogenizer using different valve units.....	33
Figure 4-1	Schematic representation of gas-liquid-solid fluidized bed for cocurrent upward gas-liquid-solid systems with liquid as the continuous phase.....	40
Figure 4-2	Pressure drop and bed height VS superficial velocity for a bed of solid.....	42
Figure 4-3	Some of many design of mixing impeller.....	45
Figure 4-4	Flow pattern of a radial-flow turbine in an unbaffled column.....	48
Figure 4-5	Flow pattern of a radial-flow turbine in a baffled column with draft tube.....	49
Figure 4-6	The relation between Reynolds number and Drag coefficient.....	51
Figure 4-7	Measurement of turbine.....	55

	PAGE
Figure 5-1 Schematic diagram of fluidized bed unit .....	60
Figure 5-2 Photograph of fluidized bed column.....	61
Figure 5-3 Cell size distribution of yeast whole cells.....	64
Figure 5-4 Pycnometer.....	64
Figure 5-5 Schematic of system for study the effect of pump circulation	66
Figure 5-6 Schematic diagram of the yeast cell disruption using three-phase fluidized bed with agitation .....	70
Figure 6-1 Yeast cell size distribution at various temperatures.....	80
Figure 6-2 Yeast cell morphology at various temperature .....	81
Figure 6-3 Yeast cell size distribution at various suspension feed rates using the centrifugal pump .....	83
Figure 6-4 Yeast cell morphology at various suspension feed rates using the centrifugal pump.....	84
Figure 6-5 Yeast cell size distribution at various impeller speed in fluidized bed without draft tube (measured by Beckman Coulter LS 230) $U_i = 0$ cm/min, $U_g = 0$ cm/min, $N = 500, 1500, 2000, 3000$ rpm Absence of glass beads .....	87
Figure 6-6 Yeast cell size distribution at various impeller speed in fluidized bed without draft tube (measured by Mastersizer S) $U_i = 0$ cm/min, $U_g = 0$ cm/min, $N = 500$ and $3000$ rpm Absence of glass beads .....	88
Figure 6-7 Yeast cell morphology at various impeller speed in fluidized bed without draft tube after operated for 180 min (observed by Olympus Microscope B071) $U_i = 0$ cm/min, $U_g = 0$ cm/min, $N = 500, 1500, 2000, 3000$ rpm Absence of glass beads .....	89
Figure 6-8 Yeast cell size distribution at various impeller speed in fluidized bed with draft tube (measured by Beckman Coulter LS 230) $U_i = 0$ cm/min, $U_g = 0$ cm/min, $N = 500, 1500, 2000, 3000$ rpm Absence of glass beads .....	91

Figure 6-9	Yeast cell morphology at various impeller speed in fluidized bed with draft tube after operated for 180 min (observed by Olympus Microscope B071) $U_i = 0$ cm/min, $U_g = 0$ cm/min, $N = 500, 1500, 2000, 3000$ rpm Absence of glass beads .....	92
Figure 6-10	Yeast cell size distribution at various impeller speed in fluidized bed with draft tube (measured by Beckman Coulter LS 230) $U_i = 0$ cm/min, $U_g = 0$ cm/min, $N = 500, 1500, 2000, 3000$ rpm Bead size = $1000 \mu\text{m}$ Bead loading = 1/3 volume of annular fluidized bed .....	94
Figure 6-11	Yeast cell size distribution at various impeller speed in fluidized bed with draft tube (measured by Mastersizer S) $U_i = 0$ cm/min, $U_g = 0$ cm/min, $N = 3000$ rpm, Bead size = $1000 \mu\text{m}$ Bead loading = 1/3 volume of annular fluidized bed .....	95
Figure 6-12	Influence of impeller speed on yeast cell disruption in fluidized bed with draft tube $U_i = 0$ cm/min, $U_g = 0$ cm/min, $N = 500, 1500, 2000, 3000$ rpm Bead size = $1000 \mu\text{m}$ Bead loading = 1/3 volume of annular fluidized bed .....	98
Figure 6-13	The phenomena of grinding the yeast cell in breaking zone .....	93
Figure 6-14	Yeast cell morphology at various impeller speed in fluidized bed with draft tube after operated for 180 min (observed by Olympus Microscope B071) $U_i = 0$ cm/min, $U_g = 0$ cm/min, $N = 500, 1500, 2000, 3000$ rpm Bead size = $1000 \mu\text{m}$ Bead loading = 1/3 volume of annular fluidized bed .....	100
Figure 6-15	Yeast cell size distribution at various superficial gas velocity in fluidized bed with draft tube (measured by Beckman Coulter LS 230) $U_i = 0$ cm/min, $U_g = 0, 10, 20, 40$ cm/min, $N = 0$ rpm Absence of glass beads .....	103

	PAGE
Figure 6-16	Yeast cell size distribution at various superficial gas velocity in fluidized bed with draft tube measured by Mastersizer S $U_l = 0$ cm/min, $U_g = 0, 10, 20, 40$ cm/min, $N = 0$ rpm Absence of glass beads ..... 104
Figure 6-17	Yeast cell morphology at various superficial gas velocity in fluidized bed with draft tube after operated for 180 min (observed by Olympus Microscope B071) $U_l = 0$ cm/min, $U_g = 0, 10, 20, 40$ cm/min, $N = 0$ rpm Absence of glass beads ..... 105
Figure 6-18	Yeast cell size distribution at various superficial gas velocity in fluidized bed with draft tube (measured by Beckman Coulter LS 230) $U_l = 0$ cm/min, $U_g = 0, 10, 20, 40$ cm/min, $N = 0$ rpm Bead size = 1000 $\mu\text{m}$ Bead loading = 1/3 volume of annular fluidized bed ..... 107
Figure 6-19	Yeast cell morphology at various superficial gas velocity in fluidized bed with draft tube after operated for 180 min (observed by Olympus Microscope B071) $U_l = 0$ cm/min, $U_g = 0, 10, 20, 40$ cm/min, $N = 0$ rpm Bead size = 1000 $\mu\text{m}$ Bead loading = 1/3 volume of annular fluidized bed ..... 108
Figure 6-20	Yeast cell size distribution at various superficial liquid velocity in fluidized bed with draft tube (measured by Beckman Coulter LS 230) $U_l = 0$ cm/min, $U_g = 0, 10, 20, 40$ cm/min, $N = 0$ rpm Absence of glass beads ..... 110
Figure 6-21	Yeast cell size distribution at various superficial liquid velocity in fluidized bed with draft tube (measured by Beckman Coulter LS 230) $U_l = 0$ cm/min, $U_g = 0, 10, 20, 40$ cm/min, $N = 0$ rpm Bead size = 1000 $\mu\text{m}$ Bead loading = 1/3 volume of annular fluidized bed ..... 111

	PAGE
Figure 6-22	Influence of superficial gas velocity on yeast cell disruption $U_l = 0$ cm/min, $U_g = 0, 10, 20, 40$ cm/min, $N = 0$ rpm Bead size = 1000 $\mu\text{m}$ Bead loading = 1/3 volume of annular fluidized bed ..... 112
Figure 6-23	Yeast cell morphology at various superficial liquid velocity in fluidized bed with draft tube after operated for 300 min (observed by Olympus Microscope B071) $U_l = 0, 10, 20$ and $30$ cm/min, $U_g = 0$ cm/min, $N = 0$ rpm Bead size = 1000 $\mu\text{m}$ Bead loading = 1/3 volume of annular fluidized bed ..... 113
Figure 6-24	Yeast cell size distribution at various impeller speed in fluidized bed with draft tube (measured by Beckman Coulter LS 230) $U_l = 0$ cm/min, $U_g = 10$ cm/min, $N = 500, 1500, 2000, 3000$ rpm Absence of glass beads ..... 115
Figure 6-25	Yeast cell size distribution at various impeller speed in fluidized bed with draft tube (measured by Beckman Coulter LS 230) $U_l = 0$ cm/min, $U_g = 40$ cm/min, $N = 500, 1500, 2000, 3000$ rpm Absence of glass beads ..... 116
Figure 6-26	Yeast cell size distribution at various impeller speed in fluidized bed with draft tube (measured by Beckman Coulter LS 230) $U_l = 0$ cm/min, $U_g = 10$ cm/min, $N = 500, 1500, 2000, 3000$ rpm Bead size = 1000 $\mu\text{m}$ Bead loading = 1/3 volume of annular fluidized bed ..... 117
Figure 6-27	Yeast cell size distribution at various impeller speed in fluidized bed with draft tube (measured by Beckman Coulter LS 230) $U_l = 0$ cm/min, $U_g = 40$ cm/min, $N = 500, 1500, 2000, 3000$ rpm Bead size = 1000 $\mu\text{m}$ Bead loading = 1/3 volume of annular fluidized bed ..... 118



- Figure 6-28 Influence of impeller speed on yeast cell disruption in the fluidized bed with draft tube  
 $U_i = 0$  cm/min,  $U_g = 10$  cm/min,  $N = 500, 1500, 2000, 3000$  rpm  
 Bead size =  $1000 \mu\text{m}$   
 Bead loading = 1/3 volume of annular fluidized bed ..... 119
- Figure 6-29 Influence of impeller speed on yeast cell disruption in the fluidized bed with draft tube  
 $U_i = 0$  cm/min,  $U_g = 40$  cm/min,  $N = 500, 1500, 2000, 3000$  rpm  
 Bead size =  $1000 \mu\text{m}$   
 Bead loading = 1/3 volume of annular fluidized bed ..... 120
- Figure 6-30 Influence of superficial gas velocity on yeast cell disruption in the fluidized bed with draft tube  
 $U_i = 0$  cm/min,  $U_g = 0, 10$  and  $40$  cm/min,  $N = 1500$  rpm  
 Bead size =  $1000 \mu\text{m}$   
 Bead loading = 1/3 volume of annular fluidized bed ..... 121
- Figure 6-31 Influence of superficial gas velocity on yeast cell disruption in the fluidized bed with draft tube  
 $U_i = 0$  cm/min,  $U_g = 0, 10$  and  $40$  cm/min,  $N = 3000$  rpm  
 Bead size =  $1000 \mu\text{m}$   
 Bead loading = 1/3 volume of annular fluidized bed ..... 122
- Figure 6-32 Influence of superficial gas velocity on yeast cell disruption in the Fluidized bed with draft tube  
 $U_i = 10$  cm/min,  $U_g = 0$  and  $40$  cm/min,  $N = 3000$  rpm  
 Bead size =  $1000 \mu\text{m}$   
 Bead loading = 1/3 volume of annular fluidized bed ..... 124
- Figure 6-33 Content of protein released at various superficial gas velocity in the fluidized bed with draft tube  
 $U_i = 10$  cm/min,  $U_g = 0$  and  $40$  cm/min,  $N = 3000$  rpm  
 Bead size =  $1000 \mu\text{m}$   
 Bead loading = 1/3 volume of annular fluidized bed ..... 125

- Figure 6-34 Yeast cell size distribution at various superficial liquid velocity in fluidized bed with draft tube (measured by Beckman Coulter LS 230)  
 $U_l = 10, 20, 30$  cm/min,  $U_g = 10$  cm/min,  $N = 3000$  rpm  
 Bead size =  $1000 \mu\text{m}$   
 Bead loading = 1/3 volume of annular fluidized bed ..... 127
- Figure 6-35 Influence of superficial liquid velocity on yeast cell disruption in the Fluidized bed with draft tube  
 $U_l = 10, 20, 30$  cm/min,  $U_g = 10$  cm/min,  $N = 3000$  rpm  
 Bead size =  $1000 \mu\text{m}$   
 Bead loading = 1/3 volume of annular fluidized bed ..... 128
- Figure 6-36 Content of protein released at various superficial liquid velocity in the fluidized bed with draft tube  
 $U_l = 10$  and  $20$  cm/min,  $U_g = 10$  cm/min,  $N = 3000$  rpm  
 Bead size =  $1000 \mu\text{m}$   
 Bead loading = 1/3 volume of annular fluidized bed ..... 129
- Figure 6-37 Yeast cell size distribution at different bead size in the fluidized bed with draft tube (measured by Beckman Coulter LS 230)  
 $U_l = 10$  cm/min,  $U_g = 10$  cm/min,  $N = 3000$  rpm  
 Bead size =  $1000$  and  $2000 \mu\text{m}$   
 Bead loading = 1/3 volume of annular fluidized bed ..... 131
- Figure 6-38 Influence of bead size on yeast cell disruption in the fluidized bed with draft tube  
 $U_l = 10$  cm/min,  $U_g = 10$  cm/min,  $N = 3000$  rpm  
 Bead size =  $1000$  and  $2000 \mu\text{m}$   
 Bead loading = 1/3 volume of annular fluidized bed ..... 132
- Figure 6-39 Yeast cell morphology at different bead size in fluidized bed with draft tube at 300 min (observed by Olympus Microscope B071)  
 $U_l = 10$  cm/min,  $U_g = 10$  cm/min,  $N = 3000$  rpm  
 Bead size =  $1000$  and  $2000 \mu\text{m}$   
 Bead loading = 1/3 volume of annular fluidized bed ..... 133

- Figure 6-40 Yeast cell size distribution comparison between low impeller speed in fluidized bed without draft tube and high impeller speed in fluidized bed with draft tube (measured by Beckman Coulter LS 230)  
 $U_i = 10 \text{ cm/min}$ ,  $U_g = 10 \text{ cm/min}$ ,  $N = 25$  and  $3000 \text{ rpm}$   
 Bead size =  $1000 \mu\text{m}$   
 Bead loading = 1/3 volume of annular fluidized bed ..... 135
- Figure 6-41 Comparison of degree of cell disruption examined under the condition of low impeller speed in fluidized bed without draft tube and high impeller speed in fluidized bed with draft tube  
 $U_i = 10 \text{ cm/min}$ ,  $U_g = 10 \text{ cm/min}$ ,  $N = 25$  and  $3000 \text{ rpm}$   
 Bead size =  $1000 \mu\text{m}$   
 Bead loading = 1/3 volume of annular fluidized bed ..... 136
- Figure 6-42 Comparison of yeast cell morphology investigated under the condition of low impeller speed in fluidized bed without draft tube and high impeller speed in fluidized bed with draft tube (observed by Olympus Microscope B071)  
 $U_i = 10 \text{ cm/min}$ ,  $U_g = 10 \text{ cm/min}$ ,  $N = 25$  and  $3000 \text{ rpm}$   
 Bead size =  $1000 \mu\text{m}$   
 Bead loading = 1/3 volume of annular fluidized bed ..... 137

## NOMENCLATURES

A	:	the cross section area of column (m)
$A_p$	:	the projected area of particle measured in plane perpendicular to direction of motion of particle (-)
a	:	an exponent
$C_D$	:	drag coefficient (-)
$D_a$	:	diameter of impeller (m)
$D_t$	:	diameter of tank (m)
$dP/dz$	:	the static pressure gradient.
E	:	the height of impeller above the column floor (m)
g	:	the gravitational acceleration ( $m/s^2$ )
H	:	the effective height of bed expansion (m)
H	:	the depth of liquid in column (m)
J	:	the width of baffles (m)
j	:	the number of CSTRs (-)
k	:	the disruption rate constant ( $s^{-1}$ )
L	:	the length of impeller blades (m)
$L_0$	:	the height of bed at fixed bed (m)
$L_{mf}$	:	the height of bed at minimum fluidization (m)
m	:	the mass of particle (kg)
N	:	the number of passes through homogenizer (passes)
$N_{re,p}$	:	Reynolds number (-)
P	:	the operating pressure (psia)
$\Delta P$	:	pressure drop (psia)
q	:	the total volume of fluid throughput the CSTR ( $m^3$ )
R	:	the weight of protein released per unit weight of packed yeast (mg/ml)
$R_m$	:	the maximum measured protein release (mg/ml)
S	:	the cross-section area of empty column (m)

$u_{mf}$	:	minimum fluidized bed velocity (m/s)
$u_t$	:	terminal velocity (m/s)
$V$	:	the total volume of the mill ( $m^3$ )
$W$	:	the weight of solid particle in the bed (kg).
$W$	:	the impeller width (m)
$\mu$	:	fluid viscosity (kg/ m.s)
$\rho_g$	:	gas density ( $kg/m^3$ )
$\rho_l$	:	liquid density ( $kg/m^3$ )
$\rho_s$	:	solid density ( $kg/m^3$ )
$\epsilon_g$	:	gas holdup (-)
$\epsilon_l$	:	liquid holdup (-)
$\epsilon_{mf}$	:	minimum porosity (-)
$\epsilon_s$	:	solid holdup (-)
$\phi_s$	:	the sphericity (-)
$\tau$	:	the mean residence time in the mill



สถาบันวิทยบริการ  
จุฬาลงกรณ์มหาวิทยาลัย

# CHAPTER 1

## INTRODUCTION

### 1.1 Background of Work

The importance of microorganisms as a source of commercially useful chemicals, antibiotics and enzymes has been recognized for a very long time. Nearly all chemicals of microbial origin produced industrially today are the extracellular substances. Those chemicals generally exist in the microbial cell, but are then excreted into the surrounding environment. However, a much larger proportion of the potentially useful microbial products is retained within the cells. For instance, a vast majority of the enzymes is intracellular matter.

Recently many intracellular enzymes have begun to be produced industrially: for example, glucose oxidase for food preservation, penicillin acylase for antibiotic conversion, and asparaginase for possible cancer therapy. Other examples of intracellular microbial enzymes produced commercially are given in Table 1-1.

The isolation of intracellular material requires that either the microbial cell is genetically engineered so that what would normally be intracellular is excreted into the environment, or it must be disintegrated by physical, chemical or enzymatic means to release its contents into the surrounding medium. However, the genetic manipulation of microbial cells to make them leaky is limited in scope. Making the cell fully permeable to any significant fraction of the intracellular products and enzymes would not only be difficult, but also will imply discontinued existence of the cell. On the other hand, the unit operations of microbial cell disruption for intracellular product isolation will become of increasing importance, instead. Generally, mechanical techniques are employed because they represent a unit operation

applicable to all type of cells and processes. Also, these techniques have been scaled to commercial production with great success, in contrast with other lytic techniques, which have unique problems in large-scale production.

**Table 1-1.** Some examples of intracellular microbial enzymes produced commercially  
(Chisti et al, 1986; Gianfreda et al, 1976; Choi et al, 1997)

Enzyme	Source	Examples of use
Invertase	<i>Saccharomyces cerevisiae</i>	Confectionery
L-Asparaginase	<i>Escherichia coli</i>	Treatment of acute lymphatic leukemia
Catalase	<i>Aspergillus niger</i>	Removal of H <sub>2</sub> O <sub>2</sub> after milk sterilization
Cholesterol oxidase	<i>Nocardia rhodochrous</i>	Serum cholesterol analysis
$\beta$ -Galactosidase	<i>Kluyveromyces fragilis</i> <i>Saccharomyces lactis</i>	Hydrolysis of lactose in milk/whey
Glucose isomerase	<i>Bacillus coagulans</i> <i>Streptomyces sp.</i>	Production of high-fructose glucose syrups
Glucose oxidase	<i>Aspergillus niger</i> <i>Penicillium notatum</i>	Serum glucose analysis Removal of oxygen from foods
Glucose-6-phosphate dehydrogenase	Yeast	Clinical analysis
Panicillin acylase	<i>Escherichia coli</i>	Deacylation of benzylpenicillin

So far, two technologies, namely, mechanical disruption; (I) homogenization, and (II) beads mill have dominated the market. Both have their origin in other industries and have been adapted successfully for biotechnology. Each technique makes use of the principle of high mechanical shear, and has features that make them unique in the treatment of bacterial, fungal, yeast, algal and eukaryotic cells. But the disadvantages of both are high investment cost, hard to scale up, especially for homogenizer. In this study, we have tried to



utilize a three-phase fluidized bed with an agitator as a newly developed technique for the disruption of baker's yeast (*Saccharomyces cerevisiae*) cells.

Three-phase gas-liquid-solid fluidized bed has gained considerable attention as evidenced in their commercial or demonstrated applications in physical, chemical, petrochemical, electrochemical, and biochemical processing. Especially biochemical processes, there are numerous applications of three-phase fluidization systems, such as ethanol fermentation, enzyme immobilization, penicillin production, and bacitracin production etc (Fan L. S., 1989). Those successful biochemical applications of gas-liquid-solid fluidization lead to a challenging idea of applying it to cell disruption process.

The system of interest in this work consists of slurry of yeast suspension, air bubble and glass beads as liquid phase, gas phase and solid phase, respectively. The liquid is flowed continuously while the gas is introduced as discrete bubbles. The flow of liquid and gas is cocurrent upward, and the solids are in non-stationary state. Cell disruption can take place based on shear forces exerted by glass beads as grinding medium and by liquid flow through the gap of the draft tube installed in the column of fluidized bed. In addition, the interaction between gas bubbles and microbial cells is supposed to affect the cell disruption. The advantages of this technique are easy to scale-up and low investment cost because of the simple structure. Moreover, it is capable of being operated continuously. In order to study the influence of operating parameters such as superficial gas velocity, superficial liquid velocity and speed of agitator on the efficiency of disruption, the particle size distribution, protein release, and microscopy study have been investigated in this work.

## 1.2 The Objective of Work

To study the effect of operating parameters on yeast cells disruption using three-phase fluidized bed with agitator

## 1.3 The Scope of Work

1. The laboratory-scale three-phase fluidized bed with agitator will be designed and fabricated.
2. The influences of operating parameters of the three-phase fluidized bed with agitator on the yeast cells disruption will be examined:
  - Impeller Speed
  - Superficial gas velocity
  - Superficial liquid velocity
  - Bead size

## 1.4 The Benefits of Work

The benefits that may be derived from this research work are as follows:

1. The operating conditions, which are appropriate for of cell disruption using three-phase fluidized bed with agitator can be identified.
2. Understanding of cell disruption mechanism takes place inside the three-phase fluidized bed with agitator.

สถาบันวิทยบริการ  
จุฬาลงกรณ์มหาวิทยาลัย

## CHAPTER 2

### LITERATURE REVIEWS

Disruption of microorganisms is often required in large-scale production of microbial products, such as enzymes, toxin, and therapeutic proteins. Mechanical disruption techniques are widespread in the industrial processes because they are applicable to all types of cells and have been scaled up to commercial production with great success, in contrast with other lytic techniques, which have unique problems in large-scale production (Millis, J. R., 1997). This chapter reviews about the research and progress in the mechanical cell disruption, especially these involved with application of three-phase fluidized bed with agitator as a newly developed technique for yeast cell disruption.

Currie et al (1972) investigated the release of protein from baker's yeast (*Saccharomyces cerevisiae*) by disruption using a 4.2 liter vertical agitator mill. Protein released from disruption in the mill was a first-order process. The rate constant was influenced by six operating parameters as temperature (5-42°C), agitator speed (500-1800 rpm), bead size (0.5, 0.8, 1.1, 2.0, and 2.8 mm), weight of beads (3-9 kg), feed rate of yeast suspension (1-8 l/min), and yeast concentration (0.3-0.75 g packed yeast/ml). It was found that the disruption efficiency increased with the agitator speeds, loading of beads, while it decreased when the feed rate of yeast suspension increased. For the effect of the temperature, it had insignificant on cell disruption.

Marffy and Kula (1974) investigated the influence of operating parameters upon the disintegration process with the Dyno-Mill disintegrator, a horizontal high-speed agitator, on enzyme releases from brewer's yeast cell (*Saccharomyces carlsbergensis*). The operating parameters taken into account were speed of impeller (2000-4500 rpm), feed rate of yeast suspension (4-40 l/hr), beads diameter (0.10-0.25 mm, 0.25-0.50 mm, and 0.75-1.00 mm)

and yeast concentration. Analysis of the experimental data showed that the enzyme release expressed as an approximately first-order process. The rate constant was used as standard to compare the efficiency of cell disruption processes. It was shown that rate constant increased with the increasing rotational speed, and the higher density of the initial cell suspension. While increasing of the flow rate caused decreasing of rate constant. Bead diameter 0.33 mm was found to be optimal to disrupt the yeast used in their work.

Cunningham et al (1975) ruptured the 0.1 g (dry weight)/ml of petroleum-grown yeast (*Candida tropicalis*) to produce the single cell protein by using various disintegration methods such as decompression, sonic oscillation, homogenization, freeze-thaw, stone-milling, and manual grinding. They defined the efficiency of cell disruption using the percentage of protein releases, which assayed by Lowry method. The results showed that the sonic oscillation, decompression with nitrogen gas, and homogenization could increase the soluble protein content by 61%, 29%, and 21%, respectively by comparing with the amount of protein released before processing. For the efficiency of other rupture methods was approximately 5% soluble protein.

Rehacek and Schaefer (1977) disintegrated *Saccharomyces cerevisiae* and *Candida utilis* by using a 20-liter continuous high-speed horizontal mill. The disintegration efficiency and heat production depended on the many operating parameters which were angle of agitator disks (75° and 81°), agitator speed (600, 1200, 1800, 2400 rpm), feed rate of cell suspension (50, 100, 150, and, 200 l/hr), and bead loading (75, 80, and 88% by volume). The degree of disintegration (x) was expressed as  $x (\%) = [100 \times (n - n_1) / n]$ , where n is the number of cells in the non-treated suspension, and  $n_1$  is the number of the cells in the treated suspension. The number of cells was determined using microscopic method (at least 30 microscopically images were employed in every condition). The results showed that the moderate disc angle of approximately 80° was the most useful for disintegration because it gave high degree of disintegration, without excessive heat generation and power consumption. It was also found that employing an oblique disk resulted in the movement of grinding beads both in radial and axial direction. The higher density of beads increased the higher the degree of disintegration and energy consumption. In addition, the degree of

disintegration was increased with the agitator speed but it decreased when the feed rate was increased.

**Engler and Robinson (1979)** investigated the degree of cell disruption using microscopic method. Microscopy may be used to count the number of whole cells before and after pass the process, but it consumed a large time because a large number of samples must be taken into account. Coulter counter could be employed with confidence, however, the procedure was not sensitive enough for application to bacterial suspension. In conclusion, they proposed that the best method was the determination of released dissolved protein in the suspending medium, which could be confirmed with the experimental data of the *Saccharomyces cerevisiae* and *Candida utilis* disruption using Manton-Gaulin homogenizer.

**Kelemen, and Sharpe (1979)** studied the disruption of variety of cell using a commercial cell disrupter, which manufactured and supplied by Stansted Fluid Power Limited, Stansted, England. This machine could be operated as continuous process and could disrupt large volumes of cells. The cell disruption could be conducted by the subjecting cells into extremely high pressure through a short orifice. Cell disruption could be observed qualitatively by phase-contrast microscope. The detailed morphological damage was also observed by electron microscope. And a quantitative estimation of non-disrupted cells was carried out by viable counts. It was clearly found that little or no disruption occurred until a certain level of applied pressure was reached, and that subsequently the proportion of cells disrupted increased rapidly with the increasing pressure until almost of all the cells were disrupted. *Saccharomyces cerevisiae* required  $1.5 \times 10^8$  Pa for the complete disruption. In addition, it was found that cell disruption depended on the shape and chemical composition of the cell wall. The cell with rod shape was disrupted more easily than spheres, while gram-negative rods, although similar in size to a gram-positive rods, was disrupted more easily.

**Mosqueira et al (1981)** characterized viscosity and density of yeast suspension with 45% (w/v) yeast concentration using a viscometer and pycnometer, respectively. High-

pressure homogenizer was used to disrupt the yeast cells. Experimental result showed that after the four passes through homogenizer for 25 min the apparent viscosity of the suspension linearly increased from 7 cP to 9 cP, while the apparent viscosity of the supernatant increased from 1.8 cP to 2.1 cP. Both suspension and supernatant exhibited the non-Newtonian behavior due to the releasing of glycan from yeast cell wall. For density of the debris suspension and separated supernatant increased a little while yeast concentration was increased from 4 to 45% (w/v).

**Agerkvist and Enfors (1990)** determined the protein releases, the particle size distribution, and the viscosity of disrupted *E. coli* suspensions after application of three different disintegration methods. A glass bead disintegrator (Dyno Mill KDL) filled with glass beads of 0.25-0.50 mm and stirred at 4500 rpm was employed. The mean residence times of the cell suspension were 2, 3, and 4 min corresponding to flows of 9, 6, and 4.5 l/hr. Then Manton Gaulin 15M-8TA homogenizer was operated batchwise at 60 MPa giving cell flows of about 200 l/h. The last method was employing Microfluidizer M-110, in which the cells were disrupted by discrete-passes of the suspension through the reaction chamber at 60 MPa with a flow of 18 l/h. The result showed that three disintegration methods gave approximately the same value of protein and enzyme releases but gave different physical properties of the disintegrated cell suspension, which in turn affected on the separability of the cell debris from the protein solution. The separation degree of biomass using centrifugation was only slightly affected by increasing degree of disruption (increasing protein releases) in the bead mill, while an increase in the degree of disruption in the high-pressure homogenizers drastically reduced the centrifugal degree of separation. However, increasing of degree of disruption resulted in shorter filtration times for three disintegration methods. The experimental results also showed further that the cell concentration had only a minor influence on protein release in the Microfluidizer.

**Milburn and Dunnill (1994)** examined the effect of freezing and thawing as pretreatment on homogenization and bead milling to release the virus-like particles (Ty-VLPs) from recombinant cells of *Saccharomyces cerevisiae*. The homogenizer was operated at flow rate of 70l/h, an operating pressure of 34.5 to 68.9 MPa, and with 6-10 discrete



passes of the cell suspension through the disruption valve. While the bead mill, filled up to 80% of its volume with glass beads of 0.5 mm diameter, was operated at the tip speed of 10 m/s. The degree of cell disruption was determined by protein assay using the dual wavelength method of Ehresmann. The effect of pre-treatment was identified that when the cells was frozen and thaw before disruption, they had 4-times resistance to be homogenized. This effect increased with the number of freezing and thawing cycles, but was independent of the time that the cells remained frozen. Therefore, it could be concluded that freezing and thawing cells had resistance two times higher than that of non-pretreatment process.

**Carlson et al. (1995)** disintegrated *E. coli* using five different mechanical cell disruption methods to extract intact plasmids, which were sonication, nebulization, homogenization, microfluidization, and bead milling. The recovery yields of intact plasmids from these diverse methods were measured using quantitative gel electrophoresis. The results showed that although cell disruption was accomplished by all the methods, but only two methods, microfluidization and bead mill, resulted in high recovery of intact plasmids. It was found that sonication, nebulization, and homogenization resulted in almost complete degradation of the plasmid under any conditions. Microfluidization provided 20-40% of the intact plasmids was recovered in the solution after one pass at 1500-2000 psi. On the other hand, the best processing method for the intact plasmids recovery was bead milling, in which over 90% of the plasmids was solubilized without substantial degradation. Other methods could recover no greater than 20% of the total intact plasmids.

**Siddiqi et al. (1996)** simulated the particle size distribution as function of operating pressure and number of passes through homogenizer based upon the Boltzmann function. 45% wet w/v of fresh packed baker's yeast (*Saccharomyces cerevisiae*) suspension was taken to process in Manton Gaulin high-pressure homogenizer. Particle size distribution (PSD) of the yeast suspension was measured using an electrical sensing zone (ESZ) method. The experimental results showed that there was little breakage below a threshold pressure of 115 bar above which breakage was critically dependent upon the number of passes through the homogenizer.



Otero et al (1996) designed the simple process to produce yeast protein concentrate, semi-pure glucomannan, cell-wall protein and yeast extract from homogenized baker's yeast (*Saccharomyces cerevisiae*). The first step in the fractionation of yeast was rupture of cell envelope. Degree of disruption was the function of the working pressure, P, and number of passes through the homogenizer, N. The optimum condition was N = 3-5 passes for obtaining 90% disruption of *S. cerevisiae* slurries, at P = 54-60 MPa. After centrifuged, yeast suspension was separated into two fractions as debris and supernatant, which two fractions were processed in the next step. From the supernatant, the yeast protein concentrate and yeast extract was produced. While primary debris was processed as semi-pure glucomannan and yeast cell-wall protein. Crude protein (total nitrogen) was determined by the Kjeldahl method. The quantitative of protein of yeast protein concentrate, yeast extract was 72 and 36 %(w/w), respectively. Whereas, yeast cell-wall protein, semi-pure glucomannan, and primary glycan from debris were 71, 3.7 and 36% (w/w), consequently.

Morohashi et al (1997) studied the release process of protein from dry baker's yeast, *Saccharomyces cerevisiae*, using an agitating bead mill. Glass beads were employed as the grinding media in 0.85% NaCl yeast suspension. The beads' mean diameter and specific gravity were 0.42 mm and 2.49, respectively. It was clearly shown that the protein release process was seriously affected by operating conditions, which were agitating speed of impeller (245, 390, and 630 rpm), weight of glass beads (0.3, 0.35, and 0.4 kg), the volume of cell suspension (0.075, 0.1, and 0.15 dm<sup>3</sup>) and concentration of cell suspension (0.01, 0.05, and 0.10 kg/dm<sup>3</sup>). Initially, the concentration of protein released increased with the disruption time, after it reached a maximum, subsequently it decreased gradually due to the denaturation of protein, caused by shearing, impacting and frictional action between colliding glass beads. The disruption time necessary for a maximum disruption became shorter if the concentration of cell suspension became lower. When the agitating speed and the weight of glass beads was higher, the maximum disruption time also became shorter, a decreasing in the volume of cell suspension also shortened the disruption time.

Choi et al (1997) assessed the disruption of *Lactobacillus casei* sp. *casei*, which releases of aminopeptidase using Microfluidizer under a pressure of 41.3 -158.5 MPa with

flow rate from 330-520 ml/min. From the experimental, the cell disruption was found to rely on both operating pressure and number of passes of the Microfluidizer. The operating pressure had greater effect on the disruption than did the number of passes. The optimum operating pressure for enzyme extraction was 76 MPa with loss of minimum enzyme activity about 15-20%.

**Siddiqi et al (1997)** studied the protein release and cells debris size distribution of disrupted baker's yeast cell (*Saccharomyces cerevisiae*) in high-pressure homogenizer. Experiments were carried out with three concentrations of yeast cells (1, 10, and 45% (w/v)). It should be noted that 45% packed yeast was typical condition for the highest concentration adopted in industrial disruption. Particle size distribution (PSD) of whole yeast, which had a modal size of approximately 4.5  $\mu\text{m}$ , and cell debris measured using an electrical sensing zone (ESZ) method, while the soluble protein release was analyzed based on the Bradford method. Thus protein release data confirmed that total protein release (96 mg protein/ g packed yeast) was achieved by the end of the fifth pass at 500 bar (most of the whole cells were disrupted). Beyond the fifth pass pumping of the cell suspension through the homogenizer caused a further degree of fine debris formation, which was hard to separate. In addition, the PSD and the total protein release were highly affected by the applied pressure for two valve geometries (micron lab40 design and lab60 and K3 design) and flow rates.

**Shimizu et al (1998)** utilized the Theta-composer as a new type beads mill with glass beads as disruption medium to study the yeast cell disruption. They investigated the influence of the parameters such as rotor speed and vessel speed on the release characteristics of soluble proteins and some enzymes. They found that the rate of protein release increased with increasing of the rotor speed. Because of the change in the distribution of the cell diameter due to the cell disruption, it was suggested that there was a critical point of the yeast cell disruption at the rotor speed 2500 rpm, and the release rate of the soluble protein was 4.4 times as fast as the rate of the cell disruption.

Heim et al (1999) presented the effect of various operating parameters on the disintegration of baker's yeast (*Saccharomyces cerevisiae*) suspension in a bead mill with a multi-disk impeller. The operating parameters were the concentration of microorganism suspension (0.05-0.20 g dry mass/ml), disk-to-disk distance (5-40 mm) and rotational speed of the impeller (1000-3500 rpm). To determine the degree of yeast disintegration, Ultraviolet (UV) absorption method was used to assay the quantitative of RNA and DNA nucleic acids releases. Experiments were carried out as batch operation. Modeling of the process by describing its kinetics using the first-order differential equation was confirmed to be adequate. They found that when the concentration of yeast suspension increased over 0.14 g/ml, the process rate constant became increased. The increasing disintegration effect could be observed at the rotational speed higher than 2000 rpm for all impeller geometries.

Ricci-Silva et al (2000) disrupted *Saccharomyces cerevisiae* cells at 5°C in a 200-ml vertical bead mill using glass beads (diameter 0.5 mm). The studied parameters were agitator speed (1100, 1700, 2300, and 3100 rpm), glass beads volume (50, 75, and 100 ml) and cell concentration (170, 250, and 325 g/l). The total protein concentration, the activity of glucose-6-phosphate dehydrogenase (G6PCH), and the number of intact cells were determined. It was found that as increasing the disruption time and the agitator speed, the percentage of cell disrupted became higher. Moreover, the disintegration rate achieved the highest value (around  $6 \times 10^{11}$  disrupted cells/min) at 3100 rpm for 3 min, and became independent to the agitation after 6 min operation. The concentration of glass beads employed for milling affected protein release and the rate of cell disruption. One hundred milliliters of glass beads was the most efficient for both parameters. The suitable volume of glass beads was 50% of the whole chamber volume to avoid the high increase in the temperature. It was found that the percentage of cell disintegration was high at low initial cell concentrations. Moreover, G6PDH liberation and the cell disruption were found to be coupled events.

## CHAPTER 3

### CELL DISRUPTION

#### 3.1 Cell Wall Structure of *Saccharomyces cerevisiae*

Yeast cells are either spherical or ellipsoidal in shape, being typically between 2  $\mu\text{m}$  and 12  $\mu\text{m}$  in diameter. The cell wall surrounding the yeast cell is approximately 25-100 nm thickness (typically less than 2% of the diameter). In the case of baker's yeast cells, the wall thickness is approximately 70 nm and increases with the age of cell (Shamlou et al., 1995). The cell wall is a complex structure made up of several different biopolymers, including glucans, protein, mannans and small amounts of chitin. Chemical analysis of the yeast cell wall shows that 55–60% of the wall is made up of  $\beta(1-3)$  and  $\beta(1-6)$  linkage glucan. Mannan has been located on the outer surface of the wall. It appears to cover the entire cell surface and is attached to a crosslinked protein network via asparagine residues. The protein present in the wall has a high content of glutamic acid and aspartic acid. Included in the protein of the yeast cell walls are enzymes, such as acid phosphatase, invertase, melibiase, and proteases (Hough et al, 1971).

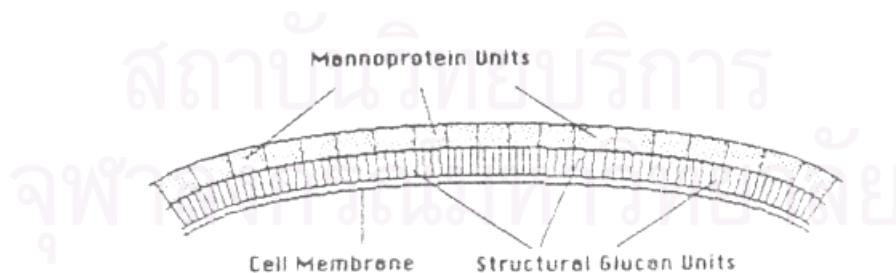


Figure 3-1. Two-layer structure of yeast cell wall including the cell membrane  
(Redrawn from Hunter J.B. and Asenjo J.A., J. Biotechnol. Bioeng. 1988, 31, p. 929)

Figure 3-1 illustrates two-layer structure of cell wall including the cell membrane which preserves the cells from a rapidly change of osmotic pressure in their natural habitat and mechanical breakage. Generally, the mean compressive force necessary to rupture the wall of the yeast cells is in the range of 40–150  $\mu\text{N}$ . However, the relative strength of the cell wall depends on culture conditions, growth rate, time of harvest, and storage conditions (Kleinig and Middelberg, 1998).

Knowledge of cell wall structure and composition can help develop more efficient methods of cell lysis. Because cells are relatively expensive raw material, the complete disintegration of the cells is desired with high product yields. However, biologically active proteins usually withstand only moderate temperatures and pH values and are the target of proteolytic enzymes liberated from cell. This fact limits the process conditions and process time. The physical state of the product, in soluble or solid form can be critical in choosing the appropriate method. Complete release of the product often requires a lengthy treatment of the raw material, which may lead to product deterioration and yield losses. These mentioned concern must be taken into account for the design of the cell disruption process.

### 3.2 Classification of Disruption Techniques

A useful classification of the cell disruption methods is given in Figure 3-2. It should be noted that the classification of techniques is rather arbitrary. For example, autolysis may be classified as an enzymatic method although it is often induced by chemical or physical shock. It is quite general to describe the non-mechanical and mechanical methods for cell disruption.



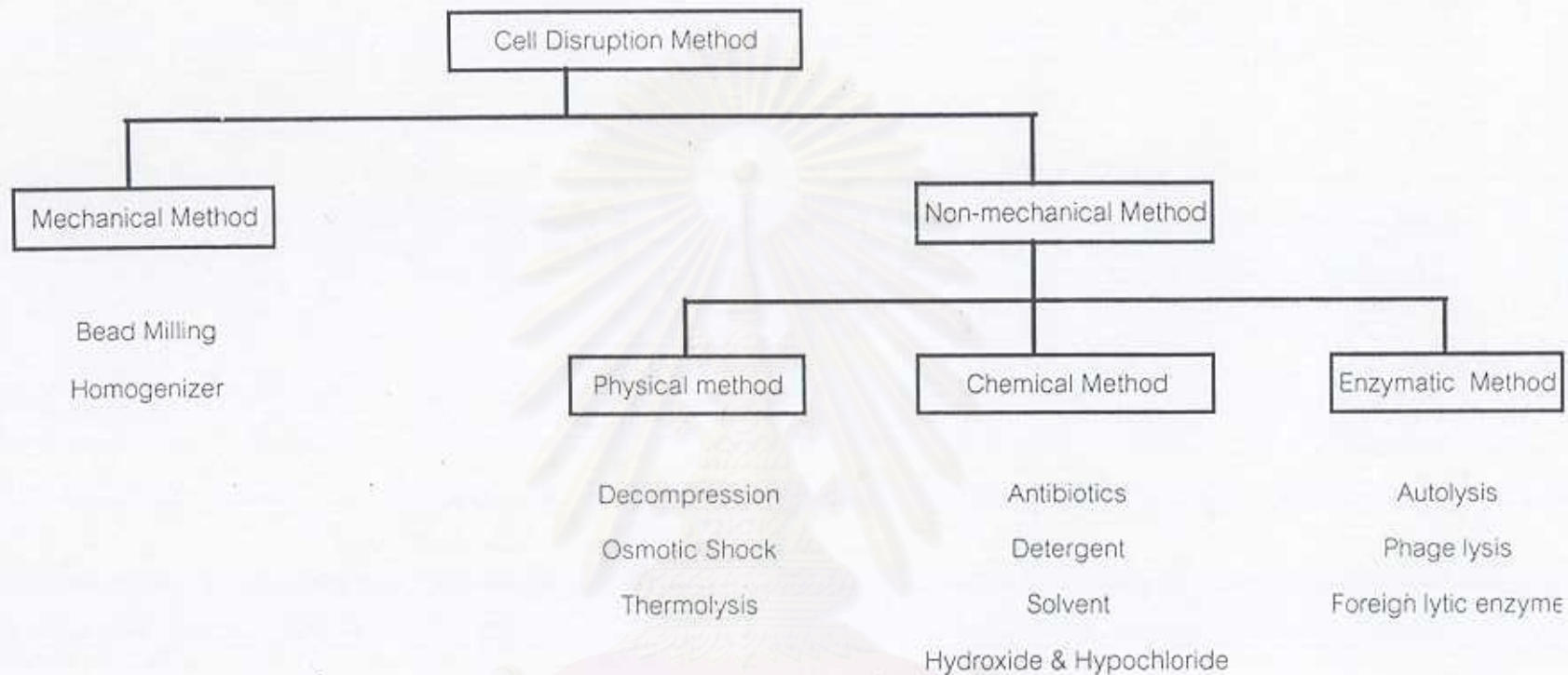


Figure 3-2. Classification of cell disruption techniques.

### 3.2.1 Non-mechanical Disruption

The non-mechanical method of cell rupture shown in Figure 3-2 is dominated by physical, chemical, and enzymatic method. These three methods are described in the following paragraphs.

#### 3.2.1.1 Physical Disruption

Important physical method for cell disruption such as decompression, osmotic shock, and thermolysis, will be described in follows.

##### Decompression

In explosive decompression is a cell suspension, which is mixed with pressurized subcritical or supercritical gas for a specified time. Gas enters the cell, and expands on release of the applied pressure causing disruption. The technique has the advantage that it is extremely gentle, resulting in large debris and consequent ease of debris removal where the desired product is soluble. Unfortunately, it generally has a low efficiency. Results are also highly dependent on the rate of pressure release and the time of contact between the gas and suspension.

##### Osmotic shock

In osmotic shock is dumping a given volume of cells into pure water-often about twice the volume of cells. Water rapidly enters the cell, increasing the internal pressure and causing lysis. The cells swell because they contain comparatively high concentration of solutes, which causes an osmotic flow of water into the cells. In some cases, they swell so much that they burst. Their contents, released into the surrounding solution, can then be separated.

##### Thermolysis

Thermolysis in a large scale process may become increasingly common. Results are dependent on the type of organism, its growth phase and pre-shock storage temperature. The technique has several advantages, for example, it may be operated to kill the host, thus eliminating the possible release of recombinant organisms



downstream. In addition, the technique leads to large cellular debris that may be easily separated from a soluble product. The technique also suffers some possible disadvantages such as significant increase in viscosity and the appearance on non-Newtonian viscoelastic behavior may be observed. Further, large debris will be undesirable where the product is a solid inclusion body, as it will be difficult to separate by fractional centrifugation.

### 3.2.1.2 Chemical Disruption

The outer wall of microorganisms can be disrupted or permeabilized by a variety of chemical treatments. These methods are shown in Figure 3-2, and will now be discussed in greater detail.

#### 1. Antibiotics

The example of available antibiotics is  $\beta$ -lactam and polymycin. The  $\beta$ -lactam antibiotics affect peptidoglycan synthesis by the blockage of peptidoglycan precursor synthesis. Without peptidoglycan, the cell is unable to maintain its osmotic pressure and consequently disrupts, releasing intracellular proteins. For polymycin, a cationic polypeptide antibiotic with an aliphatic chain, it disorganizes and penetrates the outer membrane before causing lysis by binding to, and distorting the cytoplasmic membrane. Despite their ability to cause rapid lysis, the use of antibiotics for large scale work has not been reported. This is partly because their effectiveness depends on the state of the culture. Another consideration is their generally high cost.

#### 2. Detergents

The second major method of chemically rupturing cells is solubilization by detergents, which are amphipathic molecules having a hydrophilic portion, which is often ionic, and a hydrophobic portion, usually a hydrocarbon. Typically, a concentrated detergent solution is added to about half the solution's volume of cells. The detergent solubilizes lipids in the cell walls, and thus ruptures these walls via formation of micelles between detergent and lipids in the cell walls. The resulting suspension can be centrifuged to remove cell fragments, and then run through an adsorption column or an extractor to isolate the intracellular product. . Results are very concentration dependent and

vary with the critical micelle concentration of the detergent. The detergent are anionic (e.g. sodium dodecyl sulphate (SDS) and include the soaps which are the salts of fatty acids), cationic (e.g. tetra alkyl ammonium salts), and non-ionic (e.g. Triton X and Brij series).

### 3. Solvents

A great number of solvents have been used both in the laboratory and in the industry such as chloroform, toluene, amylacetate, and ethylacetate etc. These solvents work by permeabilizing cells thus allowing soluble protein release. It probably acts by dissolving hydrophobic components in the wall, such as the inner membrane phospholipids. Results were highly dependent on the solvent concentration, cell concentration, and the temperature. Although solvents can be applied inexpensively in almost any scale, many enzymes are denatured in their presence. Moreover, there are hazards associated with the handling of large volumes of inflammable components.

### 4. Hydroxide and Hypochlorite

Alkaline lysis is saponification of the lipids in the cell wall. It is and extremely harsh but effective technique if the product of interest is resistant to degradation at high pH. The use of alkali to lyse bacteria has considerable potential for application on a large scale such as the isolation of polyhydroxybutyrate (PHB) from *Alcaligenes eutrophus*, and L-asparaginase from *Eswinia carotovora* etc. The advantages of this technique are inexpensive and can be applied easily in almost any scale of operation. Addition, it found that no viable cells remain in the process liquor. However, the concentration of NaOH required will destroy many biological activities and lead to denaturation or degradation of protein.

### 3.2.1.3 Enzymatic Disruption

As shown in Figure 3-2, there are three enzymatic methods: autolysis, phage lysis and lysis by the addition of foreign lytic enzymes.

#### 1. Autolysis

The process relies on the production of lytic enzymes by the host that degrade the cell wall thus increasing its porosity and eventually causing lysis. It is often induced by mild chemical or physical treatments such as solvent shock, pH shock, and thermal shock. It is affected by a large number of variables, making generalization and extrapolation to new systems difficult (Middelberg, 1995).

#### 2. Phage lysis

This lysis technique causes by addition of phage into cell suspension such as the disruption of *E. coli* by phage using bacteriophage T4. However, phage disruption is generally unattractive at industrial scale due to the possibility of residual phage leading to premature lysis in subsequent batches and cellular contents may be significantly altered.

#### 3. Foreign lytic enzymes.

The addition of foreign lytic enzymes may also be used to affect protein release. Essentially, lytic enzymes attack the cell wall, degrading it from without, eventually leading to cell lysis and intracellular protein release. Enzymes are highly specific for certain substrates and consequently different enzymes are required to effect intracellular product release from different organisms.

In all cases, enzymatic lysis has the major advantages that it is highly specific action of the enzymes involved and the mild conditions under which lysis occurs. Most wall lytic proteases are very specific with little or no activity toward intracellular proteins. This can lead to purification of the product concurrently with release, and opens the opportunity for gentle, selective methods of disruption to be developed. At present, enzymatic cell lysis is restricted by the cost and availability of the enzyme, which is lost into

the extract. An important application of a cell lytic enzyme system is control of microbial contamination for preservation of food.



สถาบันวิทยบริการ  
จุฬาลงกรณ์มหาวิทยาลัย

### 3.2.2 Mechanical Disruption

In recent years mechanical devices for cell disruption have been widely investigated. A typical process flow diagram, shown in Figure 3-3, illustrates the basic engineering and placement of mechanically cells disruption equipment. Desired cells are harvested in the fermenter and then separated by centrifugation or ultrafiltration. The cell concentrate is cooled by a heat exchanger and stored in a surge vessel. The cells are pumped continuously to mechanical cell disruption unit. Homogenate is cooled, then recirculated or sent for further processing. It is essential to cool the homogenate to remove heat that is generated by the dissipation of mechanical energy. It must be noted that heat removal is a common feature for any lytic system and is necessary to prevent denaturation of biological materials.

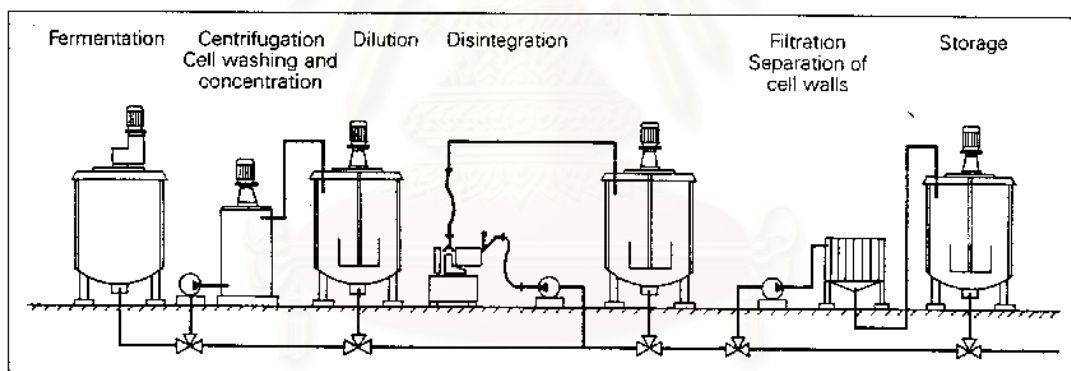


Figure 3-3. Typical process flow diagram of mechanically cells disintegration.

(Redrawn from [www.wab.com](http://www.wab.com))

It is well known that two mechanical technologies disruption have dominated the market; (I) bead mill, and (II) homogenization because of they are applicable to all type of cells. The detail of those will be described in follows.

## 1. Bead mill

Bead mill is currently preferred for large-scale cell disruption. This machine is originally developed for the comminution of pigments for the printing industry, requiring dispersion of solids into micrometer-sized particles with rather narrow size distribution (Schutte and Kula, 1990). In biotechnology, these mills are used in an adapted form for cell disruption, which is regarded as one of the most efficient techniques for physical cell rupture.

Mechanism of cell disruption in bead mill is brought about the combined forces of cavitation, shear force generated from the differential velocity of stream layer of glass beads, grinding between the beads and direct collision with the beads.

Limon-Lason and coworker (1979), a team of investigators examined batch and continuous disruption of bakers' yeast in laboratory and pilot scale bead mills and observed first-order kinetic process either batch and continuous operation. In the batch operation, the rate of protein release is directly proportional to the amount of unreleased protein as follows

$$dR/dt = k(R_m - R) \quad (3-1)$$

where  $R$  is the weight of protein released per unit weight of packed yeast,  $R_m$  is the maximum measured protein release,  $k$  is the disruption rate constant. Integration of equation (3) for  $t = 0$  and  $t = t$  (batch time) yields:

$$\ln[R_m / (R_m - R)] = \ln D = kt \quad (3-2)$$

where  $D$  is the reciprocal of the fraction of unreleased protein.

For continuous disruption, first-order kinetics held, and  $D$  can be related to the nature of mixing in the mill expressed in terms of a continuous stirred tank reactor (CSTR) in-series model, thus:

$$D = R_m / (R_m - R) = [1 + (k \times \tau / j)]^j \quad (3-3)$$

where  $\tau$  is the mean residence time in the mill (total volume of the mill,  $V$ , divided by the total throughput  $q$ ) and  $j$  is the number of CSTRs. The values of  $j$  were obtained experimentally from residence time distribution studies.

The disruption rate constant,  $k$ , is known to be a function of several operating parameters, such as, agitator speed, feed rate of suspension, bead size bead loading, temperature, equipment design, and cell concentration. Influence of those on the performance of cell disruption will be discussed in below.

a) Influence of agitator speed

Generally, increasing the agitator speed induced high shear force generation, which leads to the large of cell lysis. At the same time, the erosion of glass beads, the temperature and the power consumption also increase. So, it is necessary to analyze the efficiency of the cell disruption as a function of the agitator speed. The working range of agitator speed lies between 5 and 15 m/s, and more commonly between 8 and 10 m/s. Below these values, lysis is slow and inefficient; at higher values heat generation is excessive. (Millis J. R., 1997)

b) Influence of feed rate of suspension

The feed flow rate of cell suspension concerns the residence time distribution within the mill. Generally, cell disruption is not a simple function of residence time. The cell disruption in the mill is only slightly influenced by the feed flow rate as the first order rate constant of the process constantly decreases with flow rate (Kula and Schutt, 1983). Therefore, a high feed rate should be chosen for economic reasons.



c) Influence of equipment design

The major variables in the design of bead mill lie in geometry of mill, the agitator disk design, the arrangement of the disk on the drive shaft, and the means of separating the homogenate from the media.

Various designs of bead mills have been used for microbial cell disruption. The mill can be arranged in either a vertical or horizontal configuration. Generally, it is comprised of a cylindrical chamber equipped with a motor-driven central shaft supporting a collection of off-centered discs or other agitating element as shown in Figure 3-4 and 3-5. The chamber is filled to the desired level with glass beads, which provide the grinding action. In vertical units, the charge of grinding beads is retained in the chamber by a sieve plate covering the bottom inlet (Figure 3-4), while in horizontal units the fluid entry is above the level of the beads in the chamber and no retention mechanism is required (Figure 3-5). At the fluid exit port, three different types of bead retention systems have been employed: a sieve plate, a disc rotating in very close proximity to a plate with a central exit port in it and a vibrating slot. The latter two types of bead retention devices are believed to reduce fouling problems. Cell disintegration is mostly carried out in high-speed agitator bead mills with horizontally positioned. An advantage of the horizontal as compared to the vertical position of the grinding chamber is the almost complete elimination of gravity forces as a parameter of milling process (Kula and Schutte, 1980).

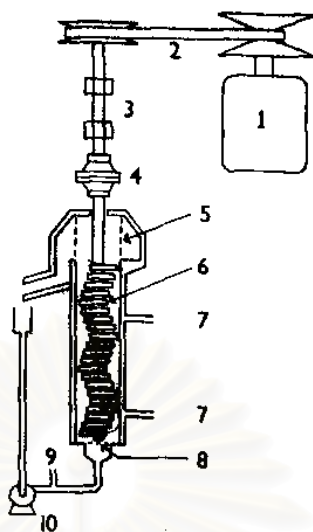


Figure 3-4. Simplified drawing of the Netzsch agitator mill system. (1) drive motor; (2) variable v-belt drive; (3) bearings; (4) Agitator coupling; (5) cylindrical sieve plate; (6) agitator discs; (7) temperature jacket inlet and outlet; (8) bottom sieve plate; (9) temperature measuring pocket; (10) recirculating pump.

(Redrawn from Carrie et al, J. Biotechnol. Bioeng. 1972, 14, p.726)

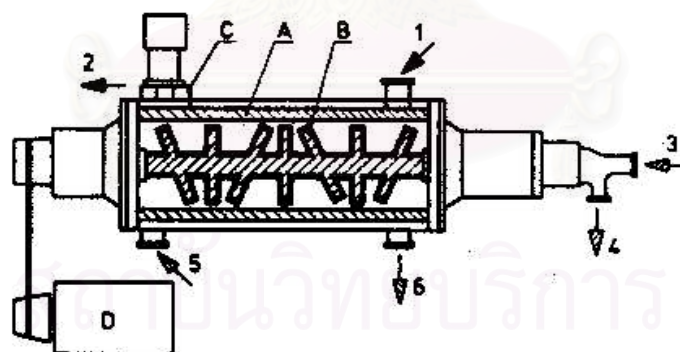


Figure 3-5. Simplified drawing of the Netzsch model LM-20 mill; (A) cylindrical grinding vessel with cooling jacket; (B) agitator with cooled shaft and disks; (C) annular vibrating slot separator, (D) variable speed drive motor; (1) product inlet; (2) product outlet; (3) agitator cooling inlet; (4) agitator cooling outlet; (5) vessel cooling inlet; (6) vessel cooling outlet

(Redrawn from Rehacek and Schaefer, J. Biotechnol. Bioeng. 1977, 19, p.1523)

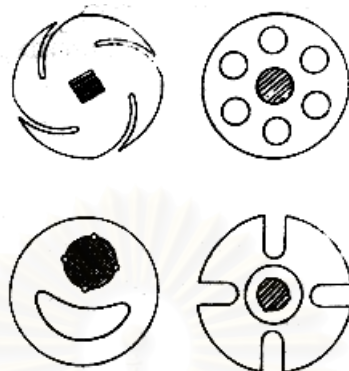


Figure 3-6. Some design of agitator disks

(Redrawn from Schutte and Kula, *Biotechnol. App. Biochem.* 1990, 12, p.610)

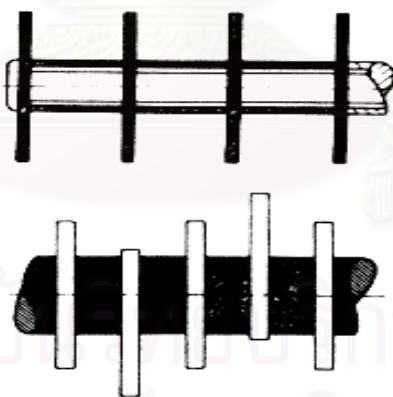


Figure 3-7. Centric and eccentric arrangement of agitator disks on the drive shaft. (Redrawn from Schutte and Kula, *Biotechnol. App. Biochem.* 1990, 12, p.610)

The agitator disk design and the arrangement of agitator disks on the drive shaft are shown in Figure 3-6 and 3-7, respectively. Notched or slotted disks are designed to act like a centrifugal pump, imparting movement on the beads. Disks may be mounted either concentrically or eccentrically on the drive shaft to prevent uneven compaction of the grinding media. Schutte and Kula (1990) reported best results with both *Saccharomyces spp* and *Brevibacterium spp* using notched, cone-shaped disks mounted concentrically on the drive shaft.

All bead mills have a device to let the ruptured cell slurry pass and retain the small grinding beads in the chamber, which design of separators may also influence operation. Three basic bead retention devices are shown in Figure 3-8. Common fixed or adjustable microslit separators are used mainly in mills with a working volume of up to 20 liters. The new types of media separators, such as, the dynamic cartridge media separator and the hydrodynamically shaped screen cartridge, are used especially for pilot, because they have an open area 3-10 times higher than a microslit, which avoids a build up in back pressure when the feed rate is increased.

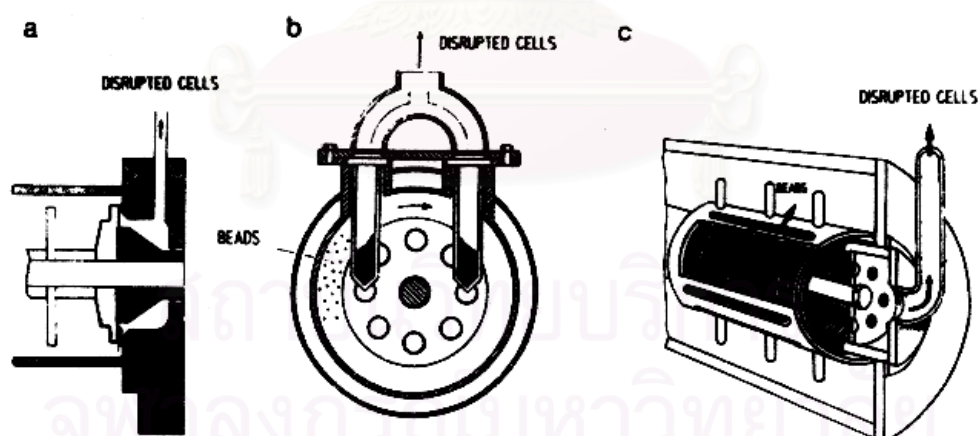


Figure 3-8. Different types of bead separators: (a) microslit separator; (b) dynamic cartridge media separator; (c) hydrodynamically shaped screen cartridge.

(Redrawn from Schutte and Kula, *Biotechnol. App. Biochem.* 1990, 12, p.613)

d) Influence of bead size

Lead-free glass or porcelain beads are the medium of choice for most biotechnology applications because of their inertness, abrasion resistance and low cost. Bead diameters are available in the range of 0.2-1.5 mm. Smaller sized beads, for example 0.2-0.5 mm, are used efficiently in smaller mills and are often selected for bacterial cells. Smaller beads generate more impacts but consume less energy. They also require very narrow slots or screen for separating the grinding media from the homogenate at the exit of the mill. Slot diameters are restricted to approximately one-third-bead diameter. Also, smaller beads (less than 0.8 mm) may float, thereby reducing effectiveness.

For use on larger cells and in larger mills, bead sizes of 0.5-1.5 mm are preferred. Above 1.5 mm, effectiveness drops rapidly. The larger beads allow larger separation dimensions hence higher flows. Schutte (1990) reported that larger beads (> 1 mm) are preferred for periplasmic enzymes or proteins, which do not require complete disintegration of the cell, whereas smaller beads are preferred for cytoplasmic enzymes or proteins. Large beads also suffer less reduction in diameter from abrasion. Useful lifetimes for beads are 100-200 h for beads less than 0.5 mm but extend to 500-700 h for beads in the range 0.5-1.0 mm. Abrasion increases in low-viscosity fluids.

e) Influence of beads loading

The bead loading is usually expressed as the percentage of the bead volume relative to the free volume of the grinding chamber. The optimal beads loading depends on the size of the glass beads employed. Working with 0.5-mm glass beads, a bead loading of 85% and for 1-mm glass beads approximately 80%, has recommended. At a bead loading below 80%, the efficiency of the cell disruption is inefficient, while at bead loading greater than 90%, the heat generation becomes a problem and the power consumption is markedly increased.

f) Influence of concentration of cell suspension

The efficiency of disruption is not strongly influenced by cell concentration. Generally, the range of 4-20% by dry weight for bacteria (Mogren et al., 1974) and 17-18% for yeast, is considered optimal. The heat generation decreases with decreasing cell concentration while the energy consumption per unit weight is increased.

g) Influence of temperature

The amount of heat generated in the chamber of a bead mill is influenced by the agitator speed and the bead loading. Temperature rising is necessary to be controlled by circulating cooling water or a refrigerant through the jacket due to protein denaturation and/or modification of physical properties of cell suspension such as viscosity (at higher temperatures, reduced viscosity would lead to greater back-mixing). However, temperature exerts a weak influence on the rate constant, with a 20% decrease as the temperature increase from 5-40°C.

## 2. High-pressure homogenizer

The high-pressure homogenizer is adapted for cell disruption from food and pharmaceutical industries like bead milling. Modifications include altering the valve design for optimal cell disruption and increasing the operating pressure. At present, the homogenizer is preferred for the large-scale disruption of non-filamentous organism.

A homogenizer has two vital parts: a positive displacement piston pump and a homogenizer valve. The number of pistons in the high-pressure pump depends on the size of homogenizer. The schematic view of high-pressure homogenizer has been shown in Figure 3-9.

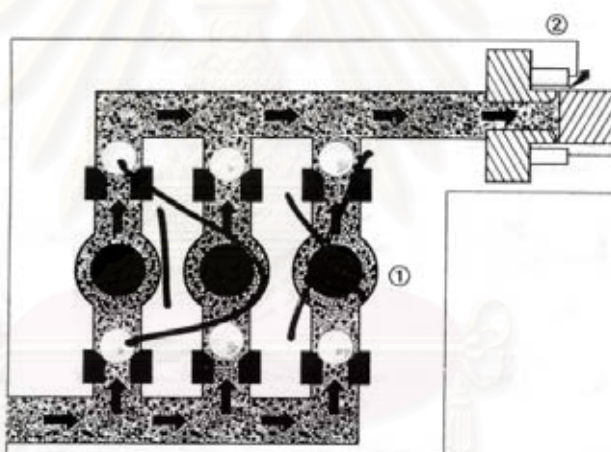


Figure 3-9. Schematic view of high-pressure homogenizer:

(1) positive displacement piston pump; (2) homogenizing valve assembly.

(Redrawn from Schutte and Kula, *Biotech. App. Biochem.* 1990, 12, p. 614.)



In principle of high-pressure homogenizer operation, a piston pump delivers the cell suspension into a valve assembly at high pressure, which pressure is controlled by altering the spring tension on the valve piston either manually or automatically. When the highly pressurized liquid enters the valve at the preset pressure, a rapid change of velocity occurs, generating extremely high hydrodynamic shear as the cell slurry passes through a valve. Disruption results from the combination of shear force and impingement on the valve.

Cell disruption in high-pressure homogenizer is described as first-order kinetics by Hetherington et al, 1971 by the equation:

$$\log[R_m / (R_m - R)] = k \times N \times p^a \quad (3-4)$$

where  $R_m$  = maximum protein release or enzyme activity;  $R$  = measured protein release or enzyme activity after  $N$  passes;  $k$  = rate constant ; and  $N$  = number of passes;  $p$  = operating pressure, and  $a$  = an exponent, which depends on the kind of microorganisms and the conditions under which the cells are grown.

Equation (3-4) shows the variables mainly influence on the cell disruption in high-pressure homogenizer as the operating pressure and the number of passes of cell suspension through the homogenizer. Typically, most applications operate within the range of 500-1000 bar (7250-14500 psi). The maximum allowable operating pressure is often dictated by the mechanical stability of the valve design, which may differ due to design or material of construction.

In addition, the disruption rate constant for high-pressure homogenizer depends on the other parameters such as design of valve unit, concentration of cell suspension, and operating temperature. Details of those will be described below.

a) Influence of valve design

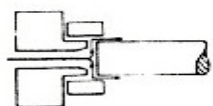
Design and selection of the valve influences shear and impingement force on cell disruption. Designs that have been shown to be effective and versatile include a flat valve, a knife-edge valve (Figure 3-10). Kula and Schutte shown the influence of flat and knife-edge valves on yeast cells disruption (Figure 3-11). Additionally, several authors report that the knife-edge valve being favored for most cell disruption applications.

b) Influence of concentration of cell suspension

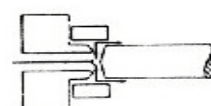
The cell concentration, expressed as percent dry solids, has been found to exert a weak influence on performance of a homogenizer. Several authors have reported little or no influence of yeast concentration over the range of 4-24%.

c) Influence of temperature

The rate of cell disruption increases with temperature. As a rule, the rate at 30°C is approximately double that at 5 °C. However, in selecting the inlet temperature for a homogenizer, must consider both the temperature rise that occurs during processing and the maximum allowable temperature of the product. Homogenization leads to a rapid rise in temperature. Typical values are 2.2-2.4 °C/100 bar. Using a typical operation pressure of 800 bar, a temperature rise of 9.6°C may be expected. The maximum allowable temperature for many proteins is considered to be 30-35°C. Using this value, it becomes necessary to feed cell slurry to the homogenizer at 5-15°C. In order to recover more released proteins, the cooling unit is necessary to prevent the denaturation of biological materials.



(a) flat valve unit



(b) knife-edge valve unit

Figure 3-10. Details of valve seats of the high-pressure homogenizer  
(Redrawn from Middelberg A.P.J. Biotechnol. Adv. 1995, 13, p.521.)

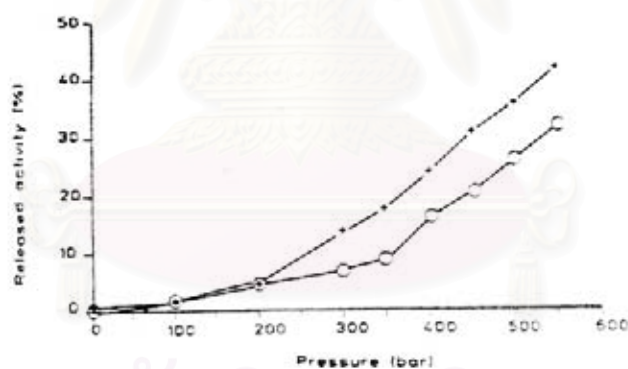


Figure 3-11. Disruption of *Saccharomyces cerevisiae* with a high-pressure homogenizer using different valve units. Symbols: (+) knife-edge valve; (o) flat valve.

Enzyme: Glucose-6-phosphat dehydrogenase.

High-pressure homogenizer: Gaulin M3 (flow rate = 400 l/h, cell concentration = 40% w/v)

(Redrawn from Kula and Schutte, Biotech. Bioeng. 1971, 12, p. 165.)

### 3.3 Disruption Measurement

Generally, the fraction of cells disrupted is determined either by the estimation of the number of whole cells remaining after the disruption process (direct methods) or by a determination of the amount of biological materials released into the suspending medium (indirect methods). Various direct and indirect methods will be briefly reviewed and comparisons between the techniques will be discussed subsequently.

#### 3.3.1 Direct Methods

The simplest measure of disruption may be determined by observational methods such as microscopy with staining to identify a loss of wall integrity. For example, Methylene-blue dye exclusion and gram staining may be employed to differentiate between yeast having intact and damaged walls. However, microscopy is too tedious and time consuming for a large number of samples. To overcome this, Melendres et al. (1992) employed Methylene-blue dye exclusion with automatic cell counting using a hemacytometer.

The volume-fraction (Siddiqi et al, 1997) or number-fraction (Shamlou et al, 1995) of physically destroyed cells can be used to monitor the cell disruption. Shimizu et al (1998) used a Coulter counter to determine the number of whole yeast cells remaining after the disruption process. Particle size analyzers have also been used to measure disruption. Wong et al (1997) has monitored cell disruption with an Elzone particle size analyzer. A clear shift to smaller sizes is observed in the disruption of *E. coli*. Disruption is defined as the ratio of the whole cell peak before and after disruption, which the cell peak is easily differentiated from cellular debris due to the high resolution of the method.

### 3.3.2 Indirect Methods

Indirect methods monitor the release of product from the cell. The most common approach is to measure total soluble protein release in supernatant of sample. Numerous methods have been developed to measure protein content. Generally, there are Kjeldahl method, Biuret method, Lowry method, Bradford method, Bicinchoninic (BCA) method, Ultraviolet (UV) 280 nm Absorption and so on. The effectiveness of the cell disintegration step is defined as a “disintegration rate (DR)” calculated according to equation (3-5).

$$DR = \frac{C(t) - C(0)}{C_{\max} - C(0)} \quad (3-5)$$

where  $C(t)$  is the concentration of soluble protein at a specific time.  $C(0)$  is the concentration of soluble protein before the disruption and  $C_{\max}$  is the maximum possible concentration of soluble protein and corresponds to complete disruption. The maximum protein concentration  $C_{\max}$  changes proportionally to the cell concentration (Bunge et al, 1992).

Engler and Robinson (1979) develop mass balances approach for measuring disruption, using Kjeldahl nitrogen analysis. The fractional release of Kjeldahl responsive material,  $R_k$ , may be estimated using equation (3-6),

$$R_k = \frac{y_0 \times C_N}{C_{NO} \times C_c - (1 - y_0) \times C_N \times M_c \times \left( \frac{\rho_c}{\rho_a} \right)} \quad (3-6)$$

where  $C_N$  is the total Kjeldahl nitrogen content in the supernatant,  $C_{NO}$  is the Kjeldahl nitrogen content of whole cells,  $\rho_a$  is the aqueous-phase density,  $C_c$  is the suspension concentration,  $y_0$  is the aqueous volume fraction of the undisrupted cell sample,  $\rho_c$  is the cell density, and  $M_c$  is the internal moisture content of cells. Engler concludes that the technique is probably less accurate because of several assumptions in the derivation. However, its advantage is relatively insensitive to protein denaturation.

In addition to monitor soluble protein release, estimation of specific enzyme activity in the supernatant is appropriated and then defines a fractional release according to equation (3-5).



สถาบันวิทยบริการ  
จุฬาลงกรณ์มหาวิทยาลัย

## CHAPTER 4

### GAS-LIQUID-SOLID FLUIDIZATION

Fluidization is defined as an operation, in which solid particles have liquid-like behavior due to the balance of the net drag force of the fluid flowing opposite to the net of gravitational force or buoyancy force of the particles. The size of solid particles, which can be fluidized, varies greatly from less than 1  $\mu\text{m}$  to 6 cm. It is generally concluded that particle distributed in sizes between 150  $\mu\text{m}$  and 10  $\mu\text{m}$  are the best for smooth fluidization (least formation of large bubbles). Larger particles cause instability and result in slugging or massive surges. Generally, the classification of fluidized bed operations depends on the number of phase in the system as follows,

1. Two-phase fluidization

Two-phase fluidized bed system consists of two phases as a solid phase and fluid phase (gas or liquid), which solid particles are fluidized in a gas or liquid. Two-phase fluidization may be gas-solid fluidization or liquid-solid fluidization.

2. Three-phase fluidization

Three-phase fluidized bed system consists of a solid phase and two immiscible-liquid, which solid particles are fluidized in two immiscible-fluid. Three-phase fluidization may be gas-liquid-solid fluidization or solid and two immiscible-liquid fluidization.

In recent years, application of three-phase fluidized bed systems for industrial processing has gained considerable attention. These examples of applications of three-phase fluidized be



are grouped according to physical, chemical (petrochemical and electrochemical) and biochemical processing as given in Table 4-1. Especially gas-liquid-solid fluidized bed with a continuous liquid phase in upward flow while gas phase is in discrete bubble cocurrent flow. Because of they have numerous advantage characteristics over the other reactors which will state in later. In this experiment, to apply gas-liquid-solid fluidization system for yeast cells disruption, it is necessary to understand the phenomena, the hydrodynamic, the design parameters of the fluidized bed and its advantages and disadvantages. The detail will be presented below.

**Table 4-1.** Examples of applications of three-phase fluidized bed processing (Fan L. S., 1989)

Physical processing	Chemical processing	Biochemical processing
Drying of calcium carbonate and polyvinylchloride	Production of zinc hydrosulfite	Aerobic biological waste treatment
Dust collection	Methanol fermentation	Production of animal cells
Crystallization	Electrode	Enzyme immobilization
Sand filter cleaning	Coal liquefaction	Ethanol fermentation
Drying of granular material	Coal gasification	Antibiotic production
Lactose granulation	Fuel gas desulfurization	Conversing of sucrose to glucose by plant cells

สถาบันวิทยบริการ  
จุฬาลงกรณ์มหาวิทยาลัย

## 4.1 The Phenomena of Gas-Liquid-Solid Fluidization

As mentioned above, the gas-liquid-solid fluidization is an operation, in which the solid particles layer behave like a fluid. The state of the particle motion in the fluidized bed operation by the upward flowing of the fluid can be subdivided into three basic operating regimes: the fixed bed regime, the expanded bed regime, and the transport regime.

If the fluid is passed upward through a bed of solid particle at a low flow rate, the fluid merely percolates through the void space between stationary particles. This is a *fixed bed regime*, which the drag force on the solid particles induced by the flow of a gas-liquid mixture is smaller than the effective weight of the particles in the systems. When, with an increasing in gas and/or liquid velocity until the drag force counterbalances the effective weight of the particles, the particles move apart and a few vibrate and move in restricted regions. This is the *expanded bed regime*. The bed is in the state of minimum fluidization or incipient fluidization. With a further increase in gas and/or liquid velocity beyond the minimum fluidization velocity until the gas or liquid velocity reaches the terminal velocity of the particle in the gas-liquid medium ( $u_t$ ). At a gas or liquid velocity above  $u_t$ , operation is in the *transport regime*.

## 4.2 The Hydrodynamic of Gas-Liquid-Solid Fluidization

The hydrodynamic behavior of three-phase fluidized bed reflects the complex interactions between the individual phases. The most prominent interaction occurs between the rising gas bubbles and the surrounding liquid-solid medium. Three distinct regions above the gas-liquid distributor are identifiable based on the prevailing physical phenomena: the distributor region, the bulk fluidized bed region, and the free board region. A schematic diagram is shown in Figure 4-1.

The distributor region refers to the region immediately above the gas-liquid distributor where gas spouts may occur. It includes the region from initial bubble formation to the establishment of the final bubble shape. The hydrodynamic behavior in the distributor region inherently depends on the gas-liquid distributor design and the physical properties of the liquid-

solid medium. The bulk fluidized bed region includes the main portion of the fluidized bed. The hydrodynamic behavior in the bulk fluidized bed region varies drastically over large ranges of operating conditions. However, for a given operating condition, there is a minimum axial transport property variation in the region. The freeboard region mainly contains entrained particles from the bulk fluidized bed region. Particle entrainment leads to a solids hold up profile above the fluidized bed surface that decreases axially in a manner similar to that in a gas-solid fluidized bed. The demarcation between the freeboard region and the bulk fluidized bed region is much more distinct for large/heavy particles than for small/light particles.

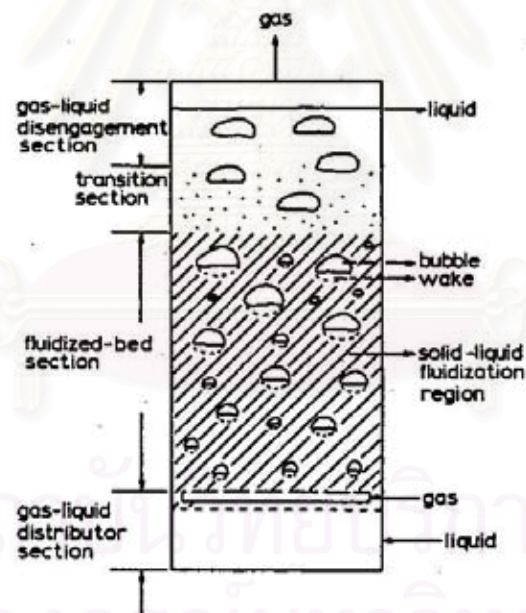


Figure 4-1. Schematic representation of gas-liquid-solid fluidized bed for cocurrent upward gas-liquid-solid systems with liquid as the continuous phase.

(Redrawn from Muroyama and Fan. AIChE J. 1985, 31, 1, p.7)

### 1. Pressure drop and phase holdup

Consider a fluidized bed column is partly filled with a fine granular material as shown schematically in Figure 4-2. The column is open at the top and has a porous plate at the bottom to support the bed and to distribute the flow uniformly over the entire cross section. Fluid is admitted below the distributor plate at a low flow rate and passes upward through the bed without causing any particle motion. If the particles are quite small, flow in the channels between the particles will be laminar and the pressure drop across the bed will be proportional to the superficial velocity. As the velocity is gradually increased, the pressure drop increases, but the particles do not move and the bed height remains the same. At a certain velocity, the pressure drop across the bed counterbalances the force of gravity on the particles or the weight of the bed, and any further increase in velocity causes the particles to move. This is point A on the graph. Sometimes the bed expands slightly with the grains still in contact, since just a slight increase in porosity,  $\epsilon$  can offset an increase of several percent in superficial velocity and keep pressure drop,  $\Delta P$  constant. With a further increase in velocity, the particles become separated enough to move about in the bed, and true fluidization begins (point B).

Once the bed is fluidized, the pressure drop across the bed becomes constant, but the bed height continues to increase with increasing flow. The bed can be operated at quite high velocities with very little or no loss of solids, since the superficial velocity needed to support a bed of particle is much less than the terminal velocity for individual particles.

If the flow rate to the fluidized bed is gradually reduced, the pressure drop remains constant, and the bed height decreases, following the line BC that is observed for increasing velocities. However, the final bed height may be greater than the initial value for the fixed bed, since solids dumped in a column tend to pack more tightly than solids slowly settling from a fluidized bed state. The pressure drop at low velocities is then less than in the original fixed bed. On starting up again, the pressure drop offsets the weight of the bed at point B, and this point, rather than point A, should be considered to give the minimum fluidization velocity,  $u_{mf}$ . To measure  $u_{mf}$ , the bed should be fluidized vigorously, allowed to settle with the fluid turn off, and

the flow rate increases gradually until the bed starts to expand. More reproducible value of  $u_{mf}$  can sometimes be obtained from the intersection of the graphs of pressure drop in the fixed bed and the fluidized bed.

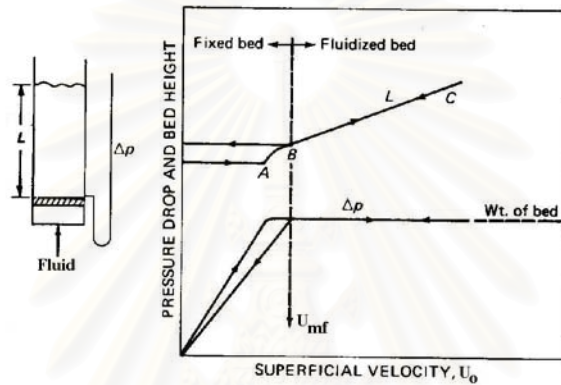


Figure 4-2. Pressure drop and bed height VS superficial velocity for a bed of solid.

(Redrawn from McCabe et al, Unit operation of chemical engineering. 1993, p.165)

The pressure drop through the bed is strongly related to the individual phase holdup in the bed, which the phase holdup is defined as the fraction of the solids, liquid or gas phase to volume of the column. In the fluidized bed section with low solids entrainment rates, the solid holdup,  $\epsilon_s$ , can be expressed as

$$\epsilon_s = \frac{W}{\rho_s SH} \quad (4-1)$$

The following relationship holds among individual holdups:

$$\epsilon_g + \epsilon_l + \epsilon_s = 1 \quad (4-2)$$

Under the steady state condition, the total axial pressure gradient (static pressure gradient) at any cross section in the column represents the total weight of the bed consisting of the three phases per volume as given by

$$-\frac{dP}{dz} = (\epsilon_g \rho_g + \epsilon_l \rho_l + \epsilon_s \rho_s)g \quad (4-3)$$

where  $\epsilon_g, \epsilon_l, \epsilon_s$  = gas, liquid, and solid holdup (-), respectively.

$\rho_g, \rho_l, \rho_s$  = gas, liquid, and solid density ( $\text{kg/m}^3$ ), respectively.

W = weight of solid particle in the bed (kg).

S = cross-section area of empty column (m).

H = effective height of bed expansion (m).

g = gravitational acceleration ( $\text{m/s}^2$ ).

and  $dP/dz$  = static pressure gradient.

The frictional drag on the wall of the column and the acceleration of the gas and liquid flows can be neglected. In equation (4-3), the term  $\epsilon_g \rho_g$  in the right hand side is usually negligibly small compared to the other terms. The evaluation of individual phase holdups based on the pressure gradient method,  $\epsilon_s$  can be directly obtained from equation (4-1) with the height of bed expansion measured experimentally while  $\epsilon_l$  and  $\epsilon_g$  can be calculated from equation (4-2) and (4-3) simultaneously with the experimentally measured static pressure gradient.



## 2. Flow regime

The various flow behaviors of the gas bubbles, which are in a discrete state in a liquid medium, depends on the particle size, the degree of the bed expansion, the liquid velocity and the gas velocity. In the case of gas-liquid-solid fluidization, three flow regimes have received many attention: the bubble coalescing regime or the churn-turbulent regime; the bubble breakup regime, the dispersed bubble, the bubble disintegration regime, or the ideal bubbly flow regime; the slug flow regime.

### a) The bubble coalescing regime or the churn-turbulent regime

At higher gas velocities, the homogeneous gas-in-liquid dispersion cannot be maintained and an unsteady flow pattern with channeling occurs. The bubbles tend to coalesce and both the bubble size and velocity become large and show wide distribution. Coalesced bubbles rise near the column center with high velocity and stir the bed violently. The coalesced bubble regime predominates at low liquid and high gas velocities. The coalesced bubbles take the form of spherical caps with a very mobile and flexible interface. These large bubbles can grow up to a diameter of about 0.15 m.

### b) The bubble breakup regime, the dispersed bubble, the bubble disintegration regime, or the ideal bubbly flow regime

The dispersed bubble regime predominates at high liquid velocities and at low and intermediate gas velocities, which is characterized by almost uniformly sized bubbles with radial distribution.

### c) Slug flow regime

In small diameter columns, at high gas flow rate, the gas bubbles can easily grow to the size of the column diameter. The large bubbles are stabilized by the column wall leading to the formation of bubble slugs. Bubble slugs can be observed in columns of diameters up to 0.15 m.



### 4.3 Agitation in Three-Phase Fluidized Bed

In this section is aimed to provide the useful information of agitator such as design of agitator, flow patterns in agitated column with and without draft tube to apply for yeast cell disruption using gas-liquid-solid fluidized bed with agitator. Details of those are summarized as follow.

#### 4.3.1 Classification of Impellers

Impellers are divided into two classes: those that generate currents parallel with the axis of the impeller shaft and those that generate currents in a tangential or radial direction. The first are called axial-flow impellers, the second radial-flow impellers.

The three main types of impellers are propeller, paddles, and turbines. Each type includes many variations and subtypes. Some of the many designs are shown in Figure 4-3

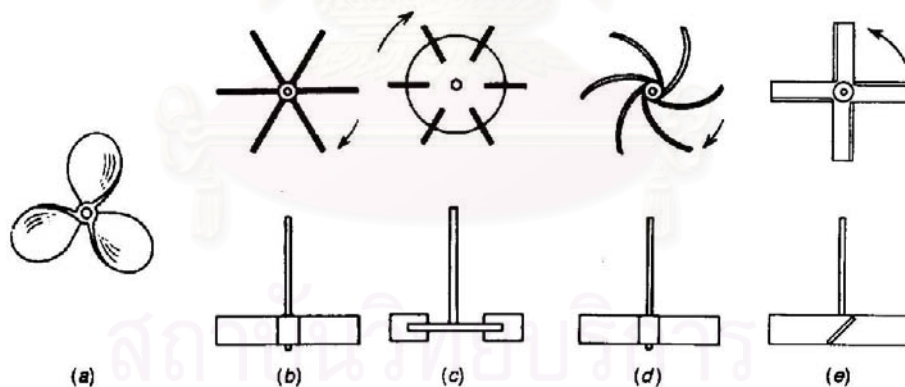


Figure 4-3. Some of many design of mixing impeller

- (a) three-blade marine propeller; (b) open straight-blade turbine; (c) bladed disk turbine;  
 (d) vertical curved-blade turbine; (e) pitched-blade turbine

(Redrawn from McCabe et al, Unit operation of chemical engineering. 1993, p.238)

### 1. Propellers

A propeller is an axial-flow, high-speed impeller for liquids of low viscosity. The flow currents leaving the impeller continue through the liquid in a given direction until deflected by the wall or the floor of the column. The highly turbulent swirling column of liquid leaving the impeller entrains stagnant liquid as it moves along. The propeller blades vigorously cut or shear the liquid. Because of the persistence of the flow currents, propeller agitators are effective in very large column.

### 2. Paddles.

Paddles turn at slow to moderate speeds in the center of a column. They push the liquid radially and tangentially with almost no vertical motion at the impeller unless the blades are pitched. The currents they generate travel outward to the column wall and then either upward or downward. Moreover, at very low speeds a paddle gives mild agitation in an unbaffled column; at higher speed baffles become necessary. Otherwise the liquid is swirled around the column at high speed but with little mixing.

### 3. Turbine

Most of turbines resemble multi-bladed paddle agitators with short blades as turning at high speed on a shaft mounted centrally in the column. Turbines are effective over a very wide range of viscosity. In low-viscosity liquid turbines generate strong currents that persist throughout the column, seeking out and destroying stagnant pockets. Near the impeller in a zone of rapid currents, high turbulence, and intense shear. The principle currents are radial and tangential. The tangential components induce vortexing and swirling, which must be stopped by baffles or by a diffuser ring if the impeller is to be most effective.

In the case of yeast cell disruption using three-phase fluidized bed with agitator, the turbine agitator is chosen because it can promote strong solid-solid impacting, induce the turbulence flow field and intense liquid shear, which will lead to high performance of yeast cell

disruption. Otherwise it has high efficiency for the dispersing a gas through the liquid in the form of small bubble, and promoting heat transfer between the liquid and the surrounding.

#### 4.3.2 Flow Patterns in Agitated Column

The velocity of the fluid at any point in the tank has three components, and the overall flow pattern in the tank depends on the variations in these three-velocity components from point to points. The first velocity component is radial and acts in a direction perpendicular to the shaft of the impeller. The second component is longitudinal and acts in a direction parallel with the shaft. The third component is tangential, or rotational, and acts in a direction tangent to a circular path around the shaft. In the usually case, the shaft is vertical and centrally located in the column, the radial and tangential components are in a horizontal plane and the longitudinal component is vertical. The radial and longitudinal components are useful and provide the flow necessary for the mixing action, while the tangential component is generally disadvantageous due to the tangential flow follows a circular path around the shaft and creates a vortex in the liquid, as shown in Figure 4-4. If solid particles are present, circulatory currents tend to throw the particles to the outside by centrifugal force, from where they move downward and to the center of the tank at the bottom. Instead of mixing, its reverse, the solid concentration occurs at the side of the bottom of the column. In unbaffled column, circulatory flow occur by all types of impellers, whether axial flow or radial flow. If the swirling is strong, the flow pattern in the column is virtually the same regardless of the design of the impeller. At high impeller speeds the vortex may be so deep that it reaches the impellers, and gas from above the liquid is drawn down into charge. Generally this is undesirable.

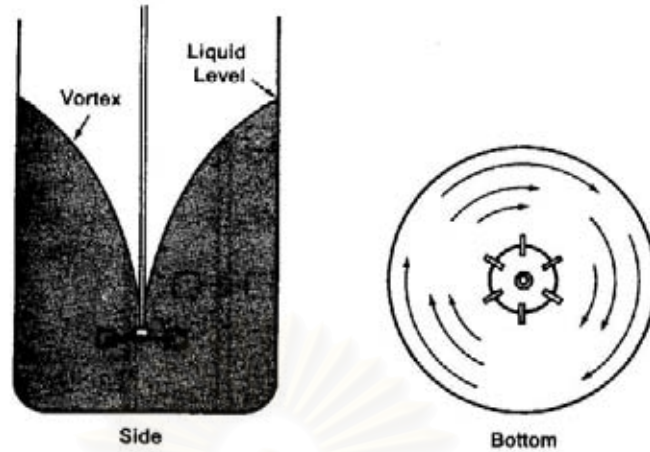


Figure 4-4. Flow pattern of a radial-flow turbine in an unbaffled column  
(Redrawn from McCabe et al, Unit operation of chemical engineering. 1993, p.239)

#### 4.3.2 Draft Tube

Naturally, the return flows to an impeller of any type of impeller from all direction will be occurred. In order to control the direction and velocity of flow to the suction of the impeller are to be controlled, draft tubes are used, as shown in Figure 4-5. These devices may be useful when high shear at the impeller is desired, or where solid particles, which are to be dispersed in liquid, tend to float to the surface of the liquid in the column. Draft tubes for turbines are mounted immediately above the impeller. However, draft tubes add to the fluid friction in the system, and increase the power consumption. In addition, they reduce also the rate of flow, so they are not used if they are required.

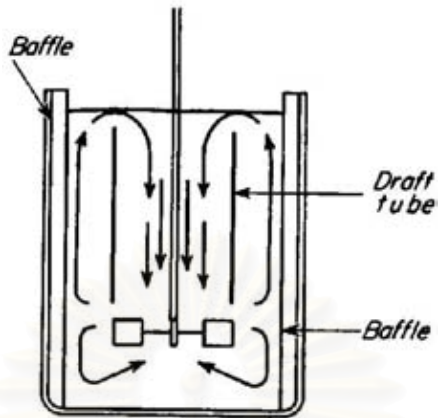


Figure 4-5. Flow pattern of a radial-flow turbine in a baffled column with draft tube.  
(Redrawn from McCabe et al, Unit operation of chemical engineering. 1993, p.392)

สถาบันวิทยบริการ  
จุฬาลงกรณ์มหาวิทยาลัย

#### 4.4 Design Parameters for Gas-Liquid-Solid Fluidization

In principle, the design and fabricate the gas-liquid-solid fluidized bed are necessary to estimate these design parameters as terminal velocity, minimum porosity, the height of bed at minimum fluidization, and minimum fluidization velocity. The equation for these parameters estimation and the standard turbine design will be stated in this section.

##### 1. Terminal velocity, $u_t$

Consider a particle moving through a fluid under the action of an external force. If the external force is the acceleration of gravity,  $g$ , which is constant. Also, the drag force always becomes larger with an increasing in velocity. The particle quickly reaches a constant velocity, which is the maximum attainable under the circumstances, and which is called the *terminal velocity*. The equation for the terminal velocity is

$$u_t = \sqrt{\frac{2g(\rho_p - \rho)m}{A_p \rho_p C_D \rho}} \quad (4-4)$$

where  $g$  = acceleration of gravity ( $m/s^2$ )

$\rho_p$  = density of particle ( $kg/m^3$ )

$\rho$  = density of fluid ( $kg/m^3$ )

$m$  = mass of particle ( $kg$ )

$A_p$  = projected area of particle measured in plane perpendicular to direction of motion of particle (-)

$C_D$  = drag coefficient (-)

If the particles are spheres of diameter,  $D_p$ ,

$$m = \frac{1}{6} \pi D_p^3 \rho_p \quad (4-5)$$

and



$$A_p = \frac{1}{4} \pi D_p^2 \quad (4-6)$$

Substitution of  $m$  and  $A_p$ , the terminal velocity become

$$u_t = \sqrt{\frac{4g(\rho_p - \rho)D_p}{3C_D\rho}} \quad (4-7)$$

In general case, the terminal velocity can be found by trial and error after guessing Reynolds number,  $N_{re, p}$  to get an initial estimate of drag coefficient,  $C_D$ , which the relation between Reynolds number and drag coefficient is shown in Figure 4-6.

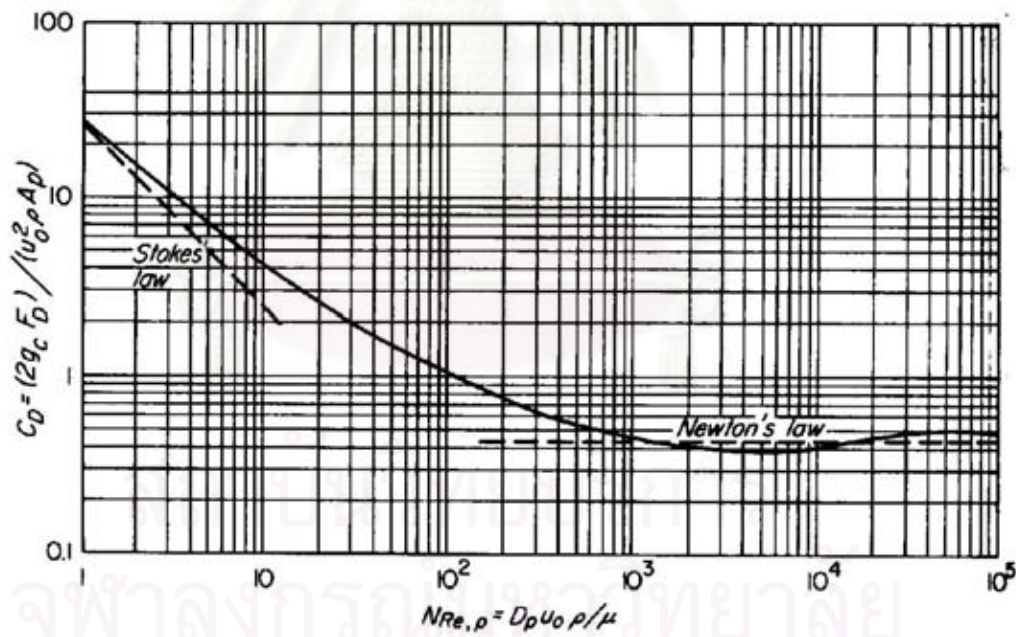


Figure 4-6. The relation between Reynolds number and Drag coefficient  
(Redrawn from McCabe et al, Unit operation of chemical engineering. 1993, p.158)



2. Minimum porosity,  $\epsilon_{mf}$  and the height of bed at minimum fluidization

The minimum porosity is the minimum voidage, which can be determined by passing the fluid up through the bed, and noting the bed height at incipient particle motion or minimum fluidization, The correlation between the minimum porosity and the height of bed at minimum fluidization is

$$\epsilon_{mf} = 1 - \frac{W}{L_{mf} A (\rho_p - \rho)} = \frac{L_{mf} - L_0}{L_{mf}} = 1 - \frac{L_0}{L_{mf}} \quad (4-8)$$

where  $W$  = weight of solids in the bed

$L_0$  = height of bed at fixed bed

$L_{mf}$  = height of bed at minimum fluidization

$A$  = cross section area of column.

3. Minimum fluidization velocity,  $u_{mf}$

Minimum fluidization velocity is the velocity of fluid, which the solid particles move apart and few vibrate. The equation for minimum fluidization velocity (will known as Ergun equation) is

$$\frac{150\mu u_{mf}}{\phi_s^2 D_p^2 \epsilon_{mf}^3} + \frac{1.75\rho u_{mf}^2}{\phi_s D_p \epsilon_{mf}^3} = g(\rho_p - \rho) \quad (4-9)$$

where  $\mu$  = fluid viscosity (kg/ m.s)

$\epsilon_{mf}$  = minimum porosity (-)

$\phi_s$  = sphericity (-)

If  $\epsilon_{mf}$  and the physical properties of fluid and solid particle are given,  $u_{mf}$  can determine by equation (4-9). However, for very small particles, only the laminar flow term of Ergun equation is significant. With  $N_{re,p} < 1$ , the equation for minimum fluidization velocity becomes

$$u_{mf} = \frac{g(\rho_p - \rho) \epsilon_{mf}^3}{150\mu} \phi_s^2 D_p^2 \quad (4-10)$$

Many empirical equations state that  $u_{mf}$  varies with somewhat less than the 2.0 power of the particle size and not quite inversely with the viscosity. Slight deviations from the expected exponents occur because there is some error in neglecting the second term of Ergun equation and because the void fraction  $\epsilon_{mf}$  may change with particle size. For roughly spherical particles,  $\epsilon_{mf}$  generally lies between 0.40 and 0.45, and increases slightly with decreasing particle diameter. For irregular solids, the uncertainty in  $\epsilon_{mf}$  is probably the major error in prediction of  $u_{mf}$ . Usually, equation (4-10) is applied for particle about 30 -300  $\mu\text{m}$  in size.

However, fluidization is also used for particles larger than 1 mm, as in the fluidized bed combustion of coal. In the limit of very large sizes, the laminar flow term becomes negligible, and  $u_{mf}$  varies with the square root of the particle size. The equation for  $N_{re,p} > 10^3$  is

$$u_{mf} = \left[ \frac{\phi_s D_p g(\rho_p - \rho) \epsilon_{mf}^3}{1.75\rho} \right]^{1/2} \quad (4-11)$$

#### 4. Standard turbine design

A turbine agitator of the type shown in Figure 4-7 is commonly used. Typical proportions are

$$D_a / D_t = 1/3$$

$$H/D_t = 1$$

$$J/D_t = 1/12$$

$$E / D_t = 1/3$$

$$W/D_a = 1/5$$

$$L/D_a = 1/4$$

where  $D_a$  = diameter of impeller

$D_t$  = diameter of tank

$E$  = height of impeller above the column floor

$H$  = depth of liquid in column

$J$  = width of baffles

$L$  = length of impeller blades

$W$  = impeller width

The listed “standard” proportions are widely accepted and are the basis of many published correlation of agitator performance.

สถาบันวิทยบริการ  
จุฬาลงกรณ์มหาวิทยาลัย

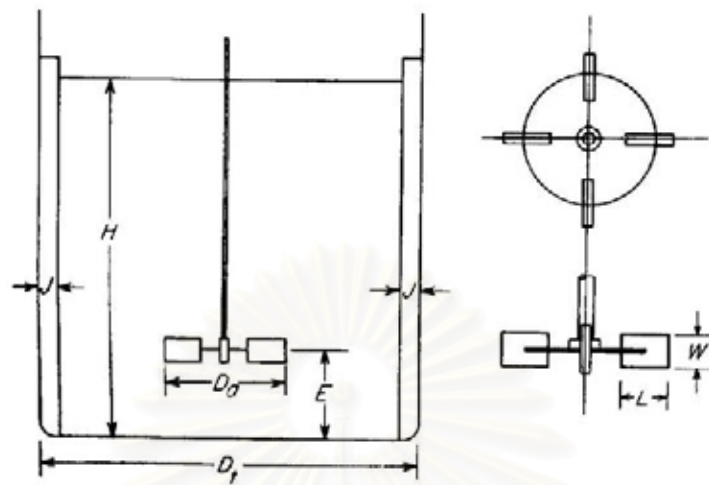


Figure 4-7. Measurement of turbine

(Redrawn from McCabe et al, Unit operation of chemical engineering. 1993, p.158)

สถาบันวิทยบริการ  
จุฬาลงกรณ์มหาวิทยาลัย

#### 4.5 Advantages and Disadvantages of Fluidized Bed

The fluidized bed has desirable and underdesirable characteristics. Its advantages are

1. The smooth, liquid-like flow of particles allows continuous automatically controlled operations with easy handling.
2. The rapid mixing of solids leads to close to isothermal conditions throughout the reactors; hence the operation can be controlled simply and reliably.
3. In addition, the whole vessel of well-mixed solids represents a large thermal flywheel the resists rapid temperature changes, responds slowly to abrupt changes in operating conditions, and gives a large margin of safety in avoiding temperature runaways for highly exothermic reactions.
4. The circulation of solids between two fluidized beds makes it possible to remove (or add) the vast quantities of heat produced (or needed) in large reactors.
5. It is suitable for large-scale operations.
6. Heat and mass transfer rates between fluid and particles are high when compared with other modes of contacting.
7. The rate of heat transfer between a fluidized bed and an immersed object is high; hence heat exchanges within fluidized beds require relatively small surface areas.

Its disadvantages are

1. For bubbling beds of fine particles, the difficult-to-describe flow of gas, with its large deviations from plug flow, represents inefficient contacting. This becomes especially serious when high conversion of gaseous reactant or high selectivity of a reaction intermediate is required.
2. The rapid mixing of solids in the bed leads to nonuniform residence times of solids in the reactor. For continuous treatment of solids, this gives a nonuniform product and poorer performance, especially at high conversion levels. For catalytic reaction, the movement of porous catalyst particles, which continually capture and release reactant gas molecules, contributes to the backmixing of gaseous reactant, thereby reducing yield and performance.

3. Friable solids are pulverized and entrained by the fluid and must be replaced.
4. Erosion of pipes and vessels from abrasion by particles can be serious.
5. For noncatalytic operations at high temperature, the agglomeration and sintering of fine particles can require a lowering in temperature of operations, thereby reducing the reaction rate considerably.



สถาบันวิทยบริการ  
จุฬาลงกรณ์มหาวิทยาลัย

## CHAPTER 5

### EXPERIMENTS

This chapter will be focused on apparatus and experimental procedures of yeast cell disintegration using three-phase fluidized bed with agitator.

#### 5.1 Fluidized Bed Unit

The apparatus used in the experiment is three-phase fluidized bed with agitator, which is shown in Figure 5-1 and 5-2. The fluidized bed unit consists of three sections, namely distribution section, fluidized bed suction, and disengaging section.

The first is the distributing section. A sieve plate, whose hole is about 500  $\mu\text{m}$ , is used as gas and liquid distributor and to support the solid particle. The distribution plate is placed on top of the distribution coaxial cone, which is packed with glass beads of 1 cm in diameter to distribute gas and liquid phase. Liquid will enter at the base of the inner cone, while gas is injected at the side of outer cone.

The second is the fluidized bed section, which consists of outer tube and a coaxial draft tube. The outer tube has height and inner diameter of 24 and 5 inch, respectively. At the wall of outer tube, there are five sampling tubes positioned at fixed axial position. In order to prevent solid leaking, the stainless still screen is soldered at the tip of each sampling tube and the top of the outer tube. The coaxial draft tube, is of 3 inch inner diameter and 16 inch in height. Its base is perforated with hole of 0.9 mm. The perforated part occupies of the total height of the draft tube. One third of volume of the annular of fluidized bed is filled with lead-free glass beads employed as the grinding medium. Their mean diameter and density are of between 0.991 – 1.397  $\mu\text{m}$ , and 2500  $\text{kg/m}^3$ , respectively.



The stainless steel agitator consists of a vertically mounted central shaft with twice impeller of 1 inch height and 2.5 inch length. The base of the impeller is fixed at the central of the fluidized bed column at a height of 2 cm from the bottom.

The third section of the system is the gas-liquid disengaging section, where the liquid is collected and recycled to the circulating tank but the air bubbles will burst and be vented to the atmosphere. During the disintegration process, the upper side of this section is covered to prevent the contamination.

All of fluidized bed unit made of stainless still, which is sterilizable. The details of the fluidized bed unit are summarized in Table 5-1.

**Table 5-1.** The details of fluidized bed system.

Capacity of fluidized bed unit	9 l
Capacity of circulating tank	20 l
Diameter of glass beads	0.991 – 1.397 $\mu\text{m}$
Pack density of glass bead	2500 $\text{kg/m}^3$
Bulk density of glass bead	1550 $\text{kg/m}^3$
Loading of bead by volume	1/3 of volume of the annular of fluidized bed
by weight	3 kg
Speed of impeller	0-3000 rpm
Gas flow rate	0-10 l/min
Liquid flow rate	0-240 l/hr

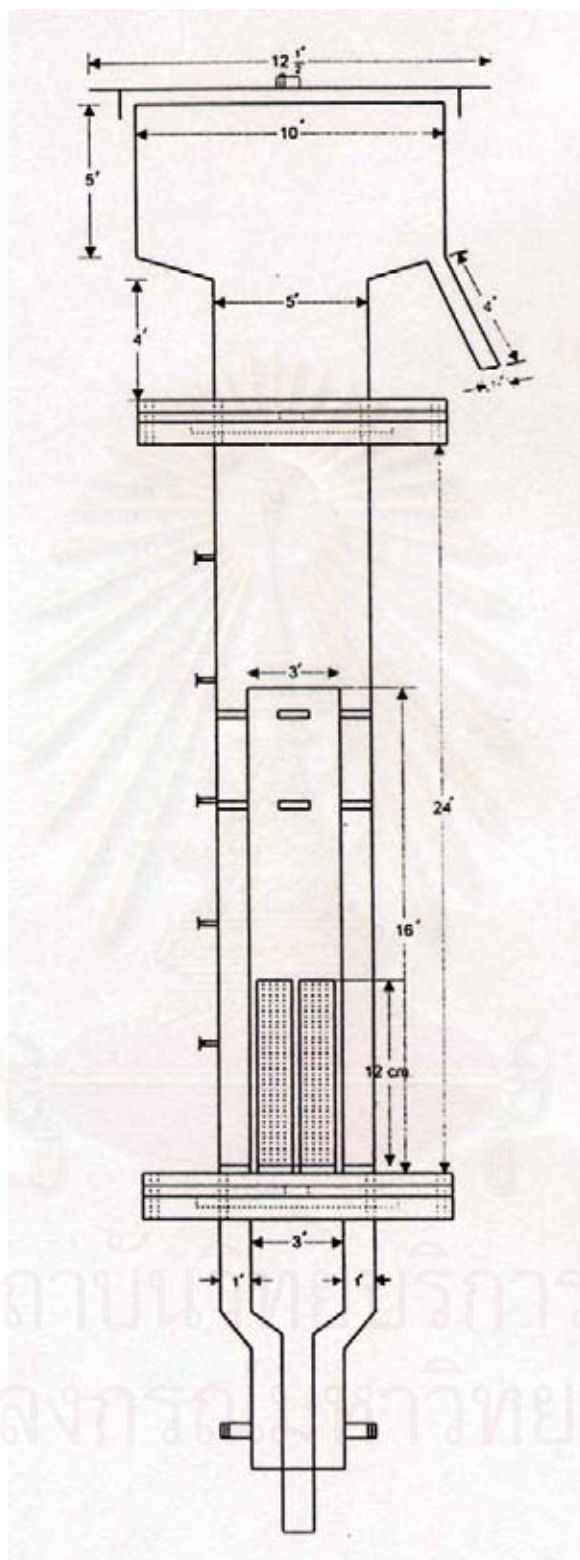


Figure 5-1. Schematic diagram of fluidized bed unit

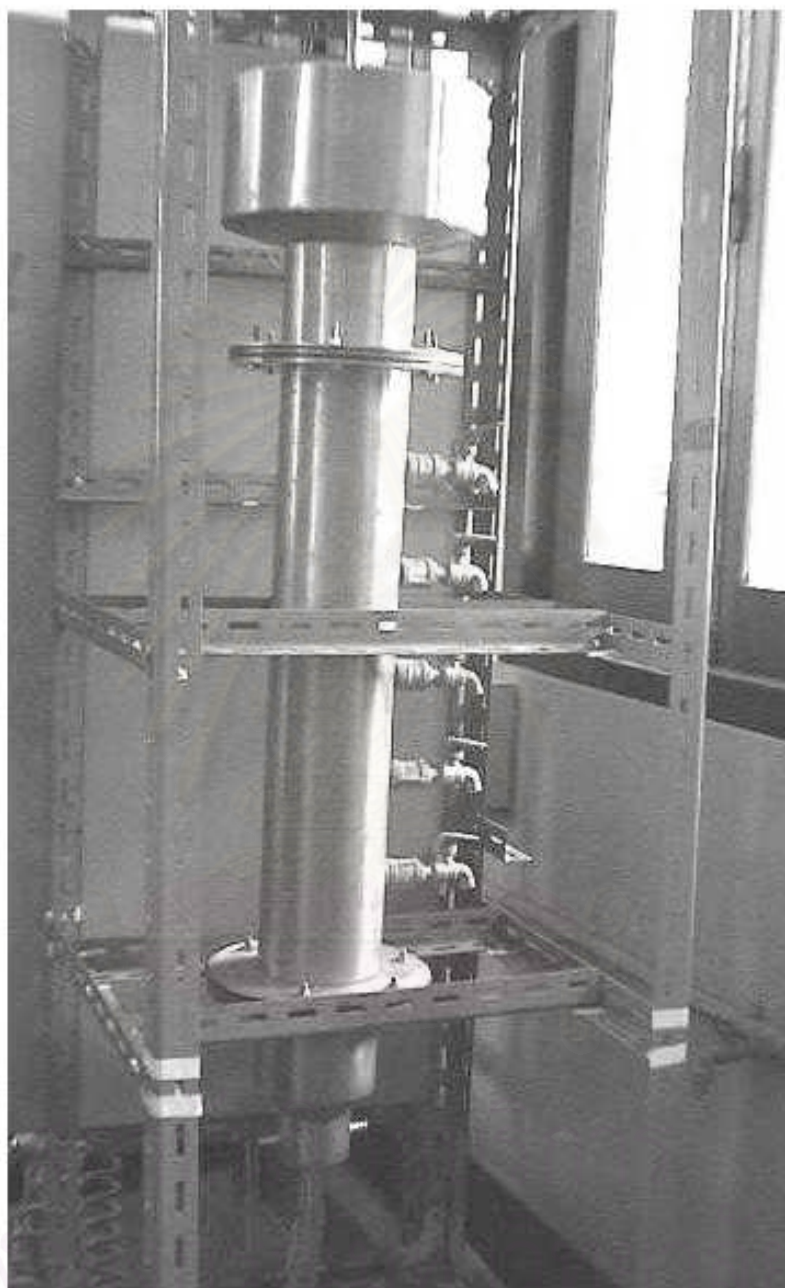


Figure 5-2. Photograph of fluidized bed column

## 5.2 Yeast Suspension Preparation

The yeast cells used in the disruption experiment are dried baker's yeast, *Saccharomyces cerevisiae*, produced commercially by Gistbrocades, Delft, The Netherlands (Kleinig and Middelberg, 1996). The yeast cells are suspended in 0.85% NaCl aqueous solution to prepare the 1 % dry weight/volume yeast concentrations (Morohashi et al., 1997). The yeast suspension is prepared immediately before the experiment at a temperature about 10°C.

### 5.3.1 Characteristic of Yeast Cells Suspension

#### 1. Yeast Cell Size Distribution

Size distribution of yeast whole cells is measured using Beckman Coulter (model LS 230, Coulter Corporation, U.S.A.). The size listing and graph of the yeast cell size distribution after preparation, are shown in Table 5-2 and Figure 5-3, respectively. It expresses the wide range of size distribution between 2.423  $\mu\text{m}$  and 8.944  $\mu\text{m}$ . There is a modal size of approximately 4.047  $\mu\text{m}$ .

#### 2. Yeast Suspension Density

The density of yeast cell suspension at concentration of 1% (w/v) and of water at approximately temperature 18 °C is measured by the Pycnometer and shown in Figure 5-4. The volume of Pycnometer is 25 ml ( $v_0$ ). The following masses are measured: empty Pycnometer ( $m_0$ ), Pycnometer containing yeast suspension sample ( $m_s$ ).

$$\text{Density of yeast suspension, } \rho_1 = \frac{m_s - m_0}{v_0} \quad (5-1)$$

The measurement result shown in Table 5-3 indicates that yeast suspension density is 992.70 kg/m<sup>3</sup> while density of water is 989.90 kg/m<sup>3</sup> at 18 °C.

#### 3. Yeast suspension viscosity

The viscosity of 1% (w/v) yeast concentration and 0.85 % NaCl solution is measured using Viscometer Cannon-Fenke. The result is shown in Table 5-4.

Table 5-2. Size listing of yeast cell distribution

Channel Diameter (Lower) $\mu\text{m}$	Diff. Number %	Channel Diameter (Lower) $\mu\text{m}$	Diff. Number %	Channel Diameter (Lower) $\mu\text{m}$	Diff. Number %
0.375	0	6.761	2	121.8	0
0.412	0	7.421	0.87	133.7	0
0.452	0	8.147	0.21	146.8	0
0.496	0	8.944	0.011	161.2	0
0.545	0	9.819	0	176.8	0
0.598	0	10.78	0	194.2	0
0.657	0	11.83	0	213.2	0
0.721	0	12.99	0	234.1	0
0.791	0	14.26	0	256.8	0
0.869	0	15.65	0	282.1	0
0.953	0	17.18	0	309.6	0
1.047	0	18.86	0	339.8	0
1.149	0	20.7	0	373.1	0
1.261	0	22.73	0	409.6	0
1.385	0	24.95	0	449.7	0
1.52	0	27.38	0	493.6	0
1.669	0	30.07	0	541.9	0
1.832	0	33	0	594.9	0
2.01	0	36.24	0	653	0
2.207	0	39.77	0	716.9	0
2.423	0.33	43.66	0	786.9	0
2.66	3.44	47.93	0	863.9	0
2.92	8.55	52.63	0	948.2	0
3.206	12.3	57.77	0	1041	0
3.519	14.4	63.41	0	1143	0
3.862	14.8	69.62	0	1255	0
4.241	13.5	76.43	0	1377	0
4.656	11.3	83.9	0	1512	0
5.111	8.61	92.09	0	1660	0
5.611	5.98	101.1	0	1822	0
6.158	3.71	111	0	2000	

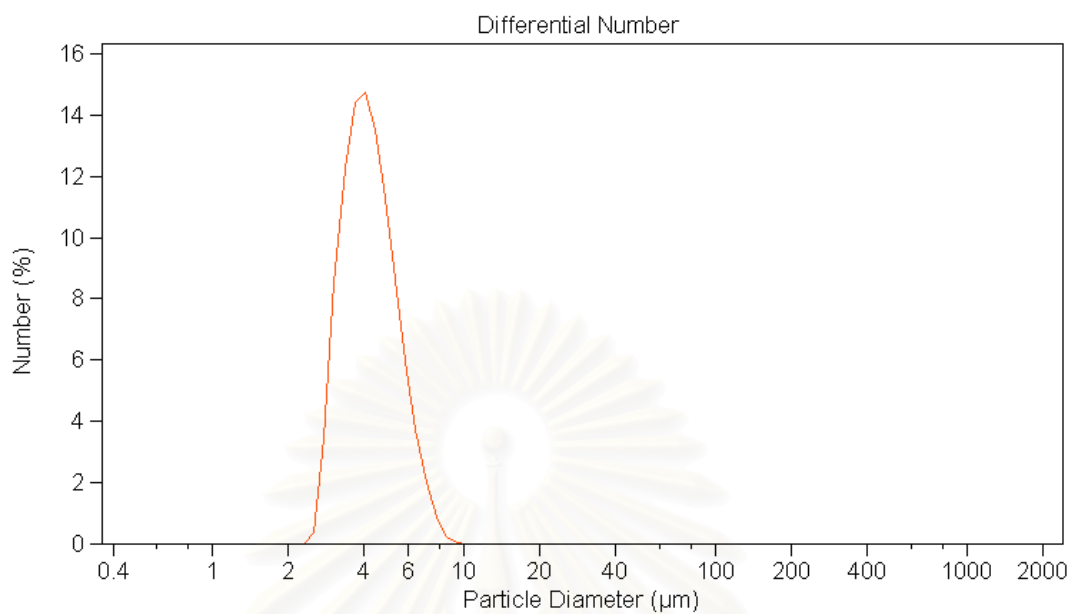


Figure 5-3. Cell size distribution of yeast whole cells



Figure 5-4. Pycnometer



Table 5-3. The result of density measurement using Pycnometer

sample	volume (ml) of			mass (g) of						density (kg/m <sup>3</sup> )
	empty Pycnometer, v <sub>0</sub>			empty Pycnometer, m <sub>0</sub>			Pycnometer containing sample, m <sub>s</sub>			
	1 <sup>st</sup>	2 <sup>nd</sup>	3 <sup>rd</sup>	1 <sup>st</sup>	2 <sup>nd</sup>	3 <sup>rd</sup>	1 <sup>st</sup>	2 <sup>nd</sup>	3 <sup>rd</sup>	
water	25	25	25	16.0046	16.0046	16.0045	40.7067	40.7669	40.7671	989.908
1% (w/v) of yeast suspension	25	25	25	16.0047	16.0045	16.0047	40.7791	40.8435	40.8447	992.7093

Table 5-4. The result of viscosity measurement using Viscometer

sample	% by weight	Capillary No.	Constant Number K	Flow time, t (s)			Hagenbach correction, J	Kinematic viscosity ν = K(t-J), mm <sup>2</sup> /s
				1 <sup>st</sup>	2 <sup>nd</sup>	3 <sup>rd</sup>		
water	100	25	0.00185	517	519	522	0	0.96
1% (w/v) of yeast suspension	0.85	25	0.00185	612	614	620	0	1.03

สถาบันวิทยบริการ  
จุฬาลงกรณ์มหาวิทยาลัย



### 5.3 Preliminary Experiments

It is necessary to understand the role of each elemental mechanism on the yeast cell disruption. Therefore, the objective of this preliminary experiments is mainly to investigate the relationship between each important operating parameters (the speed of impeller, the superficial gas velocity, the superficial liquid velocity and the diameter of the glass beads) and the degree of yeast cell disruption. While a certain operating parameter is taken into account, the remaining parameters will be fix in each experiment. However, some phenomena, such as an increase in temperature of cell suspension will also be investigated.

#### 5.3.1 Study of Influence of Temperature Rising on Yeast Cell Disruption

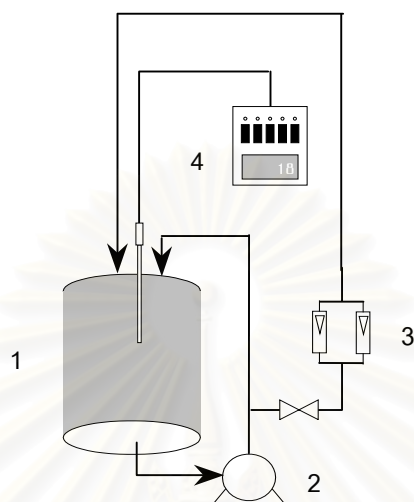
The temperature rising during the disintegration processes can be occurred in the case of the yeast suspension was circulated by pump and/or both of agitation and glass beads presented in the system. So that it is necessary to study the effect of temperature rising on yeast cell disruption. The study takes place over 5 temperatures as 10°C, 24°C, 32°C, 47°C, and 52°C, which 10°C is the temperature of yeast suspension after immediately preparation and 24°C is typically the room temperature. This experiment is carried out air oven to eliminate the shear effect from fluidized bed unit. This procedure is set as follows:

1. Prepare 100 ml of yeast suspension immediately in a beaker before the experiment, which temperature of suspension is 10°C, and take the samples as the reference samples.
2. Place the yeast suspension in air oven and heat until the temperature of suspension reach to desired temperature. The thermometer is put into the yeast suspension to monitor the temperature. Hold at the desired temperature for 10 min.
3. Carefully mix the yeast suspension to allow a representative sample. Take the samples for analytical proposes.

### 5.3.2 Study of Influence of Circulation of Yeast Suspension using Centrifugal Pump on Yeast Cell Disruption

In continuous operation, the yeast suspension is circulated from a storage tank to the fluidized bed unit using the centrifugal pump. The circulation of yeast suspension by pump can cause the cell disruption so that it is necessary to study the effect of pump on cell disruption. This study is carried out under the conditions of 3 flow rates, 80 l/hr, 160 l/hr, and 240 l/hr. The following steps constitute the influence of the pump procedure and the schematic diagram of this experiment shows in Figure 5-5.

1. Fill up the yeast suspension into the circulating tank, which is surrounded with the cooling jacket to maintain the temperature of suspension between 10°C and 24°C during the experiments.
2. Withdrawn the yeast suspension from circulating tank to centrifugal pump.
3. Switch on the pump. The outlet stream from the pump is spilt into two streams: one stream is recycled back immediately to the tank while the other is adjusted the flow rate at the desired values by liquid rotameter before is recycled back to the tank.
4. Take the yeast suspension samples from the second stream at the fixed time interval.



1. Storage Tank 2. Liquid Pump 3. Flow Meters 4. Thermocouple and Temperature Indicator

Figure 5-5. Schematic of the system for study the effect of pump circulation

สถาบันวิทยบริการ  
จุฬาลงกรณ์มหาวิทยาลัย

## 5.4 Disruption Experiments

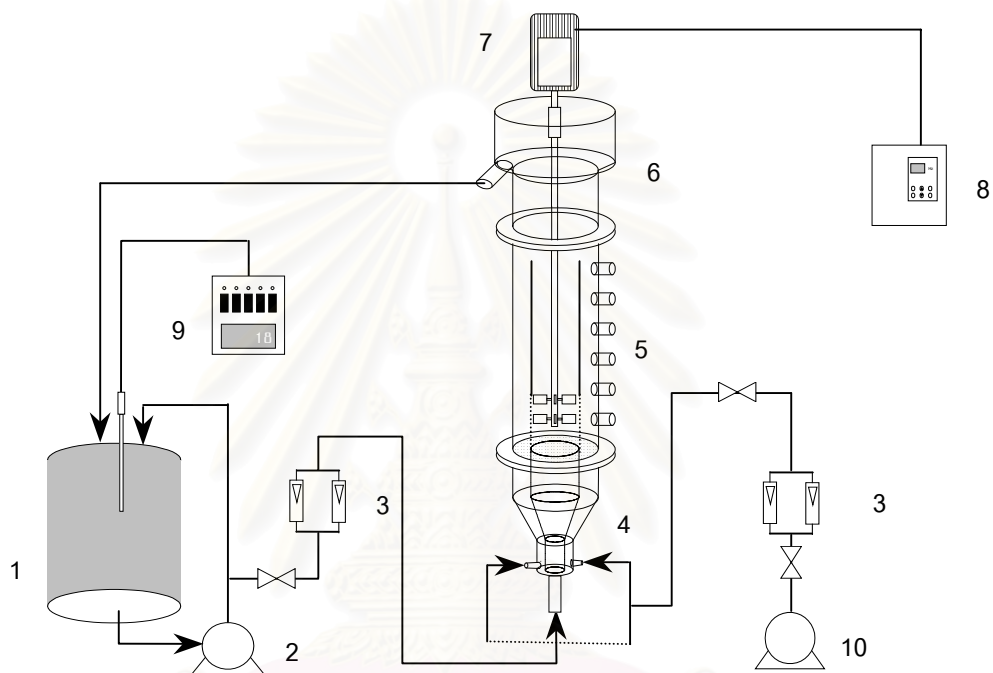
Yeast disintegration is carried out in three-phase fluidized bed unit. Lead-free glass beads, with volume of one-third that of the annular of the fluidized bed section, employed as solid phase. Yeast suspension is used as the major fluidized medium, which is the continuous phase, and air is dispersed into liquid fluidized bed. The schematic diagram of the yeast cell disruption system is shown in Figure 5-6.

### 5.4.1 Experimental Conditions

Four operating parameters are taken into account for investigating their effect on the yeast cell disruption using three-phase fluidized bed with agitator. There are the speed of impeller, superficial gas velocity, superficial liquid velocity and the bead size. The values of variables hold constant during the investigation of each separated variable to study the relationship between those operating variables and degree of yeast cell disruption. The overall of operating conditions of the disruption processes is summarized in Table 5-5.



สถาบันวิทยบริการ  
จุฬาลงกรณ์มหาวิทยาลัย



1. Storage Tank
2. Liquid Pump
3. Flow Meters
4. Distributing Section
5. Fluidized Bed Section
6. Disengaging Section
7. Impeller and Motor
8. Inverter
9. Thermocouple and Temperature Indicator
10. Air Compressor

Figure 5-6. The schematic diagram of the yeast cell disruption

using three-phase fluidized bed with agitation

**Table 5-5.** The operating condition of three-phase fluidized bed system for the study of effect of speed of impeller, superficial gas velocity, superficial liquid velocity, and size of glass beads on the yeast cell disruption

Impeller speed (rpm)	Superficial gas velocity (cm/min)	Superficial liquid velocity (cm/min)	Draft tube (with or without)	Glass beads (with or without)
0, 500, 1500, 2000,3000	0	0	with	without
500,3000	0	0	without	without
0, 500, 1500, 2000,3000	0	0	with	with 1000 $\mu$ m diameter
0	0, 10, 20, 40	0	with	without
0	0, 10, 20, 40	0	with	with 1000 $\mu$ m diameter
0	0	0, 10, 20, 30	with	without
0	0	0, 10, 20, 30	with	with 1000 $\mu$ m diameter
3000	0, 10, 20, 40	0,10, 20, 30	with	with 1000 $\mu$ m diameter
3000	10	10	with	with 2000 $\mu$ m diameter
25	10	10	without	with 1000 $\mu$ m diameter

#### 5.4.2 Experimental Procedure

Three-phase fluidized bed with agitator can operate the batch wise as well as continuous wise. For batch operation, the fluidized bed section, which is attached with cooling jacket, is filled up with yeast suspension before starting each experimental run while the liquid inlet is completely sealed. On the other hands, either fluidized bed section or circulating tank was filled up for continuous run. The yeast suspension is withdrawn from the storage tank, which is surrounded with cooling jacket, to a centrifugal pump. The outlet stream from the pump is split into two streams; the one is recycled back to the tank while the other is used to adjust the flow rate by liquid rotameter and feed to the bottom of the cone of fluidized bed unit. Air from a compressor at ambient temperature and constant pressure is fed at the flow rate of desired values by using air rotameter before it is dispersed into the column through a distributor plate. And the inverter is used to adjust the speed of impeller at the desired values. During the processes, the yeast suspension is withdrawn from the five sample tubes at the fixed time interval for analytical purposes. At each sampling, the same amount of undisrupted cell suspension is added to the tank so as to maintain the initial amount of suspension. Additionally, operating temperature is controlled between 10°C and 24 °C to eliminate the effect of temperature on cell disruption.



## 5.5 Measurement of Cell Size Distribution

To determine the cell size distribution, the laser particle size analyzer model LS 230 (Coulter Corporation, U.S.A.) is used and assumed the yeast sphericity by Fraunhofer's method (Solecki and Heim, 1999).

The distribution of yeast cell diameter at 0 min at any condition shows that initial size distribution of yeast whole cells has a modal size of approximately 4.047  $\mu\text{m}$ . In the disintegration processes, the frequency of the peak at 4.047  $\mu\text{m}$  decreases with an increase in the disruption time. There is a shift toward smaller sizes as cell disruption progresses. It is implied that the peak at 4.047  $\mu\text{m}$  correspond to the size of whole cell remained in the sample. The standardized frequency of 4.047  $\mu\text{m}$  is defined as the ratio of non-disrupted cell at certain time to the frequency at initial time (Shimizu et al, 1998), which can be represented by an equation of the form

$$\begin{aligned} \text{Ratio of non-disrupted cell (-)} \\ &= \frac{\text{average frequency of yeast whole cell at any time}}{\text{average frequency of yeast whole cell at 0 min.}} \end{aligned} \quad (5-2)$$

Then, the effectiveness of the cell disintegration is defined as a “ degree of cell disruption” calculated from following equation

$$\begin{aligned} \text{Degree of cell disruption (\%)} \\ &= (1 - \text{ratio of non-disrupted cell}) \times 100 \end{aligned} \quad (5-3)$$

Equation (5-2) and (5-3) can be employed to determine the effectiveness of the cell rupture in all disruption processes, except the study of the influence of the temperature, which the degree of cell disruption do not change with time. So that, the ratio of non-disrupted cell can be modified as follows.

$$\begin{aligned} &\text{Ratio of non-disrupted cell (-)} \\ &= \frac{\text{average frequency of yeast whole cell at any temperature}}{\text{average frequency of yeast whole cell at } 10^{\circ}\text{C}} \end{aligned} \quad (5-4)$$

where the temperature at  $10^{\circ}\text{C}$  is the temperature of yeast suspension after immediately preparation.

## 5.6 Measurement of Crude Soluble Protein Released Content

The determination of crude soluble protein released from the yeast cells is accomplished by the Kjeldahl method (Tecator Kjeldahl (KD-02)). Principle and procedure of Kjeldahl method are described below.

### 5.6.1 Principle of Kjeldahl Method

In Kjeldahl procedure, proteins and other organic food components in samples are digested with sulfuric acid in the presence of catalysts. The total organic nitrogen is converted to ammonium sulfate. The digest is neutralized and distilled into a boric acid solution. The borate anions formed are titrated with standardized acid, which is converted to nitrogen in the sample. The result of the analysis represents the *crude protein content* of the food since nitrogen also comes from non-protein component.

### 5.6.2 Procedure of Kjeldahl Method

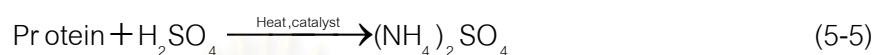
#### 1. Sample preparation

In the case of the determination of protein in the feed stock, yeast suspension before passing through the fluidized bed disruption is homogenized and mixed carefully to allow a representative sample of about 1 ml to be taken.

In the case of the determination of protein in the supernatant obtained after passed the disintegration processes, samples of disrupted cell suspension are centrifuged at 3000 g for 1 h using a refrigerated centrifuge (Beckman Co. Ltd.). Then, yeast suspension is separated into two fractions as debris and supernatant. Finally, 1 ml of the supernatant sample is taken to assay in the next step.

## 2. Digestion

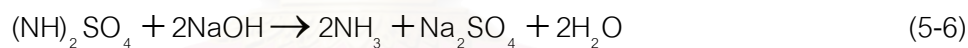
Place sample (accurately volume) in Kjeldahl flask. Add acid and catalyst; digest until clear to get complete breakdown of all organic matter. It is necessary to aware that nonvolatile ammonium sulfate is formed from the reaction of nitrogen and sulfuric acid.



During digestion, protein nitrogen is liberated to form ammonium ions; sulfuric acid oxidizes organic matter and combines with ammonium formed; carbon and hydrogen elements are converted to carbon dioxide and water.

## 3. Neutralization and Distillation

The digest is diluted with water. Alkali containing sodium thiosulfate is added to neutralize the sulfuric acid. The ammonia formed is distilled into a boric acid solution containing the indicators; methylene blue and methyl red



## 4. Titration

Borate anion (proportional to the amount of nitrogen) is titrated with standardized HCl.



## 5. Calculations

Moles HCl = Mole  $\text{NH}_3$  = Moles N in the samples

A reagent blank should be run to subtract reagent nitrogen from the sample nitrogen.

$$\% \text{ N (\% g/ml)} = \text{N HCl} \times \frac{\text{Corrected acid volume}}{\text{ml of sample}} \times \frac{14 \text{gN}}{\text{mole}} \times 100 \quad (5-9)$$

where N HCl = Normality of HCl, in moles/ 1000 ml

Corrected acid volume = (ml of std. acid for sample) – (ml of std. acid for blank)

14 = atomic weight of nitrogen

A factor is use to convert percent N to percent crude protein. Most proteins contain 16 percent N, so the conversion factor is 6.25 (100/16 = 6.25) (Cunningham et al, 1975; Engler and Robinson, 1979).

$$\% \text{ N} \times 6.25 = \% \text{ protein} \quad (5-10)$$

In this experiment, the ratio of protein after pass through the fluidized bed is defined as follows.

Ratio of protein content in the supernatant

$$= \frac{\% \text{ protein in supernatant after pass through the disintegration processes}}{\% \text{ protein in feed stock}} \quad (5-11)$$

สถาบันวิทยบริการ  
จุฬาลงกรณ์มหาวิทยาลัย

## 5.7 Microscopic Observation

Cell disruption is demonstrated qualitatively by microscopy (Microscope model B071 of Olympus, Japan). Consideration of the morphology of yeast cells at the magnification of 400. The number of sample at least 10 samples is photographed before and after being processed through the fluidized bed.



สถาบันวิทยบริการ  
จุฬาลงกรณ์มหาวิทยาลัย

## CHAPTER 6

### RESULTS AND DISCUSSIONS

In this study, for the disruption of baker's yeast cells (*Saccharomyces cerevisiae*) to recover useful intracellular proteins, a three phase fluidized bed with agitator is employed as a novel type of cell disrupter. The three-phase system mentioned here consists of yeast suspension, air bubble and glass beads as liquid, gas and solid phase, respectively. The liquid is flowed continuously while the gas is introduced as discrete bubbles. The flow of liquid and gas is cocurrent upward, and the solids are in non-stationary state. It is expected that cell disruption can take place based on shear forces exerted by liquid flow through the pinholes of draft tube installed in the column fluidized bed and by impact or shear exerted by glass beads. In addition, the interaction between gas bubbles and yeast cells is also expected to affect the cell disruption.

So far, it has been found that there are a few literatures on the application of gas-liquid-solid fluidized bed with agitator as cell disrupting equipment. In preliminary experiments, we attempt to expose the effect of each operating variable, which will provide influence on the cell disruption phenomena. These operating variables are operating temperature, the presence of coaxial draft tube, whose the lower part consists of perforated holes of 0.9 mm, agitator speed, bead size, superficial gas velocity, and superficial liquid velocity.

## 6.1 Influence of Preliminary Parameters on Yeast Cell Disruption

### 6.1.1 Influence of the temperature rising on yeast cell disruption.

In the case of presence either agitation or glass beads and/or yeast suspension is circulated by pump, the temperature rises occurred during the disintegration progresses. To remove heat generated, the cooling jacket around the fluidized bed column and circulating tank are necessary for batch and continuous processes because of the heat removal is a common feature for any lytic system and prevents denaturation of biological materials (Millis, 1997).

In these experiments, the mixture of ice, water, and salt is used to control the temperature of suspension circulated with system. However, it can not sufficiently remove the heat so that it is necessary to determine the effect of temperature on cell disruption during the processes. The study is carried out talk a range of over 5 temperatures (10, 28, 32, 47, and 52°C). The result (Figure 6-1) shows that no significant change of yeast cell size distribution is observed over the temperature 10 to 28 °C ranges. In addition, the result shows that there is no difference of crude soluble protein content in supernatant before and after being treat at 10 °C and 28 °C. When temperature is higher than 28 °C, yeast cell size distribution shifts toward smaller size. This means that cell disruption can take place with an increase in temperature between 32 – 52°C.

The morphology of yeast cells at any temperature using the microscope observation at magnification of 400 illustrates in Figure 6-2. The temperature higher than 28 °C, it was found that the yeast cells started to break down and cell debris was observed compared with the yeast cells, which were prepared at temperature of 10 °C. However, temperature lowers than 28°C gave rise to no significant effect on cell shape and no occurrence of cell debris was observed. The effect of temperature on yeast cell disruption was confirmed by the results using laser particle size analyzer.



It is concluded that the temperature exerted only weak effect on the cell disruption between 10 – 28 °C. This temperature effect on yeast cell disruption is in good agreement with that respected by Currie et al (1972) and Limon-Lason et al (1979). Undoubtedly, in all other disruption experiments are carried out at the temperature ranging from 10 - 24 °C to avoid the effect of temperature on cell disruption.

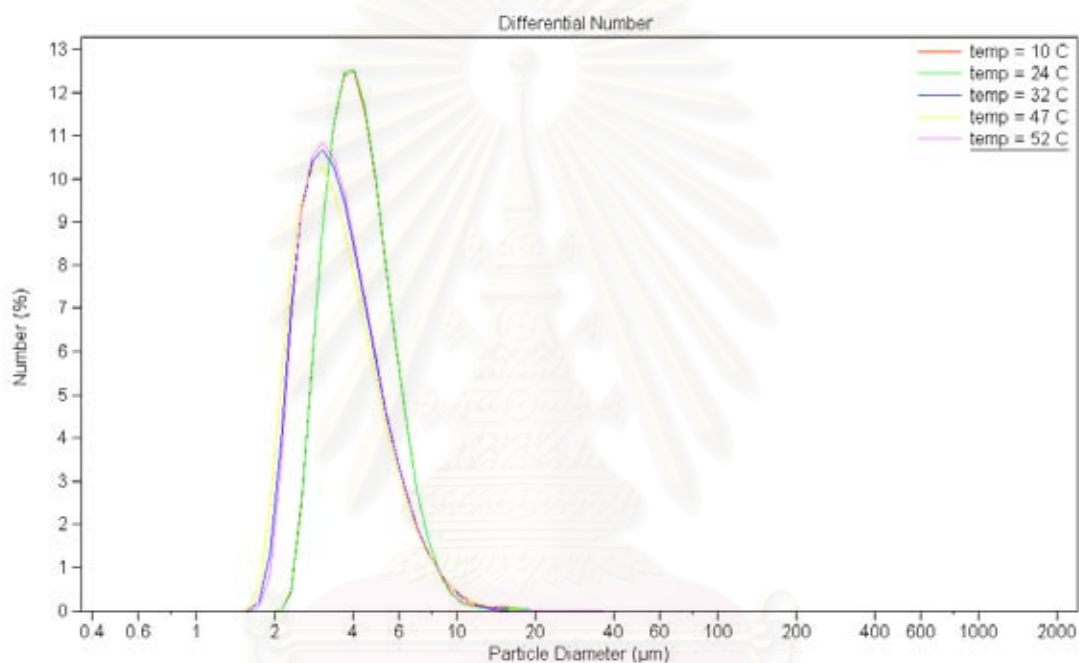
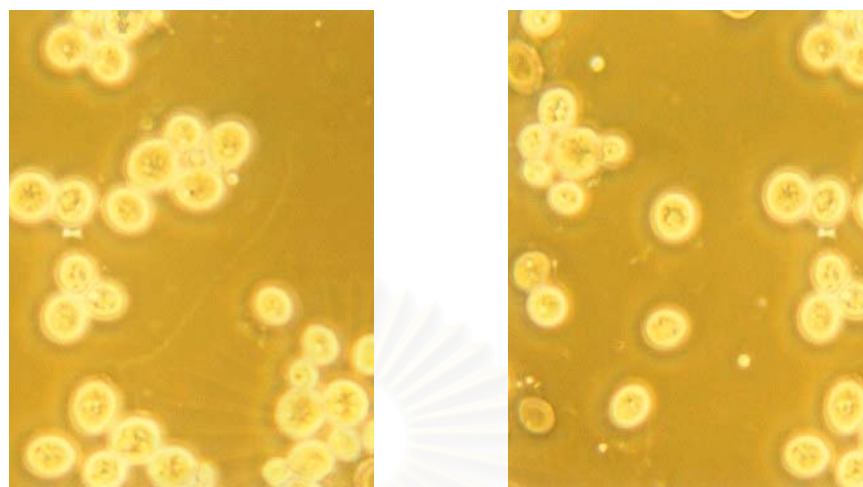
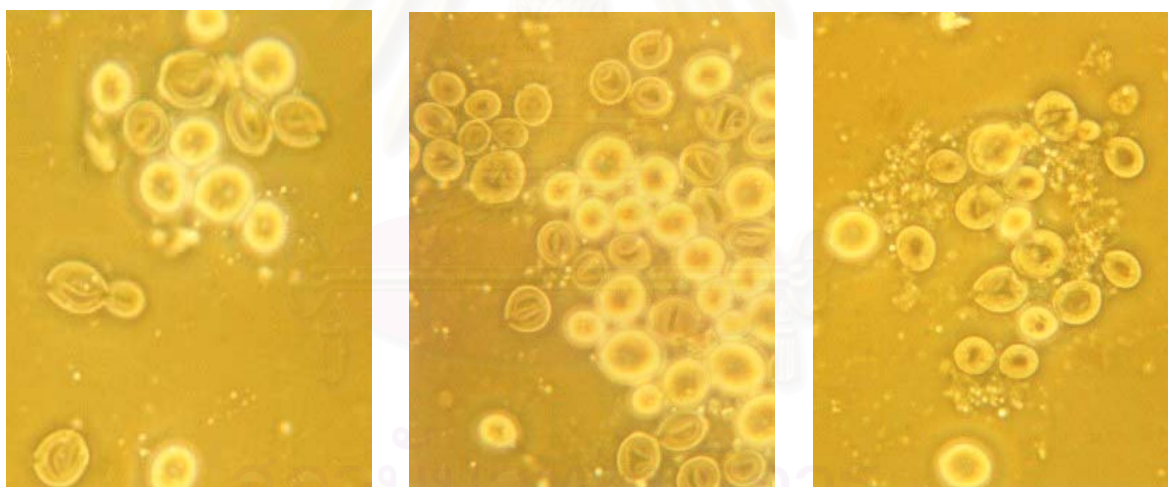


Figure 6-1. Yeast cell size distribution at various temperatures: 10, 28, 32, 47, and 52 °C  
(measured by Beckman Coulter LS 230)



(a) 10 °C

(b) 28 °C



(c) 32 °C

(d) 47 °C

(e) 52 °C

Figure 6-2. Yeast cell morphology at various temperatures

(observed by Olympus Microscope B071)

(a) 10 °C (b) 28 °C (c) 32 °C (d) 47 °C (e) 52 °C

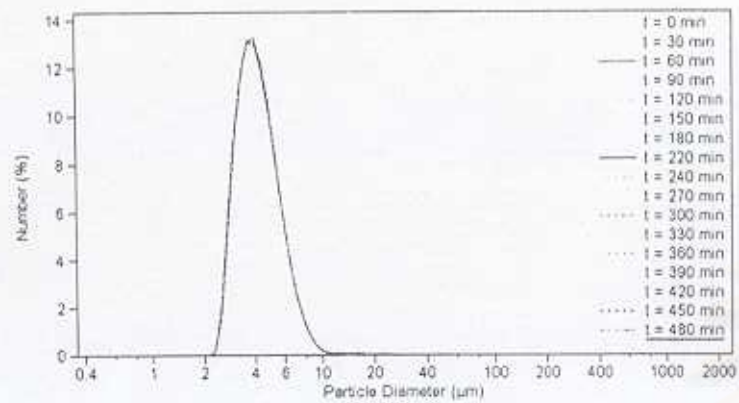
### 6.1.2 Influence of Suspension Circulation through Centrifugal Pump on Cell Disruption

Yeast cell disruption processes are circulated continuously using a centrifugal pump. Due to the fact that the high shear rate is introduced by high feed flow rate velocity through the pump, which may cause the damage of the yeast cell (Matsumoto et al, 1996). The objective of these experiments is to study the circulation effects on the yeast cell disruption, which the experiments are set up at feed flow rate between 10 cm/min and 30 cm/min.

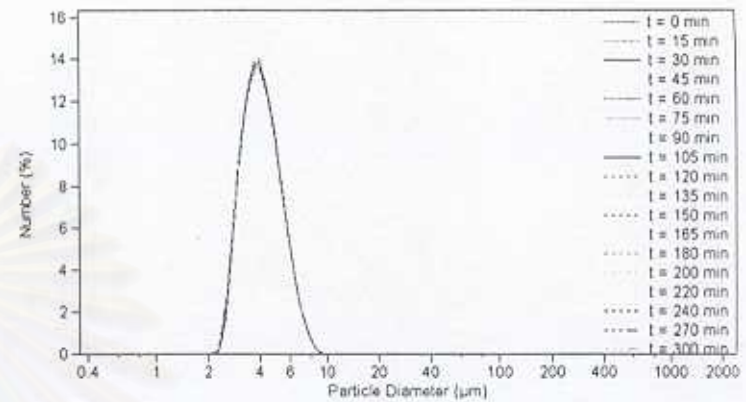
As seen in Figure 6-3, the yeast suspension samples at feed rate between 10 cm/min and 30 cm/min exhibited no change of cell size distributions compared with the size distribution at its initial state. This indicates that the circulation of yeast suspension using centrifugal pump did not affect yeast cell disruption at the feed rate between 10 cm/min and 30 cm/min (Bongkot et al, 1998).

Also, the examination of protein released assay indicates that there was no different of protein in supernatant before and after passing through the centrifugal pump over the experimental time.

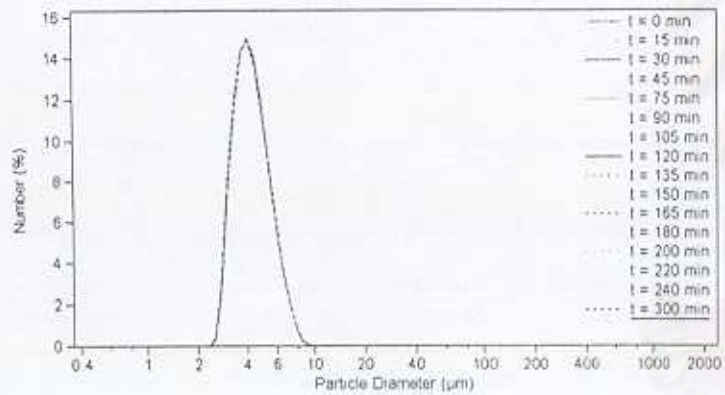
In addition, the microscopic observation clearly showed that no cell disruption took place under the condition accounted here (Figure 6-4).



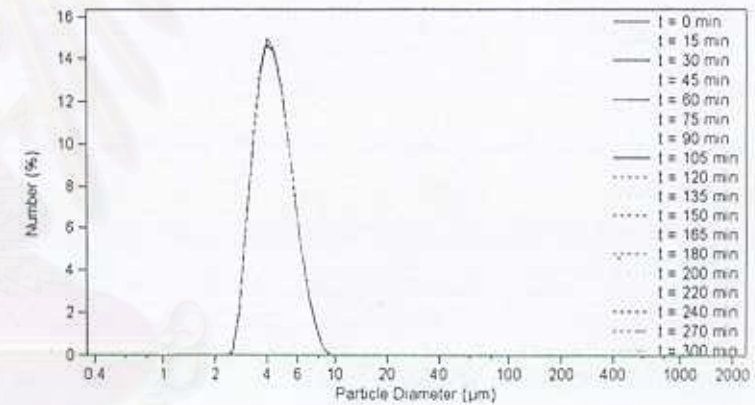
(a) 0 cm/min



(b) 10 cm/min



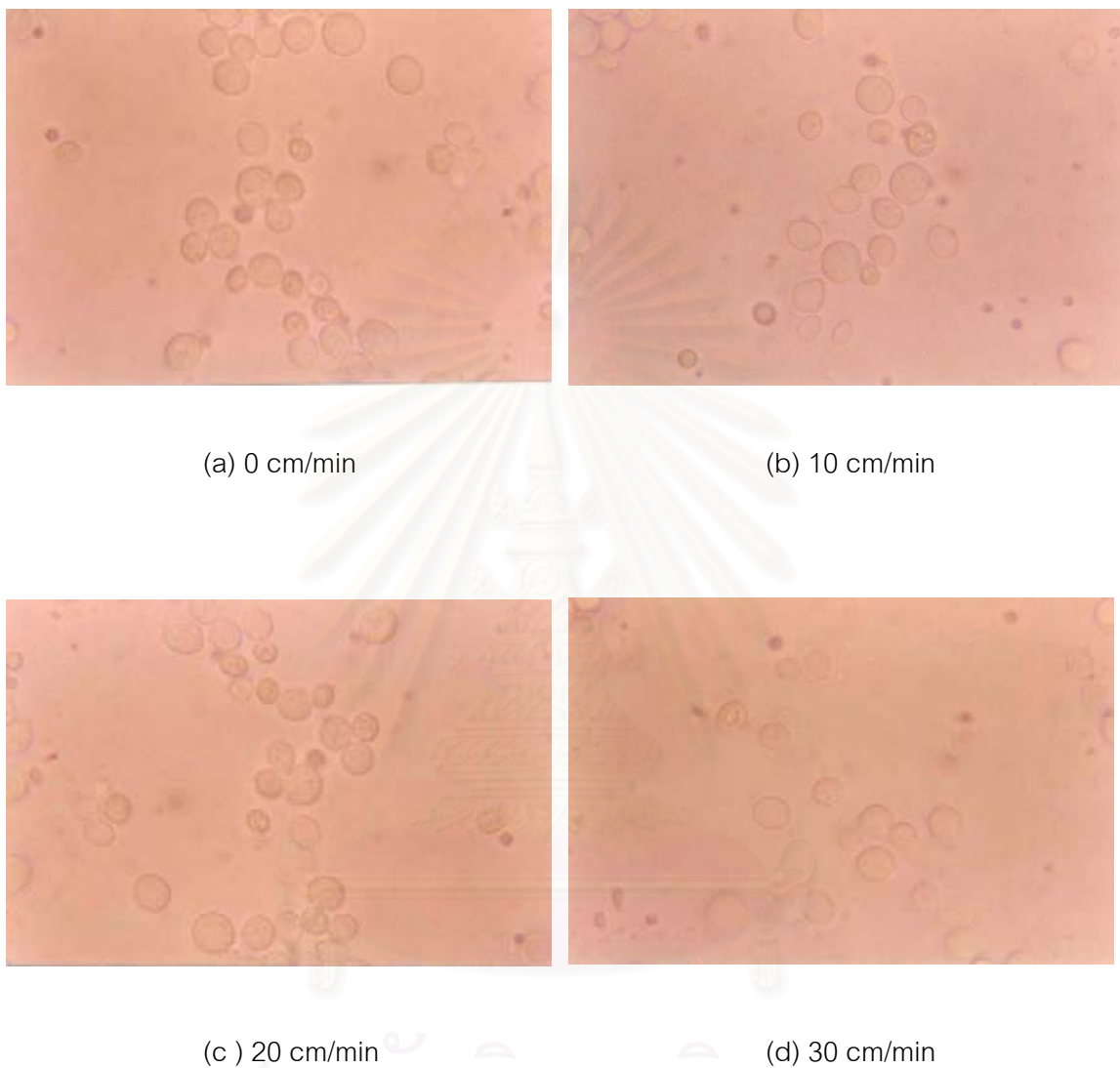
(c) 20 cm/min



(d) 30 cm/min

Figure 6-3. Yeast cell size distribution at various suspension feed rate using the centrifugal pump

(measured by Beckman Coulter LS 230)



สถาบันวิทยบริการ  
จุฬาลงกรณ์มหาวิทยาลัย

**Figure 6-4.** Yeast cell morphology at various suspension feed rates using centrifugal pump at 0, 10, 20 and 30 cm/min for 300 min (observed by Olympus Microscopoe B071)



## 6.2 Influence of Agitation on Yeast Cell Disruption

Under the yeast suspension concentration of 1 % (w/v), a set of experiments were carried out to study the effect of impeller speeds (500, 1500, 2000, and 3000 rpm) on yeast cell disruption with either absence or presence of glass beads, but there was no gas introduction and circulation of yeast suspension.

With absence of the glass beads, previous studies on microorganisms both in pellet and filamentous forms (Smith et al, 1990; Shamlou et al, 1990 and Shamlou et al, 1994) suggested that the cell wall could damage in the single-phase mixing with impeller. The most plausible mechanisms of cell disruption are based on the fluid-induced stress originated from the turbulent velocity fluctuations in the tank. Especially the small area closed to the impeller, there is a zone of strongly accelerating flow, strong vortexing and rapid change of pressure (Hetherington et al., 1971; Smith et al, 1990).

In addition, with absence of glass beads, the experiments were divided into two parts to investigate the effect of agitation on yeast cell disruption. In the first part, the influence of the agitation was investigated in the fluidized bed column without draft tube. In the second part, the effect of installation of coaxial draft tube, whose the lower part consists of perforated holes of 0.9 mm, on yeast cell disruption, was also investigated.

### 6.2.1 With absence of glass beads and draft tube

Agitation in the fluidized bed unit without the draft tube and glass beads, the yeast cell size distribution is measured using the laser diffraction technique. The instrument utilized was Beckman Coulter model LS 230. Figure 6-5 shows the cell size distribution at various impeller speed. The plots also include the initial size distribution of the yeast whole cells of which a modal size is of approximately 4.047  $\mu\text{m}$ . The initial size distribution lies between 2  $\mu\text{m}$  and 10  $\mu\text{m}$  in range. These investigation results show that there is no change of cell size diameter at any impeller speed with respect to time.

This result is repeated by using Mastersizer S Particle Size Analyzer and showed in Figure 6-6. It is also found that there was no change of the cell size distribution at any impeller speed.

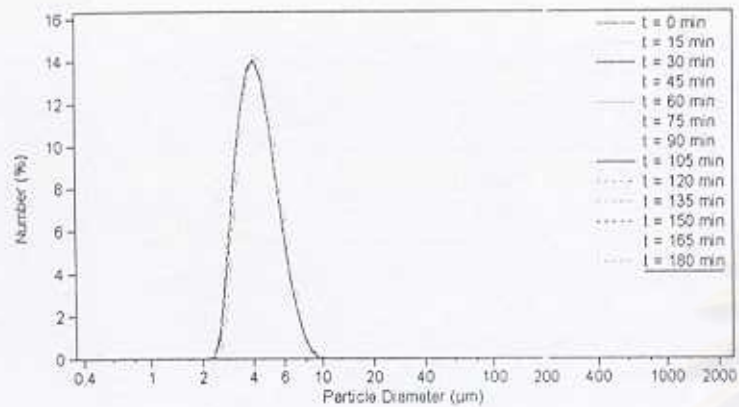
In addition, the crude soluble protein released in the supernatant, which was taken to analyzed by Kjeldahl method, shows that no protein released is detected at every the impeller speed.

The microscopy demonstrates the clear evidence of no yeast cell disruption, which also supported the results of the cell size distribution. The yeast cells were photographed before and after process at variety of the impeller speed. The morphology of yeast cells at magnification of 400 is shown in Figure 6-7. It can be seen that the speed of impeller between 500 rpm and 3000 rpm had no significant of the change of cell shape and no occurrence of cell debris cell was observed.

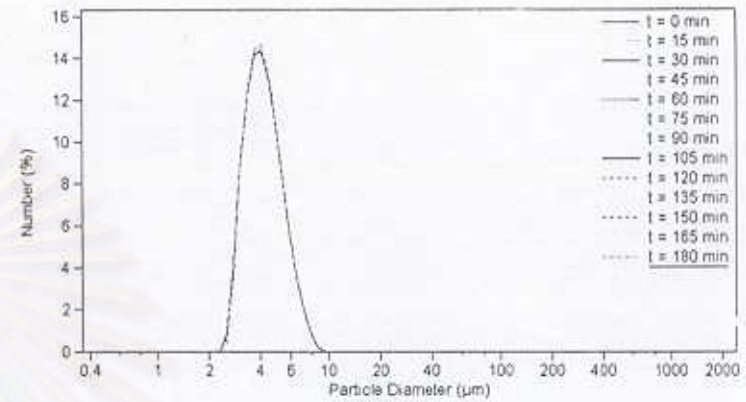
These results suggest that the agitation, at the speed of impeller between 500 rpm and 3000 rpm in the fluidized bed without the draft tube and glass beads, does not cause the yeast cell disruption. Because the fluid shear stress originated from the turbulent velocity fluctuations in the column might be too small to overcome the strength of the outer walls of the yeast cell. Therefore, the cells did not break down, the size distributions did not change and then protein released was not observed.

สถาบันวิทยบริการ  
จุฬาลงกรณ์มหาวิทยาลัย

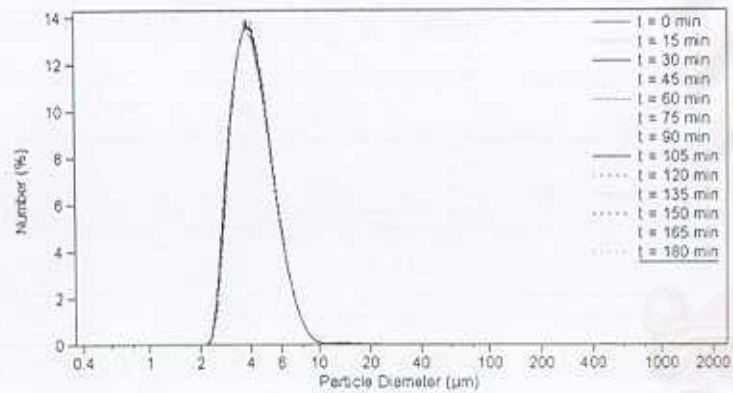




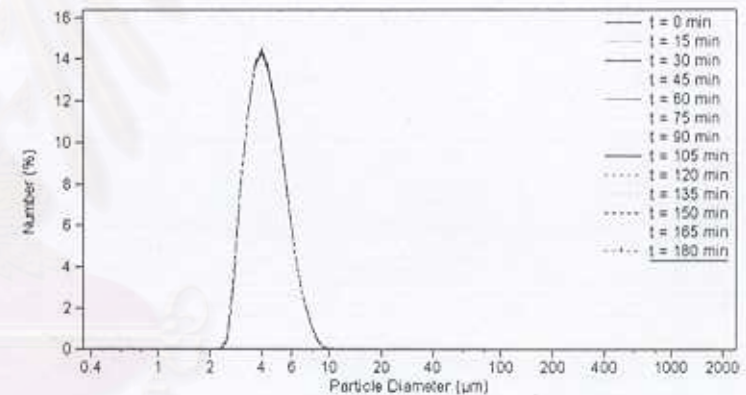
(a) 500 rpm



(b) 1500 rpm



(c) 2000 rpm



(d) 3000 rpm

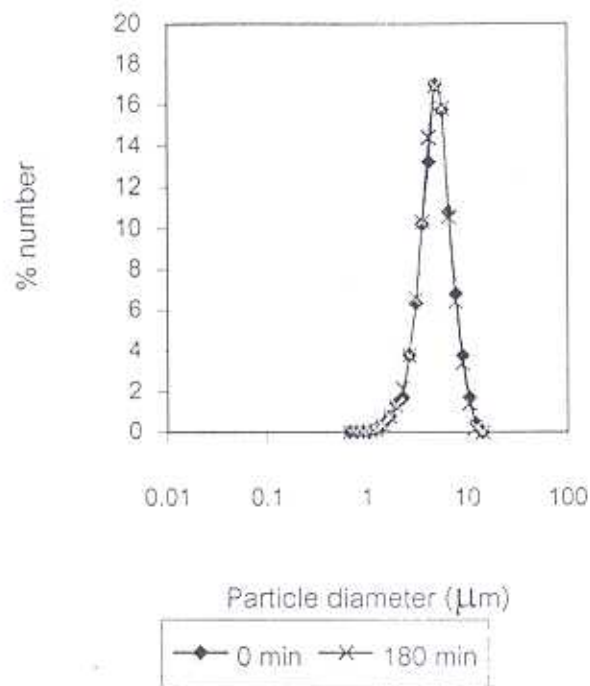
Figure 6-5. Yeast cell size distribution at various impeller speed in the fluidized bed without draft tube (measured by Beckman Coulter LS 230)

$U_i = 0$  cm/min

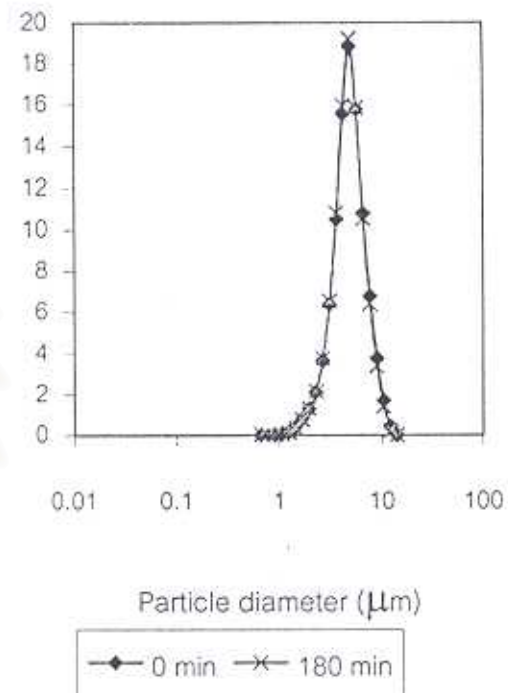
$U_g = 0$  cm/min

$N = 500, 1500, 2000$  and  $3000$  rpm

Absence of glass beads



(a) 500 rpm



(b) 3000 rpm

Figure 6-6. Yeast cell size distribution at various impeller speed in the fluidized bed without draft tube (measured by Mastersizer S)

$$U_i = 0 \text{ cm/min}$$

$$U_g = 0 \text{ cm/min}$$

$$N = 500 \text{ and } 3000 \text{ rpm}$$

Absence of glass beads

สถาบันวิทยบริการ  
จุฬาลงกรณ์มหาวิทยาลัย

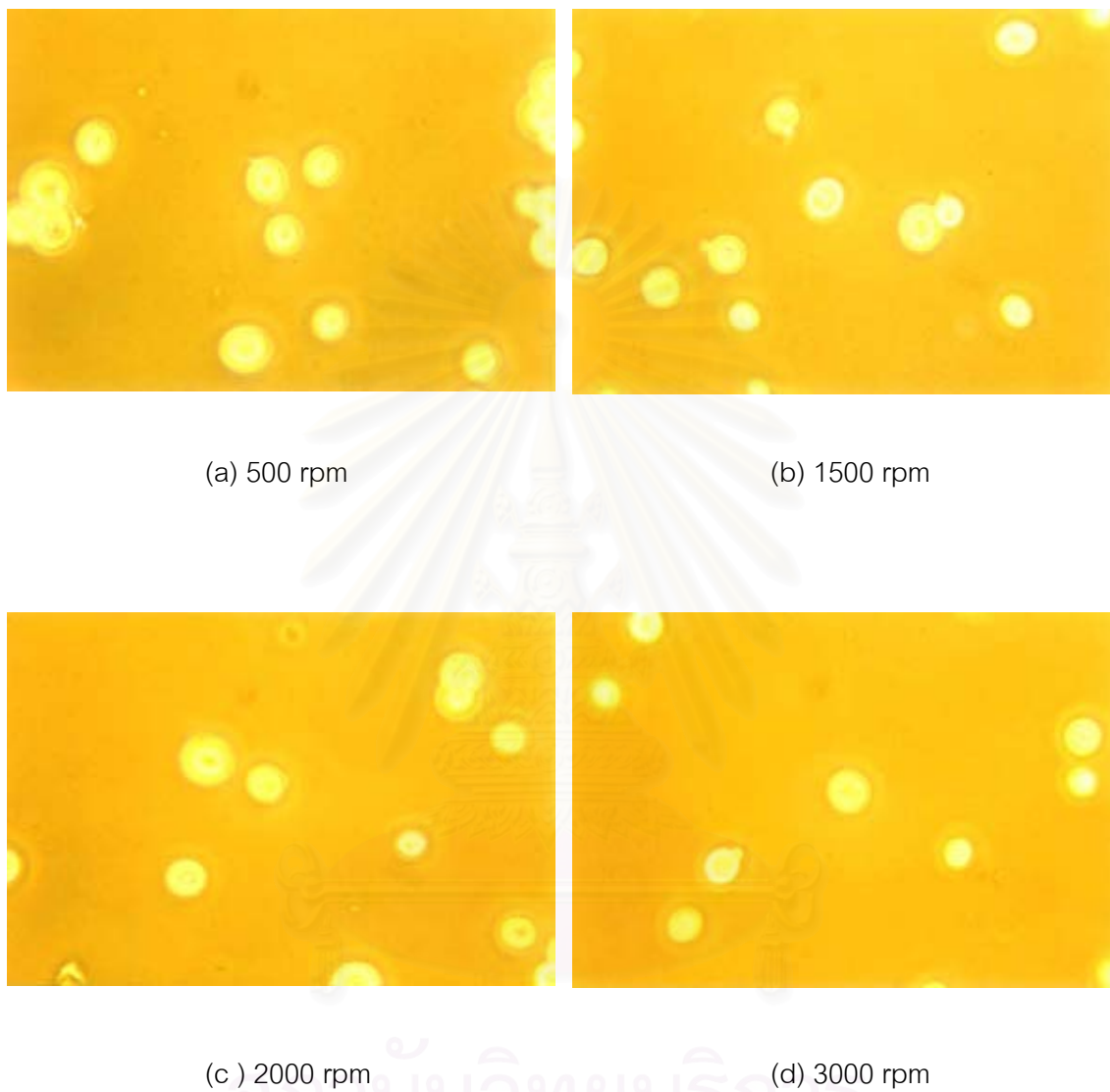


Figure 6-7. Yeast cell morphology at various impeller speed in the fluidized bed without draft tube after operated for 180 min (observed by Olympus Microscopoe B071)

$$U_i = 0 \text{ cm/min}$$

$$U_g = 0 \text{ cm/min}$$

$$N = 500, 1500, 2000, \text{ and } 3000 \text{ rpm}$$

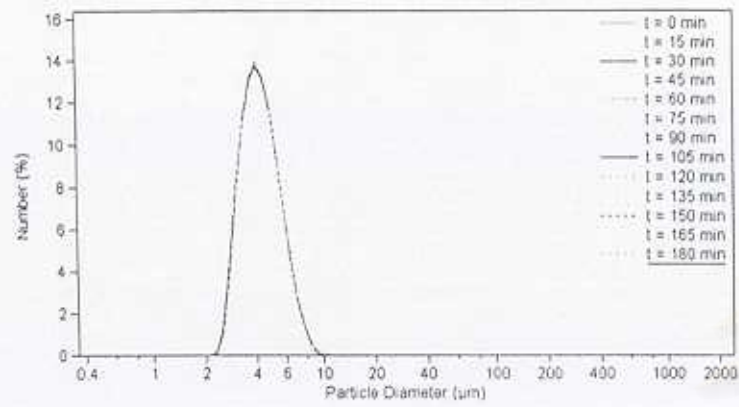
Absence of glass beads

### 6.2.2 With absence of glass beads but with presence of draft tube

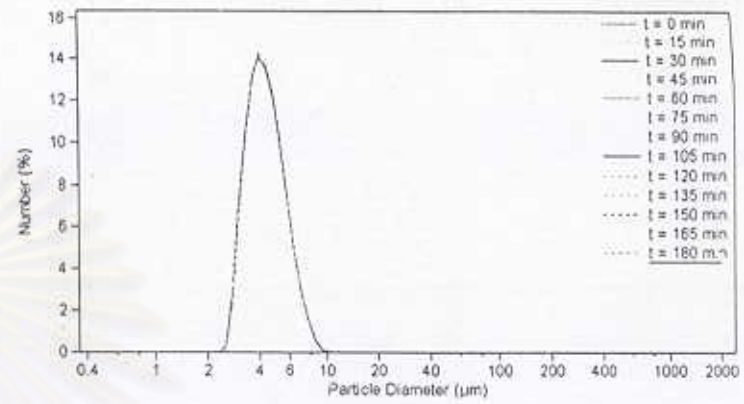
In this part the coaxial draft tube, whose the lower part consists of perforated holes of 0.9 mm, was installed to avoid the collision between the glass beads and the impeller, which may result in the erosion of the glass beads and the contamination to the product. The effect of the existing of the draft tube on yeast cell disruption was investigated by the following the cell size distribution and the protein released.

Figure 6-8 shows that there was no change of the cell size distribution at various impeller speeds. In addition, no protein released in the supernatant was observed over the range of the impeller speed at any time. Then, the morphology of yeast cells observed by microscopic method shows no significant change of cell shape and no occurrence of cell debris at every the impeller speed compared with that of the yeast cells at the initial state (Figure 6-9). These results lead to the conclusion that the shear forces exerted by liquid flow through the pinholes of draft tube did not overcome the strength of the yeast cell wall so that it do not cause the cell rupture.

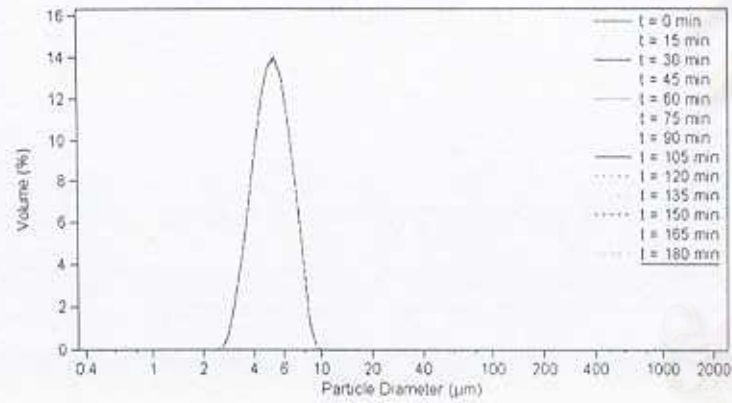
In conclusion, in the fluidized bed with agitation, without glass beads, no yeast cell disruption took place regardless of the absence or presence of draft tube. It indicates that the yeast cells are not generally considered sensitive to mechanical forces generated in the stirred column without abrasive element (Zhang et al, 1999).



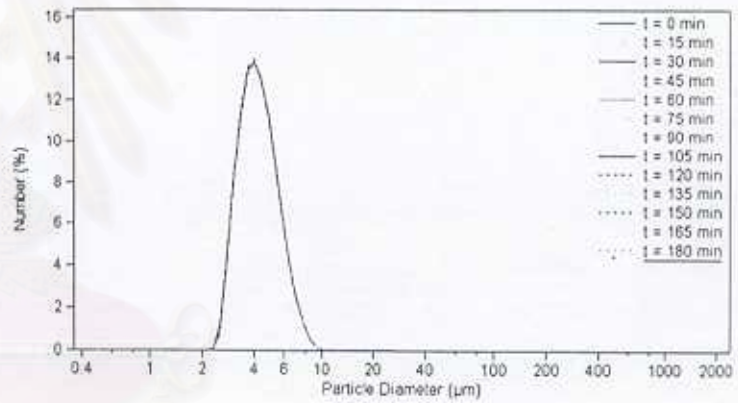
(a) 500 rpm



(b) 1500 rpm



(c) 2000 rpm



(d) 3000 rpm

Figure 6-8. Yeast cell size distribution at various impeller speed in the fluidized bed with draft tube (measured by Beckman Coulter LS 230)

$$U_i = 0 \text{ cm/min}$$

$$U_g = 0 \text{ cm/min}$$

$$N = 500, 1500, 2000 \text{ and } 3000 \text{ rpm}$$

Absence of glass beads



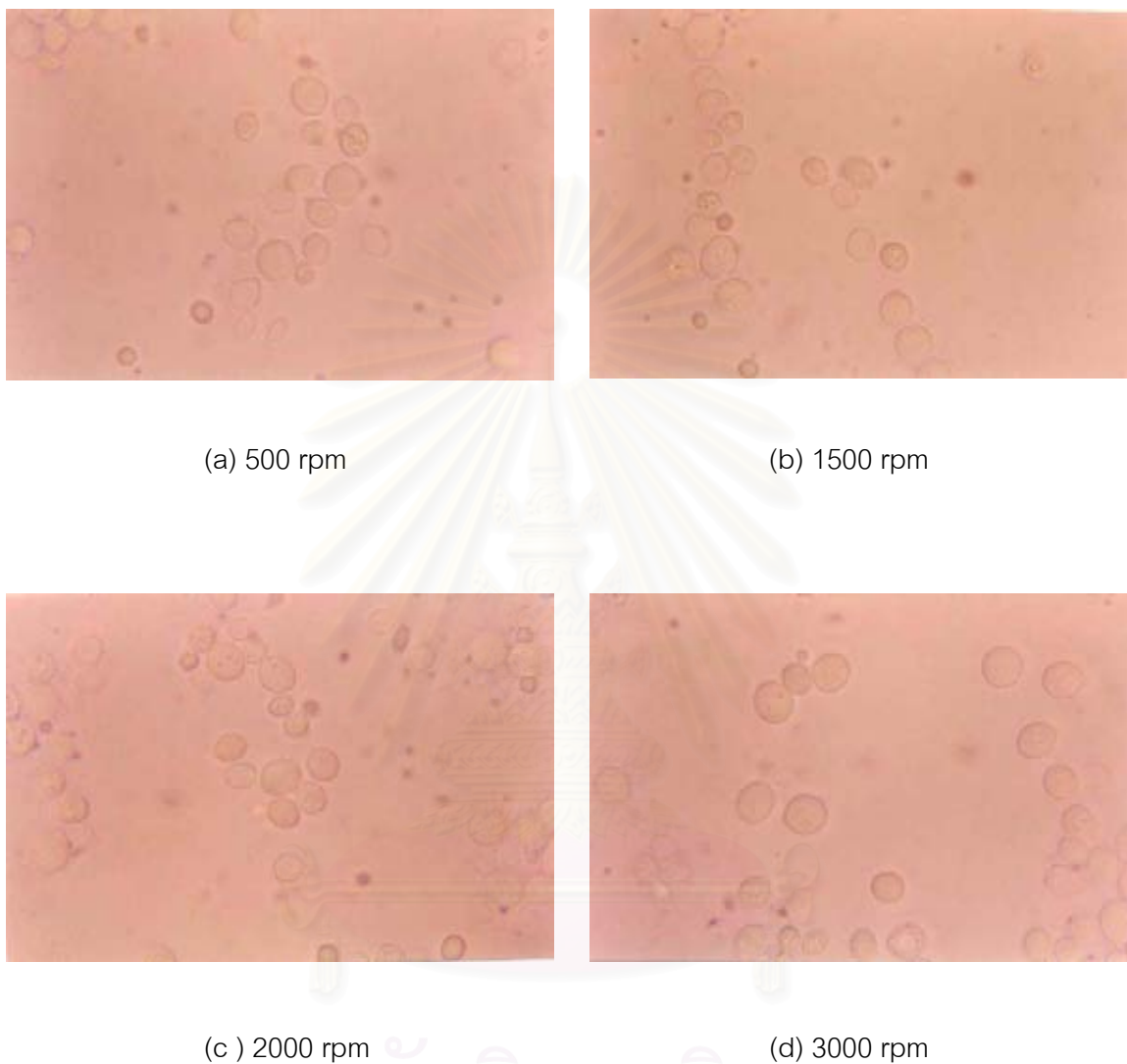


**Figure 6-9.** Yeast cell morphology at various superficial gas velocity in the fluidized bed with draft tube after operated for 180 min (observed by Olympus Microscopoe B071)

$$U_l = 0 \text{ cm/min}$$

$$U_g = 0 \text{ cm/min}$$

$$N = 500, 1500, 2000 \text{ and } 3000 \text{ rpm}$$

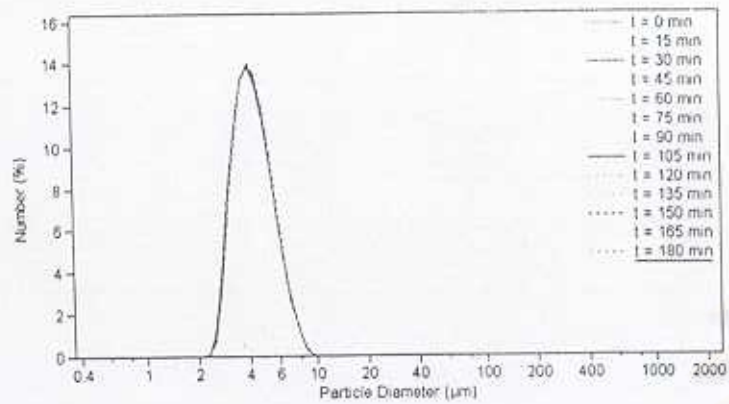
Absence of glass beads

### 6.2.3 With presence of glass beads and draft tube

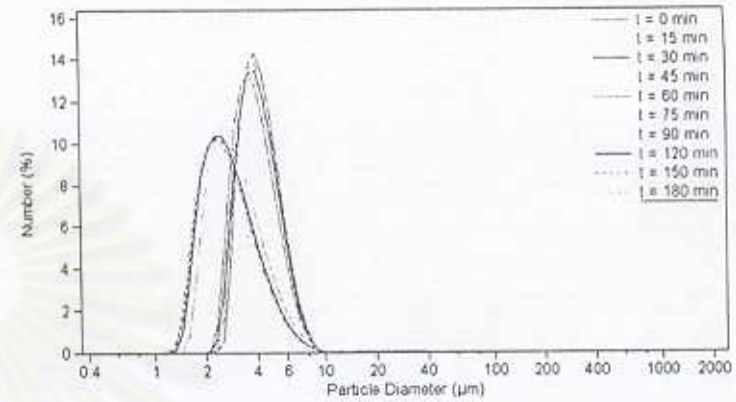
To increase the efficiency of yeast cell disruption processes, one-third of annular of the fluidized bed section had been filled with glass beads to be employed as the grinding elements. The effect of agitation with the presence of glass beads on yeast cell disruption was investigated and then presented below.

Figure 6-10 shows the yeast cell size distributions at various the impeller speeds were measured by Beckman Coulter model LS 230. The repeatability of cell size distribution at 3000 rpm was examined by Mastersizer S Particle Size Analyzer and shown in Figure 6-11. These results show that the cell size distribution shifted toward smaller size range as the cell disruption progressed. The fraction of cell debris became increased and the modal size became smaller with an increase in disruption time. Initially, the fraction of the cell debris became increased with the disruption time, after a certain length of operating time it reached a maximum, subsequently it became constant and the pseudo-steady state in the cell size distribution could be assumed (Shamlou et al, 1995).

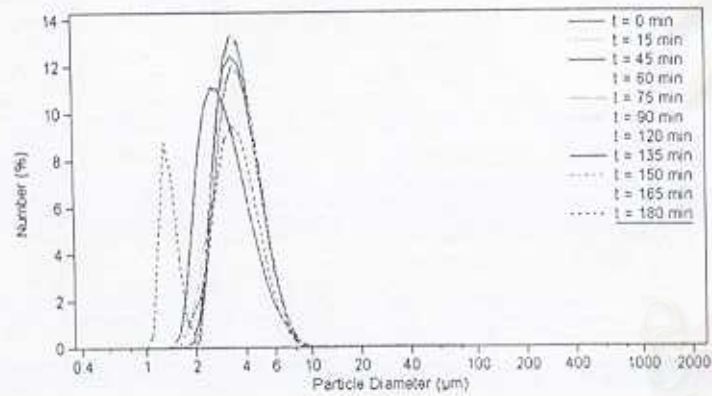




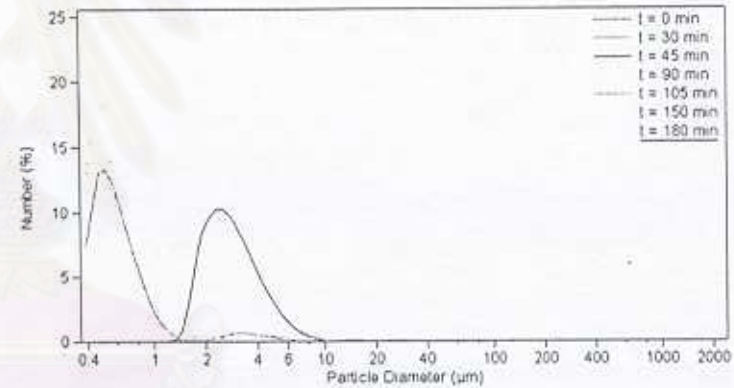
(a) 500 rpm



(b) 1500 rpm



(c) 2000 rpm



(d) 3000 rpm

Figure 6-10. Yeast cell size distribution at various impeller speed in the fluidized bed with draft tube (measured by Beckman Coulter LS 230)

$$U_i = 0 \text{ cm/min}$$

$$U_g = 0 \text{ cm/min}$$

$$N = 500, 1500, 2000 \text{ and } 3000 \text{ rpm}$$

$$\text{Bead size} = 1000 \text{ } \mu\text{m}$$

$$\text{Bead loading} = 1/3 \text{ volume of annular fluidized bed}$$

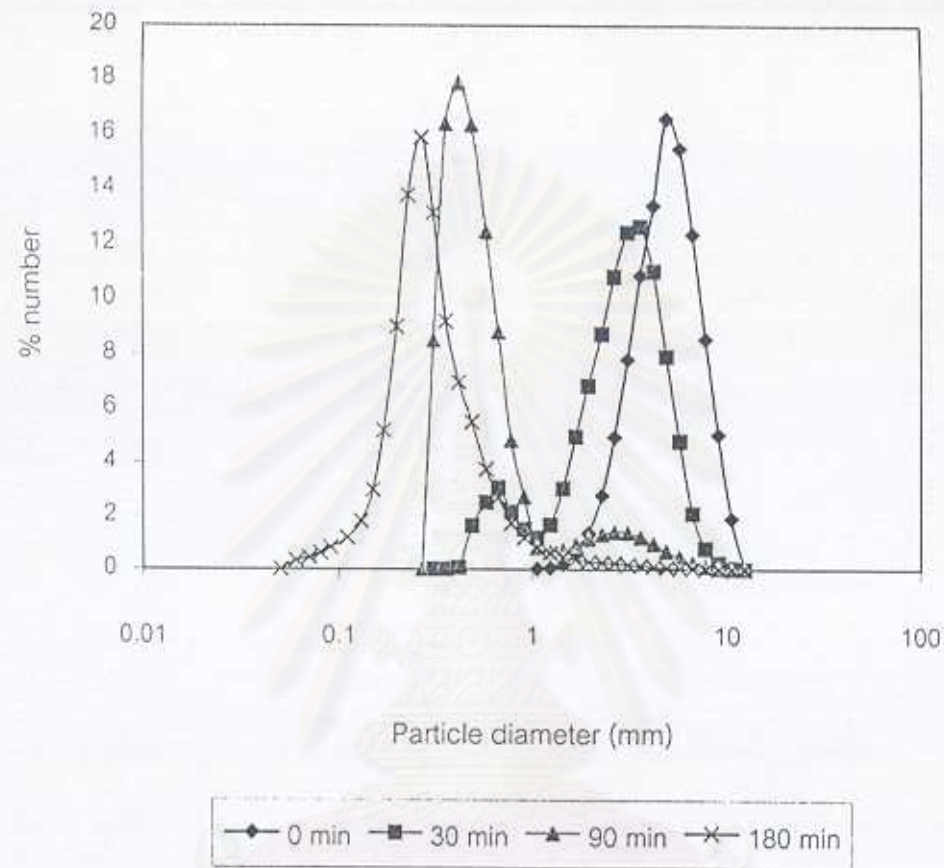


Figure 6-11. Yeast cell size distribution at impeller speed of 3000 rpm in the fluidized bed with draft tube (measured by Mastersizer S)

$U_i = 0$  cm/min

$U_g = 0$  cm/min

$N = 3000$  rpm

Bead size =  $1000 \mu\text{m}$

Bead loading =  $1/3$  volume of annular fluidized bed

สถาบันส่งเสริมบริการ  
จุฬาลงกรณ์มหาวิทยาลัย

According to Shimizu et al (1998), the ratio of non-disrupted cell remaining in the sample at any certain time is defined as.

$$\begin{aligned} &\text{Ratio of non-disrupted cell} \\ &= \frac{\text{frequency of the modal size of yeast whole cell at the any time}}{\text{frequency of the modal size of yeast whole cell at the certain time}} \end{aligned} \quad (6-1)$$

And then, the effectiveness of the cell disintegration is defined as “degree of cell disruption”, which can be calculated from the following equation

$$\begin{aligned} &\text{Degree of cell disruption (\%)} \\ &= (1 - \text{ratio of non-disrupted cell}) \times 100 \end{aligned} \quad (6-2)$$

Figure 6-12 shows the relationship between the operating time and the degree of cell disruption. The disruption time for obtaining a maximum value became shorter than when the speed of impeller was increased (Morohashi et al, 1997; Kula and Schutte, 1987; Shimizu et al, 1998). Since an increase in the agitator speed might lead to a high frequency of contact of these beads and also lead to higher shear stresses (Currie et al, 1972), it would enhance the cell disruption process to become faster.

สถาบันวิทยบริการ  
จุฬาลงกรณ์มหาวิทยาลัย

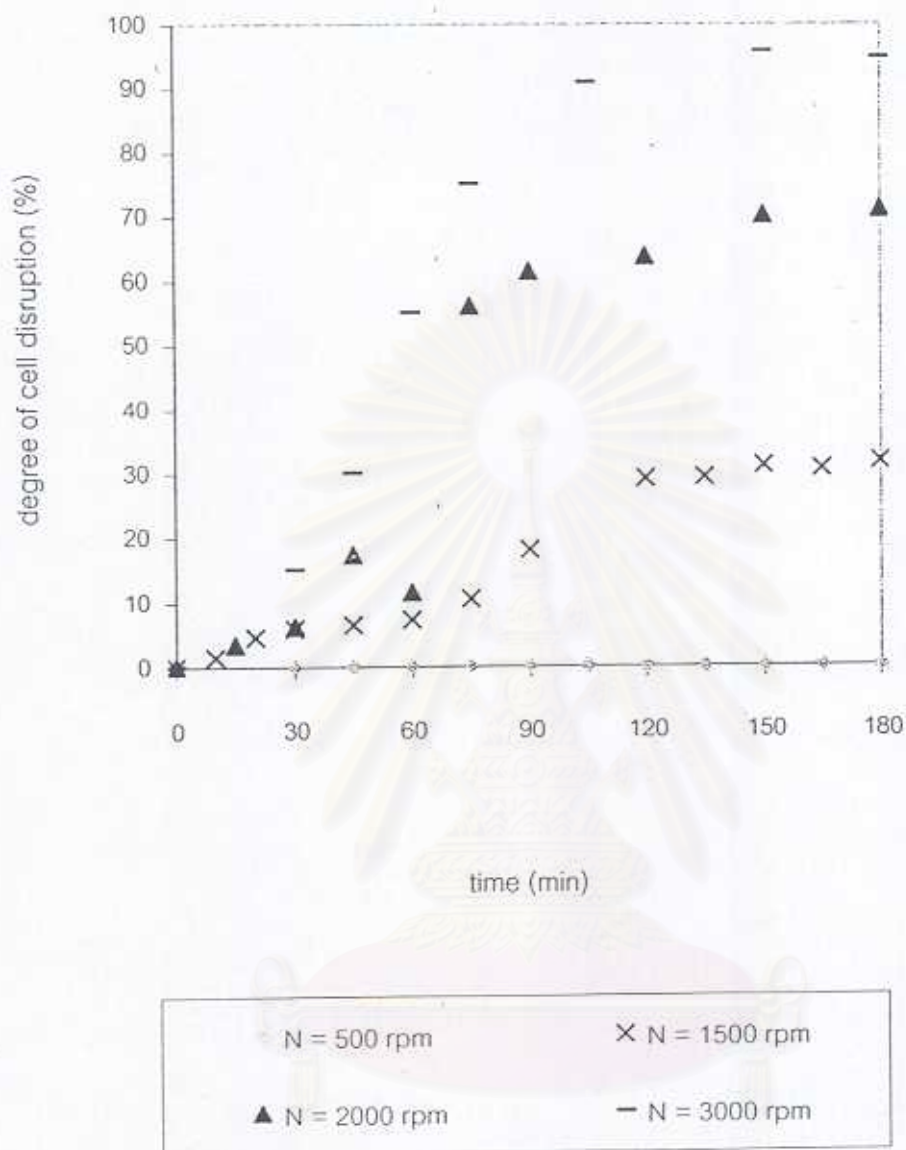


Figure 6-12. Influence of impeller speed on yeast cell disruption in the fluidized bed with draft tub

$$U_i = 0 \text{ cm/min}$$

$$U_g = 0 \text{ cm/min}$$

$$N = 500, 1500, 2000 \text{ and } 3000 \text{ rpm}$$

$$\text{Bead size} = 1000 \mu\text{m}$$

$$\text{Bead loading} = 1/3 \text{ volume of annular fluidized bed}$$

The main mechanisms of cell disruption seem to be shearing, grinding due to the beads and direct collision with the beads.

Heim and coworker (1999) have confirmed that the grinding played a significant role in the destruction of the yeast cells in a bead mill with the grinding elements and also proposed the mechanism of yeast cell disruption. The cells might be forced to enter into the breaking zone located between two grinding media (Figure 6-13). The external forces exerted by the movement of grinding media will act on the cells and then lead to the disruption.

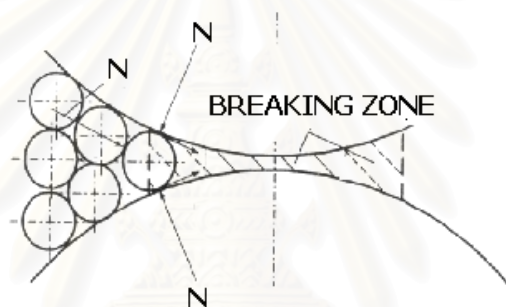


Figure 6-13. The phenomena of grinding the yeast cell in breaking zone

Shear stresses are developed in the yeast suspension due to the agitator imparted the kinetic energy to the beads, forcing them to form stream layers of different velocity. When the layer of the fluid moves faster or slower than a nearby layer of fluid or solid surfaced, leading high shear forces caused the cell destruction.

During the disintegration process, the cells might possibly be disrupted by the direct collision due to the external force exerted from the agitator.

The protein assay in the supernatant sampled from the experimental equipment was employed to confirm the effect of agitation in the fluidized bed unit with glass beads. It shows that no cell disruption occurs at 500 rpm because no protein released in supernatant was detected. While at 3000 rpm, the concentration of the protein released was found to increase with the disruption time and then reach a maximum value. This result could be used to support the yeast cell size distribution investigation.

The morphology of yeast cell examined by microscopy shown in Figure 6-14 also supports the results mentioned above. No disruption after processing at 500 rpm was observed because the yeast cells did not change of shape compared with the yeast cells at the preparation state. While the speed of impeller was increased between 1500 rpm and 3000 rpm, the cells were broken down and the intracellular materials were released. It could be concluded that the rupture of yeast cells is insignificant when the agitation speed lower than 500 rpm and the working range should lie within the range of 1500 - 3000 rpm.



สถาบันวิทยบริการ  
จุฬาลงกรณ์มหาวิทยาลัย



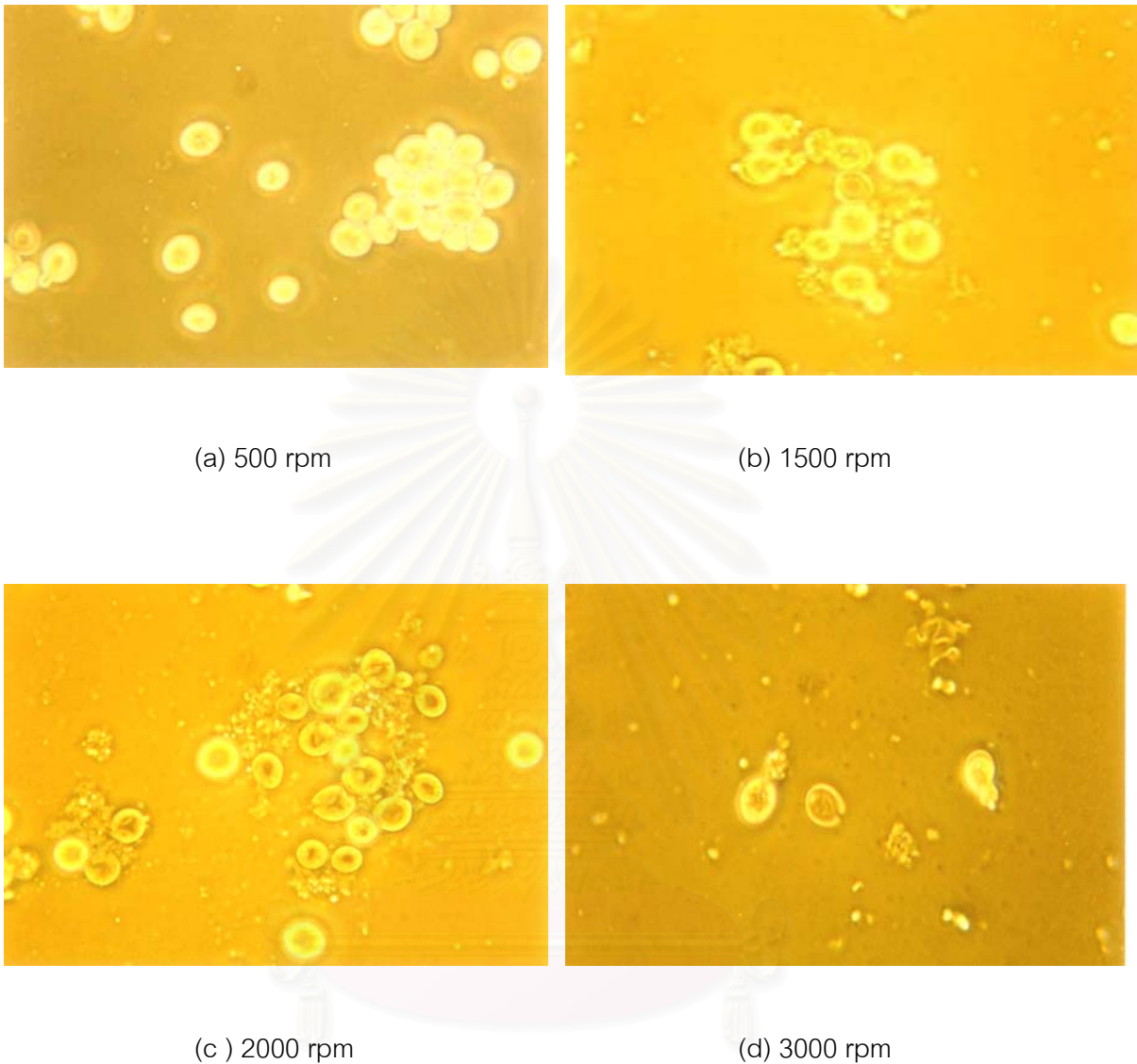


Figure 6-14. Yeast cell morphology at various impeller speeds in the fluidized bed with draft tube after operated for 180 min (observed by Olympus Microscopoe B071)

$$U_i = 0 \text{ cm/min}$$

$$U_g = 0 \text{ cm/min}$$

$$N = 500, 1500, 2000, \text{ and } 3000 \text{ rpm}$$

$$\text{Bead size} = 1000 \mu\text{m}$$

$$\text{Bead loading} = 1/3 \text{ volume of annular fluidized bed}$$



### 6.3 Influence of Superficial Gas Velocity on Yeast Cell Disruption

Some previous investigation suggested that the suspended microorganism cells could be damaged by the interaction between cell and bubble when air is introduced into the column (Kunas et al, 1990; Bavarian et al, 1991; Chalmers et al, 1991). These observations indicate that the cell-bubble interaction can be classified into three distinct regions in a bubble column.

1. cell interacts with bubble generation at the sparger
2. cell interacts with rising bubble
3. cell interacts with bubble at the air-medium interface

In the region of bubble generation, Murhammer et al.(1990) is suggested that the number of damaged cell increased when an increase in air velocity leaving the sparger, Because increasing the air velocity lead to higher levels of fluid turbulence.

In the region of bubble rising, the bubble coalescence and break up is supported to be main reason for cell rupture (Chalmers, 1994)

When a air bubble reaches to the top of the column. If no other bubble is presented at the air-medium interface, it will partially rise out of the liquid medium, forming a thin film separating the surrounding gas from the gas within the bubble. This film can be drained rapidly and make the bubble ruptured. Under the some certain conditions, the film could stabilize and the bubble would remain at the interfacial for a long period of time. If the time is sufficiently long, other bubbles will join it and form a foam layer. If a foam layer is presented at the top of the column, a bubble larger than those in the foam would slowly rise through the foam, potentially coalescing with other bubbles in the foam to form bigger bubbles (Chalmers, 1994). Handa and coworker (1987) used a microscopic video system to investigate cell rupture as a result of bubble at the air-medium interface. They find that cells oscillated near rapidly rupturing bubbles. It was also proposed that cells could be damaged as a result of physical shearing while the liquid drained around the bubbles.

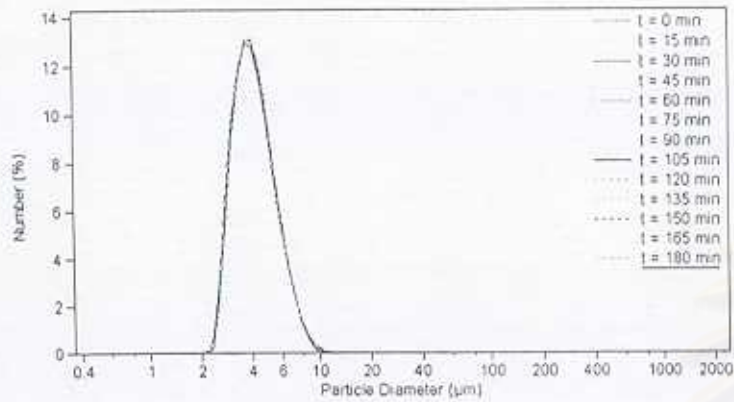
However, there are very few literature mentions on the effect of sparging of the yeast cell suspension with the gas on the yeast cell disruption. These experiments were focused on the introduction of gas bubbles into the yeast suspension to observe the influence of the gas bubbles at various superficial gas velocities on yeast cell rupture when no agitation and no circulation of suspension was employed.

### 6.3.1 With absence of glass beads but with presence of draft tube

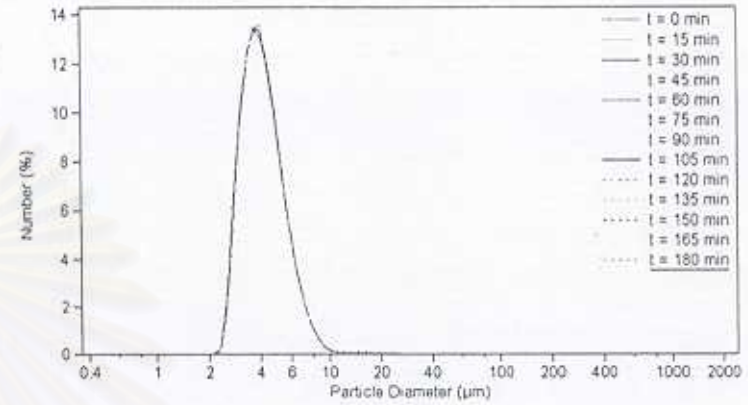
Figure 6-15 shows the cell size distributions, which are measured by Beckman Coulter model LS 230, at superficial gas velocity varied as 0, 10, 20 and 40 cm/min. There was no change in the cell size distribution when the gas was introduced into the system at every superficial gas velocity. As also seen in the Figure 6-16, no change in the cell size distribution, which measured by Mastersizer S Particle Size Analyzer, was observed.

The similar tendency of protein released is employed to confirm that the increase in superficial gas velocity between 0–40 cm/min had insignificant influence on yeast cell disruption in the bubble column regime.

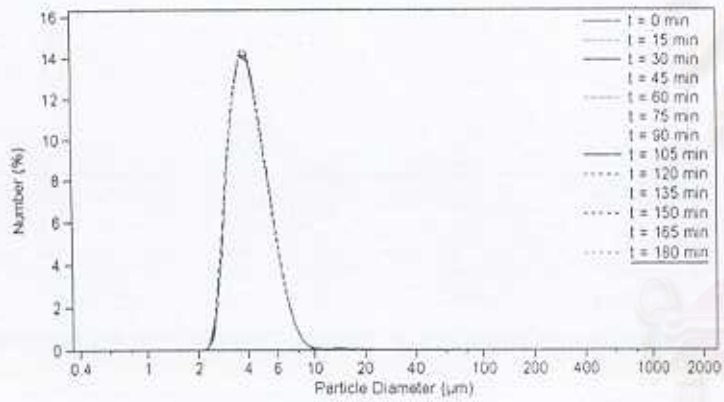
Consideration of the morphology of yeast cells using the microscopic observation at the magnification of 400 as demonstrated in Figure 6-17, the yeast cells sampled under the condition of from before and after being sparging with the gas at different of superficial gas velocities had no change in their morphology. In addition, there was no cell debris observed under any condition.



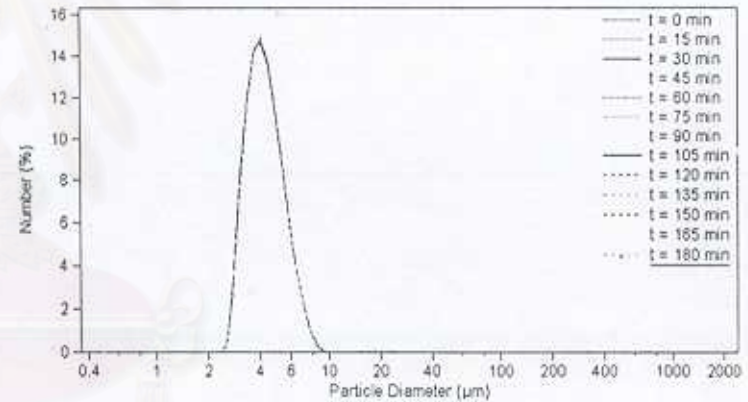
(a) 0 cm/min



(b) 10 cm/min



(c) 20 cm/min



(d) 40 cm/min

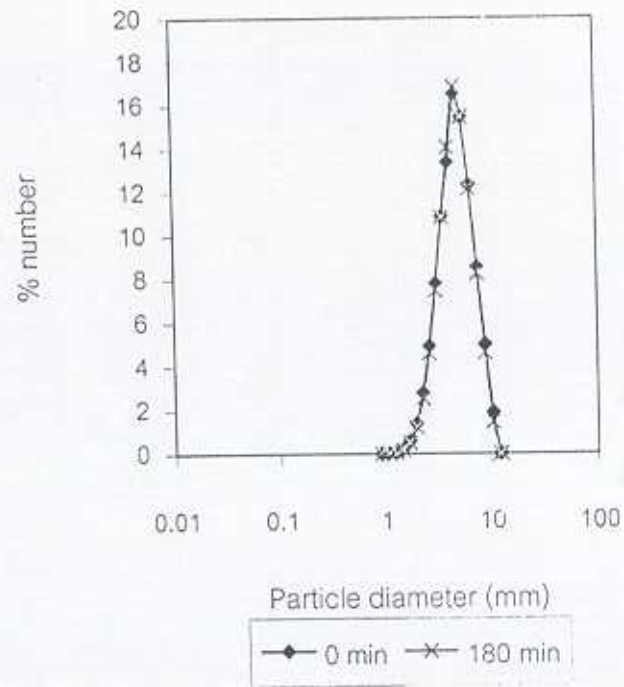
Figure 6-15. Yeast cell size distribution at various superficial gas velocity in the fluidized bed with draft tube (measured by Beckman Coulter LS 230)

$U_i = 0$  cm/min

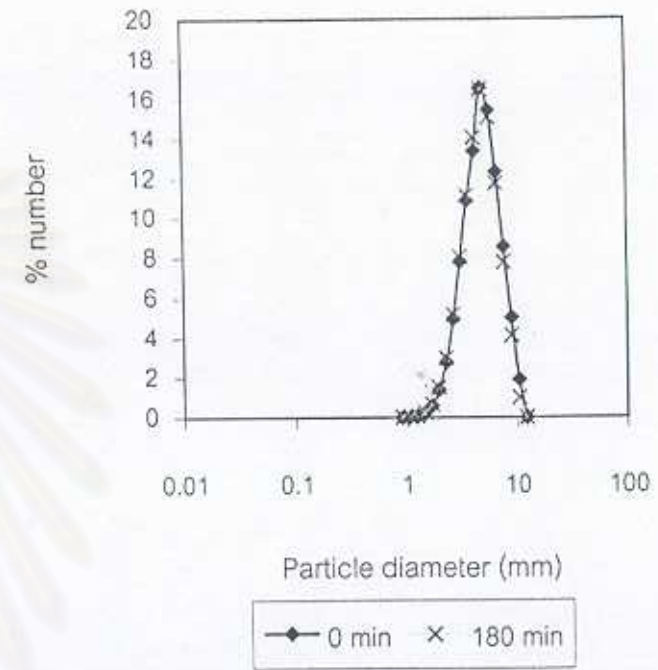
$U_g = 0, 10, 20$  and  $40$  cm/min

$N = 0$  rpm

Absence of glass beads



(a) 10 cm/min



(b) 40 cm/min

Figure 6-16. Yeast cell size distribution at various impeller speed in the fluidized bed with draft tube (measured by Mastersizer S)

$U_i = 0$  cm/min

$U_g = 10$  and  $40$  cm/min

$N = 0$  rpm

Absence of glass beads

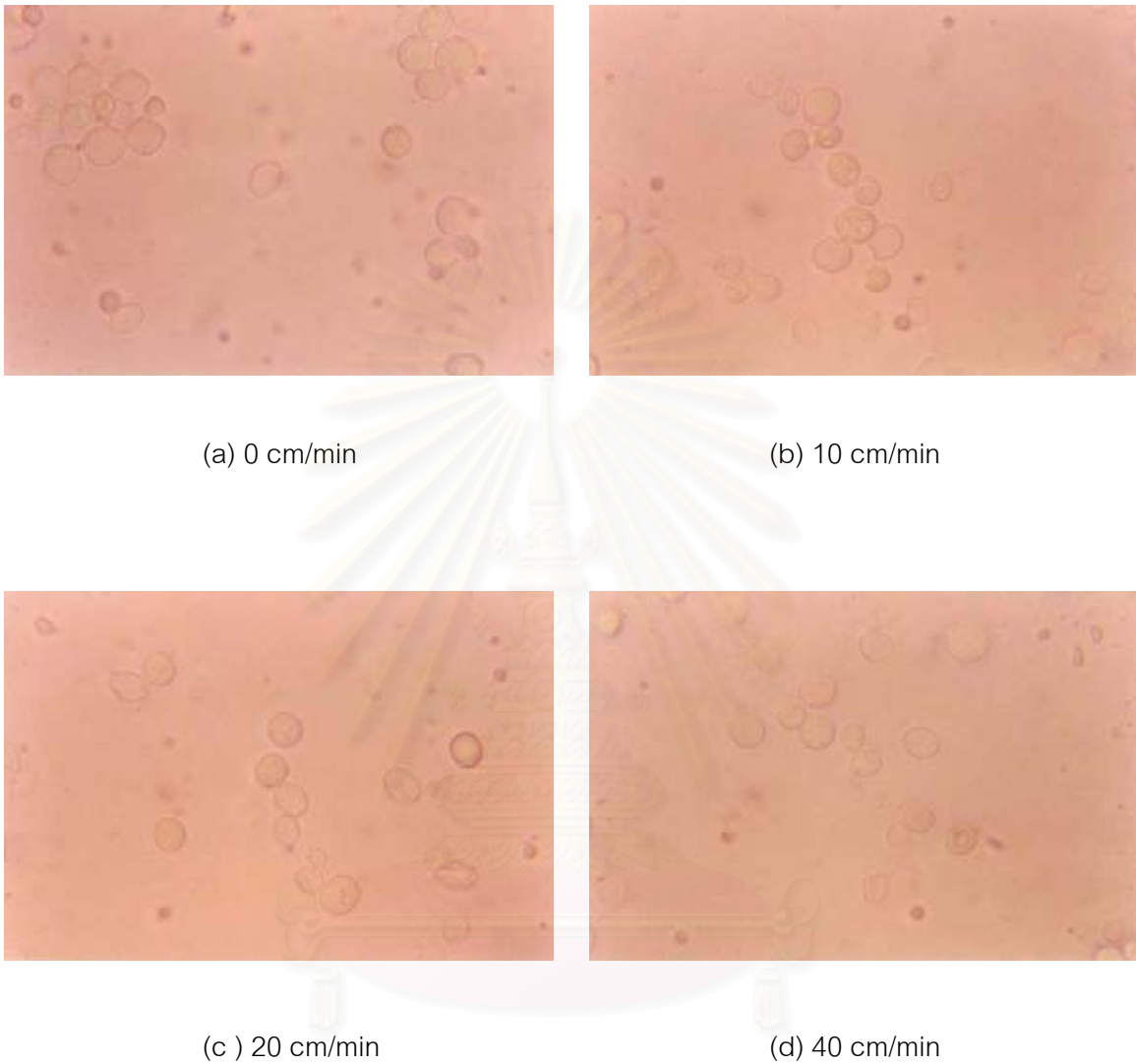


Figure 6-17. Yeast cell morphology at various superficial gas velocities in the fluidized bed with draft tube at 180 min (observed by Olympus Microscopoe B071)

$$U_l = 0 \text{ cm/min}$$

$$U_g = 0, 10, 20 \text{ and } 40 \text{ cm/min}$$

$$N = 0 \text{ rpm}$$

Absence of glass beads

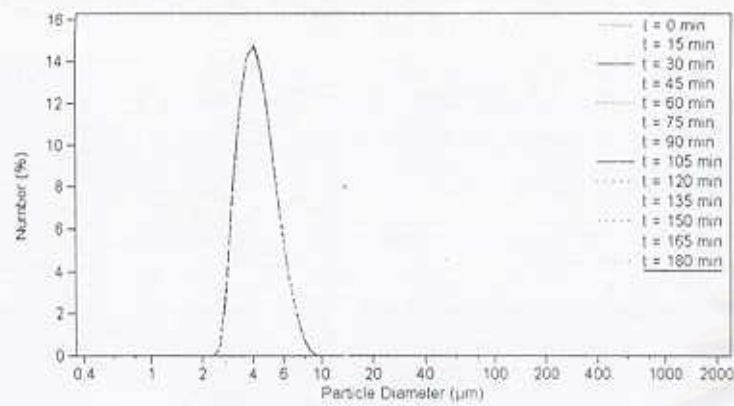


### 6.3.2 With presence of glass beads and draft tube

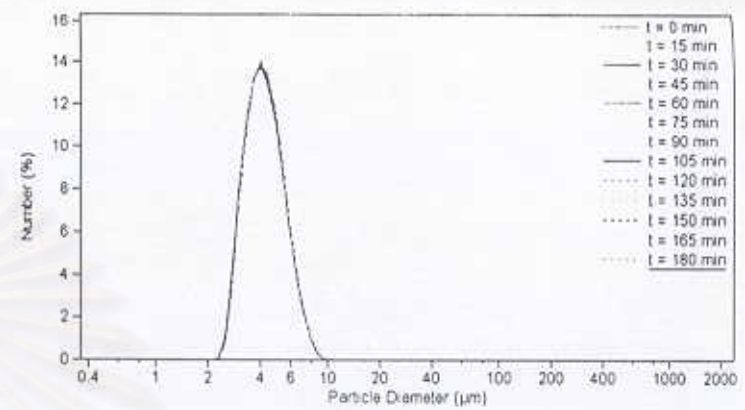
The influence of the presence of glass beads in the annular region of the fluidized bed column on the yeast cells disruption is also investigated when the air bubble is introduced.

Figure 6-18 shows that there was no change in cell size distribution with the increase in the superficial gas velocity between 10 and 40 cm/min. Also, there was no protein released in the supernatant after introducing the air bubble at any superficial gas velocity. There is no change of yeast cell morphology as shown in Figure 6-19.

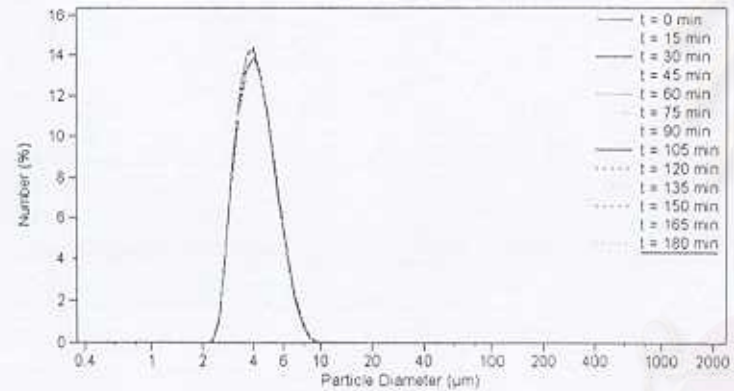
In conclusion, the interaction between the air bubble and yeast cells had insignificant effect on the yeast cell disruption. Since the strength of yeast cell wall can resist higher levels of fluid turbulence generated by the increase in air velocity leaving the sparger as well as the oscillation of the bubble coalescence and break up. These phenomena were also found in the case of the presence of glass beads. It could be concluded that the superficial gas velocity in the range of 10 and 40 cm/min did not lead to vigorous interaction sufficient enough to break up the yeast cell.



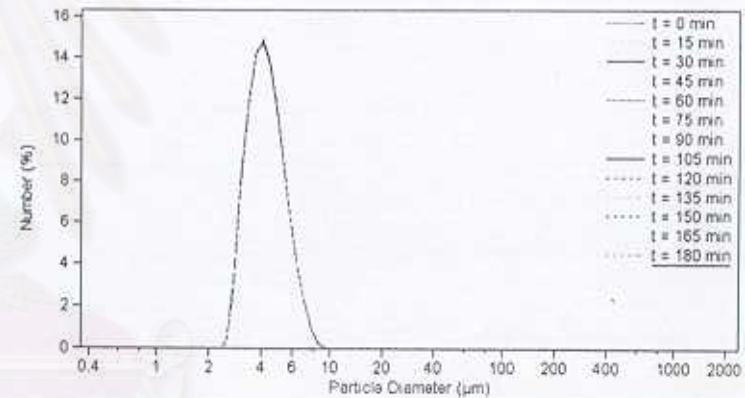
(a) 0 cm/min



(b) 10 cm/min



(c) 20 cm/min



(d) 40 cm/min

Figure 6-18. Yeast cell size distribution at various superficial gas velocity in the fluidized bed with draft tube (measured by Beckman Coulter LS 230)

$U_i = 0$  cm/min

$U_g = 0, 10, 20$  and  $40$  cm/min

$N = 0$  rpm

Bead size =  $1000 \mu\text{m}$

Bead loading =  $1/3$  volume of annular fluidized bed



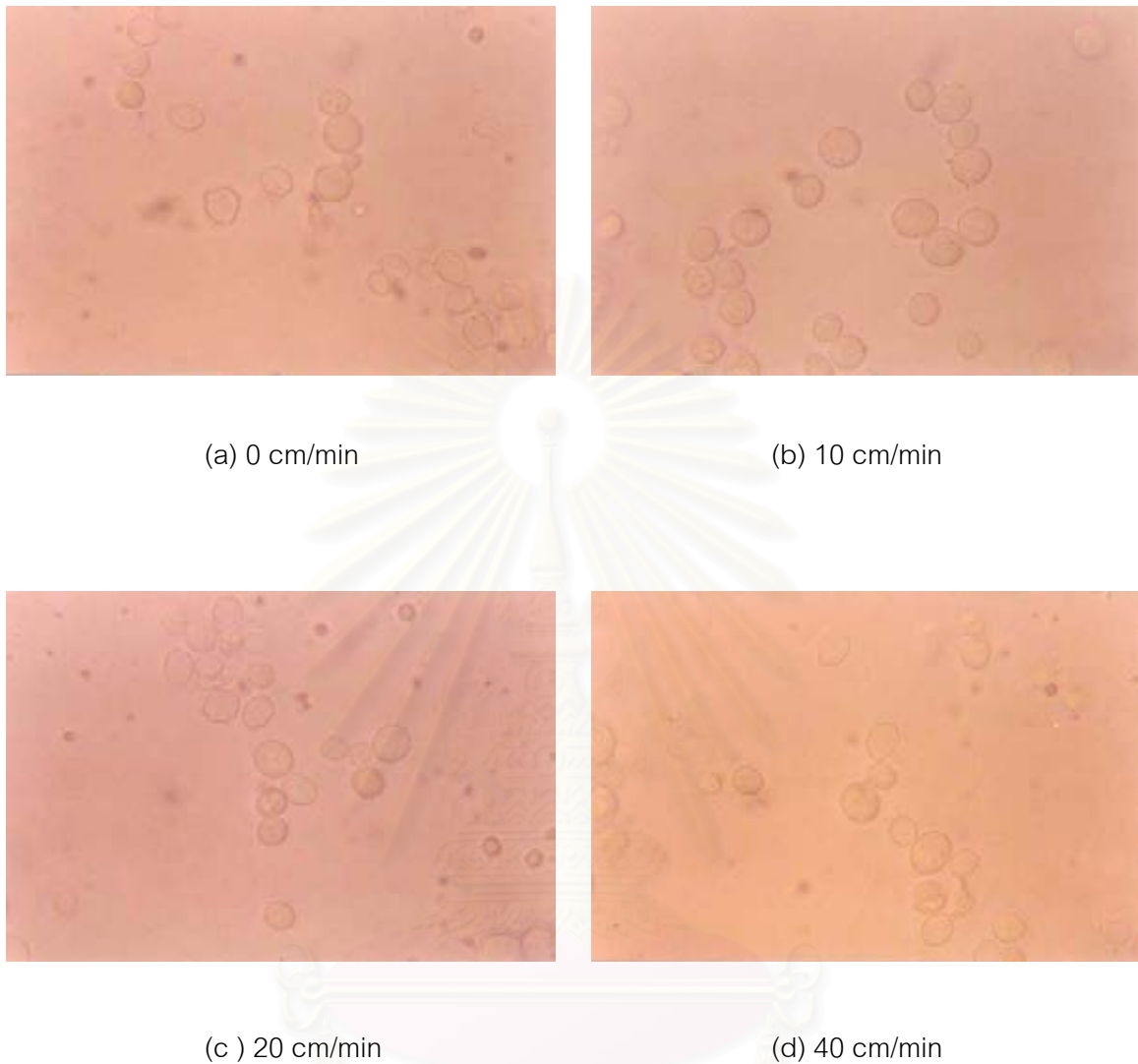


Figure 6-19. Yeast cell morphology at various superficial gas velocities in the fluidized bed with draft tube after operated for 180 min (observed by Olympus Microscopoe B071)

$$U_l = 0 \text{ cm/min}$$

$$U_g = 0, 10, 20 \text{ and } 40 \text{ cm/min}$$

$$N = 0 \text{ rpm}$$

$$\text{Bead size} = 1000 \mu\text{m}$$

$$\text{Bead loading} = 1/3 \text{ volume of annular fluidized bed}$$

## 6.4 Influence of Superficial Liquid Velocity on Yeast Cell Disruption

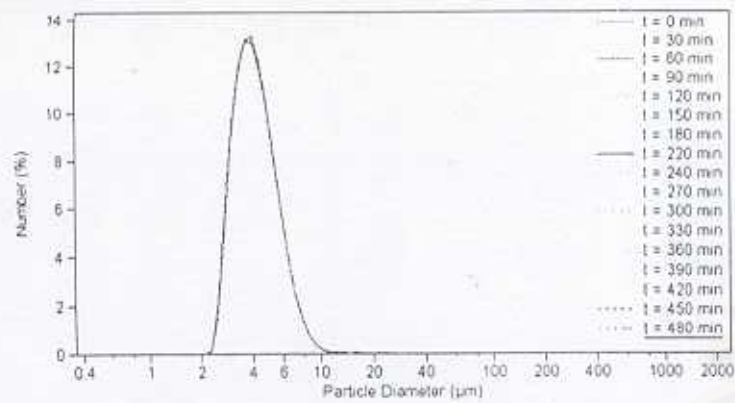
These experiments were set up to study the effect of superficial liquid velocity on the yeast cell disruption. The superficial liquid velocities accounted here were varied in the range of between 10 to 30 cm/min.

### 6.4.1 With absence of glass beads but with presence of draft tube

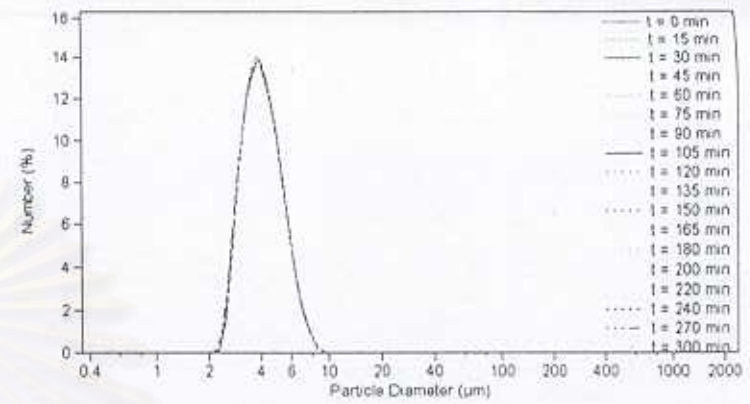
The effect of superficial liquid velocity on the yeast cell disruption in the system with draft tube but no glass beads employed was investigated here. The results showed that the superficial liquid velocity range from 10 and 30 cm/min had insignificant effect on change of cell size distribution for operation over 300 min (Figure 6-20). It can be concluded that the flow of yeast suspension through the fluidized bed with draft tube at superficial liquid velocity between 10 cm/min and 30 cm/min did not cause the disruption of the yeast cells.

### 6.4.2 With presence of glass beads and draft tube

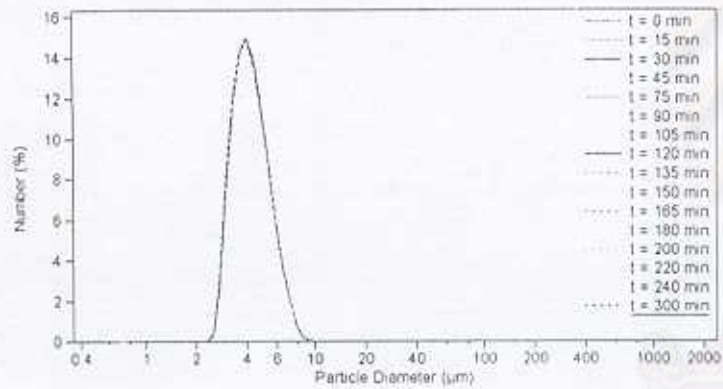
Even when the yeast suspension was pumped through the fluidized bed column, which was filled with glass beads, superficial liquid velocity in the range of 10 to 20 cm/min resulted in no change of the yeast cell size distribution. However, the superficial liquid velocity of 30 cm/min caused a shift of cell size distribution with respect to time as shown in Figure 6-21. Figure 6-22 also shows that degree of cell disruption at superficial liquid velocity 30 cm/min was about 1% after operated for 300 min. In addition, there was no protein released during the investigation. It could be implied that no significant cell disruption took place under the condition of using the superficial liquid velocity between 10 and 30 cm/min. Figure 6-23 also demonstrates the images of cell disruption observed by microscopic method. There is no damaged cell or cell debris observed under any condition mention above.



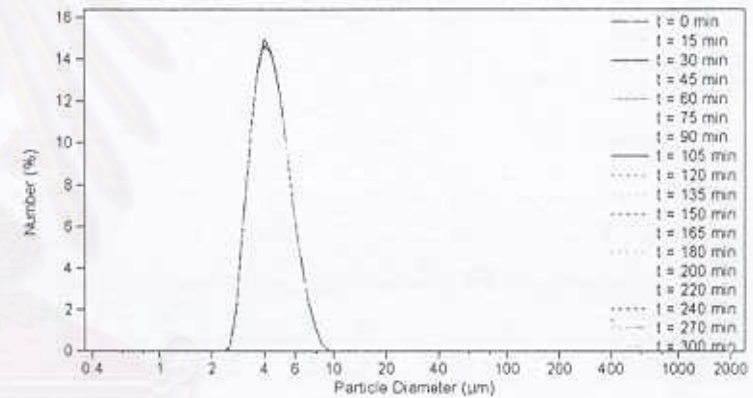
(a) 0 cm/min



(b) 10 cm/min



(c) 20 cm/min



(d) 30 cm/min

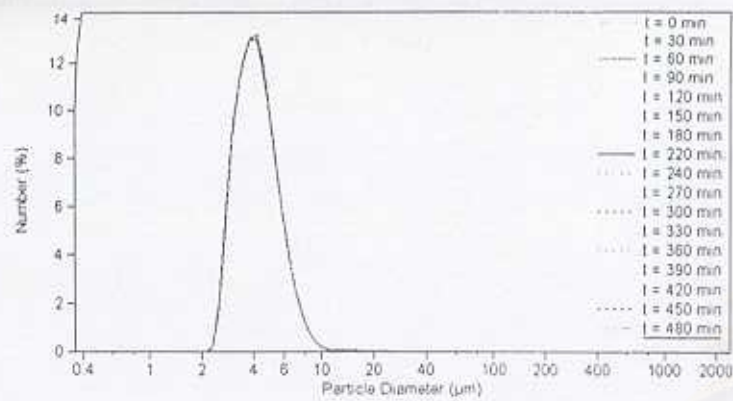
Figure 6-20. Yeast cell size distribution at various superficial gas velocity in the fluidized bed with draft tube (measured by Beckman Coulter LS 230)

$U_i = 0, 10, 20$  and  $30$  cm/min

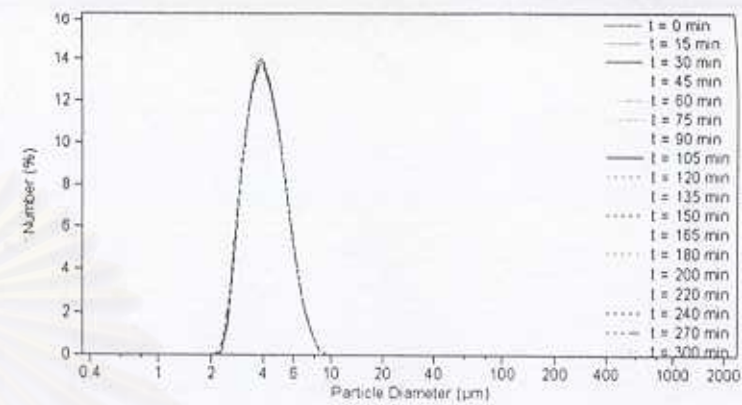
$U_g = 0$  cm/min

$N = 0$  rpm

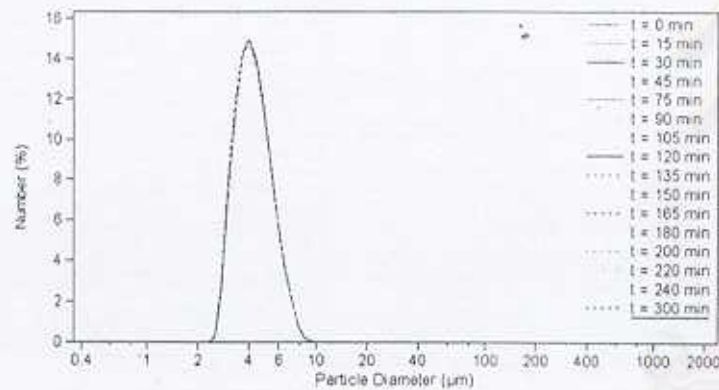
Absence of glass beads



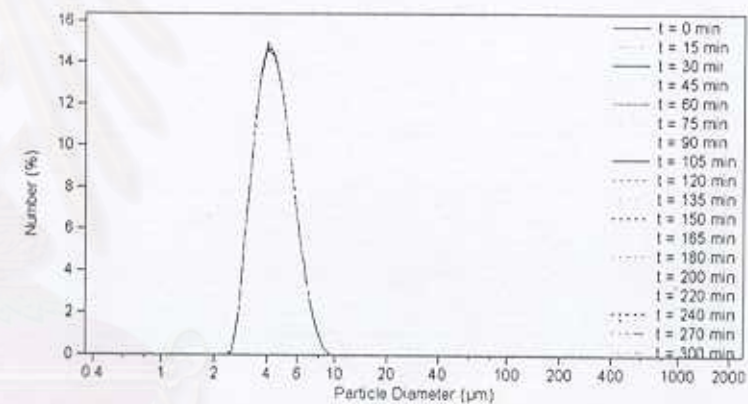
(a) 0 cm/min



(b) 10 cm/min



(c) 20 cm/min



(d) 30 cm/min

Figure 6-21. Yeast cell size distribution at various superficial gas velocity in the fluidized bed with draft tube (measured by Beckman Coulter LS 230)

$U_1 = 0, 10, 20$  and  $30$  cm/min

$U_g = 0$  cm/min

$N = 0$  rpm

Bead size =  $1000 \mu\text{m}$

Bead loading =  $1/3$  volume of annular fluidized bed



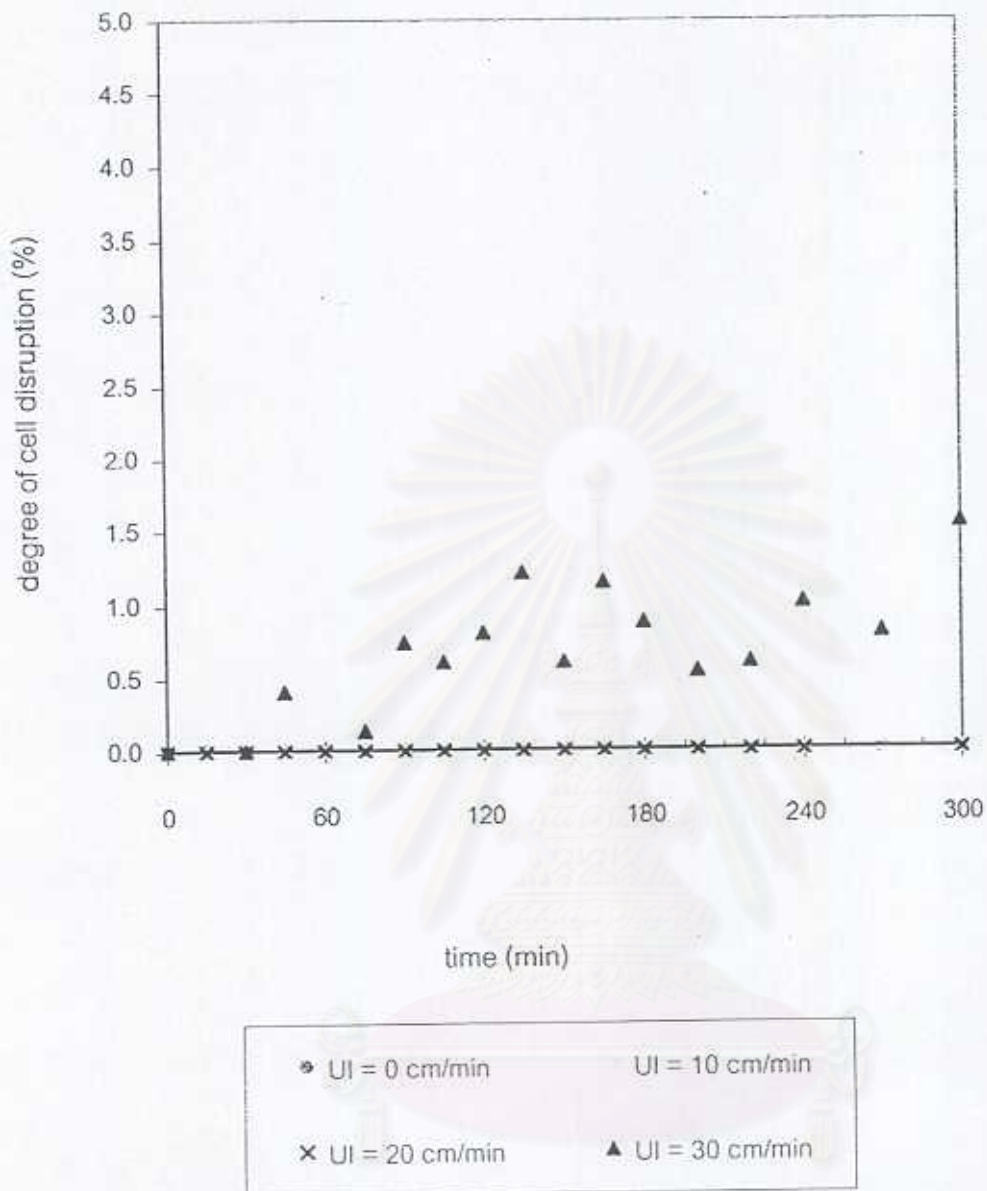


Figure 6-22. Influence of superficial liquid velocity on yeast cell disruption in the fluidized bed with draft tube

$U_j = 0, 10, 20$  and  $30$  cm/min

$U_g = 0$  cm/min

$N = 0$  rpm

Bead size =  $1000 \mu\text{m}$

Bead loading =  $1/3$  volume of annular fluidized bed

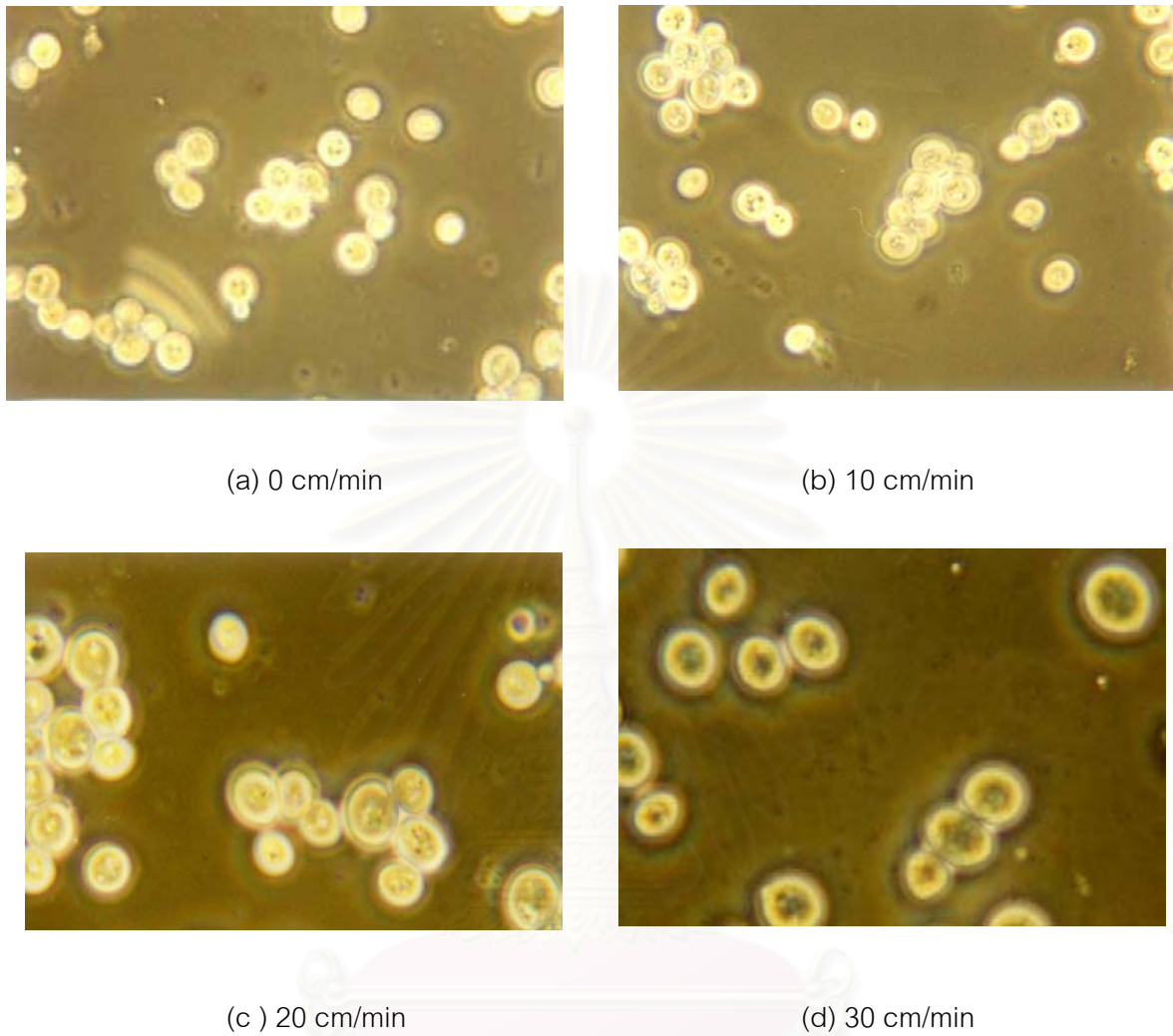


Figure 6-23. Yeast cell morphology at various superficial liquid velocities in the fluidized bed with draft tube after operated for 300 min (observed by Olympus Microscopoe B071)

$U_l = 0, 10, 20$  and  $30$  cm/min

$U_g = 0$  cm/min

$N = 0$  rpm

Bead size =  $1000 \mu\text{m}$

Bead loading =  $1/3$  volume of annular fluidized bed



## 6.5 Influence of Agitation and Superficial Gas Velocity on Yeast Cell Disruption

With the superficial gas velocity of 10 to 40 cm/min and no circulation of yeast suspension, a set of experiment was carried out to investigate the effect of impeller speeds (500, 1500, and 3000 rpm) in with the absence and presence of glass beads on the yeast cell disruption.

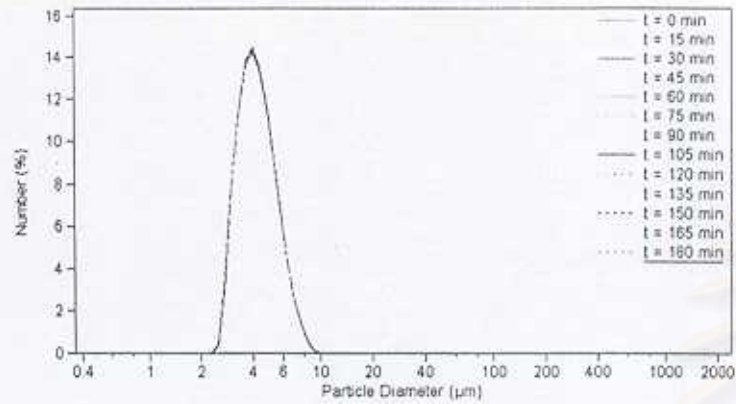
### 6.5.1 With absence of glass beads but with presence of draft tube

In the case of absence glass beads, the yeast cells size distributions are shown in Figure 6-24 and 6-25. The tendency similar to that of mentioned in section 6.2 was observed. It could be concluded here that the agitation accompanying with introduction of gas bubble had insignificant effect on the yeast cell disruption even the draft tube was installed into the system without glass beads.

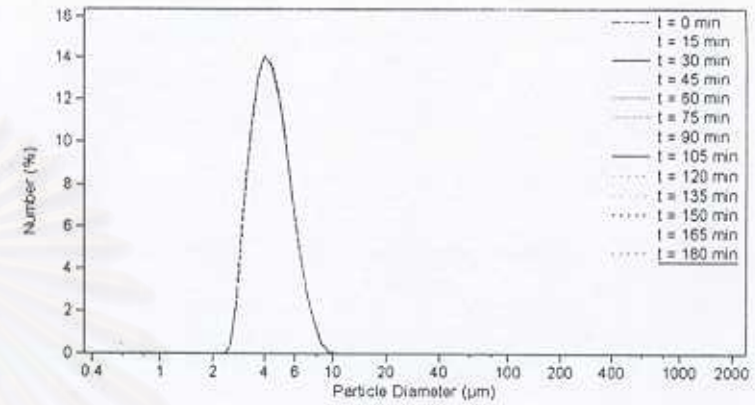
### 6.5.2 With presence of glass beads and draft tube

With the existing of the glass beads in the fluidized bed column, an increase in the impeller speed led to the cell size distribution shift toward the smaller size range regardless of the superficial gas velocity employed (Figure 6-26 and 6-27). Degree of cell disruption after operated for 180 min with the agitator speed of 3000 rpm was higher than that of 2000, 1500, and 500 rpm. Comparison of the results shown in Figure 6-28 and 6-29 suggest that there was no significant effect of the superficial gas velocity on the yeast cell disruption under the conditions of employing the agitation in the system, which was installed with the draft tube and loaded with the glass beads.

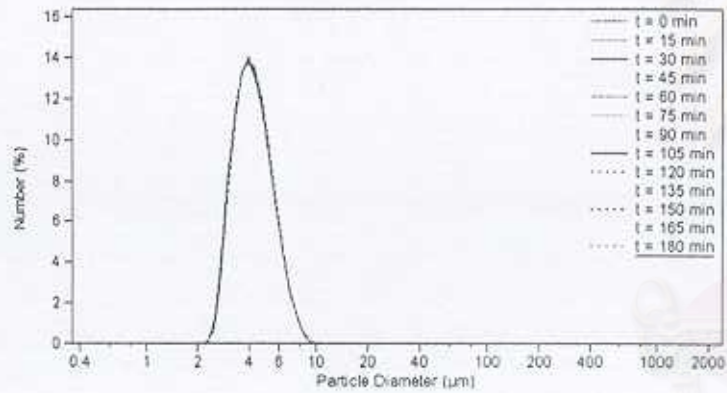
Figures 6-30 and 31 show that when the air was introduced into the system, the degree of cell disruption at a certain impeller speeds became smaller compared with that of the system without the introduction of air. Because dispersed bubbles might act as barrier of impacting among the yeast cell and other obstacles including the glass beads and the column wall. The air bubbles might decrease the vigorousness of the grinding, impacting, and shearing phenomena. Therefore, degree of cell disruption was found to decrease with the increase in the superficial gas velocity.



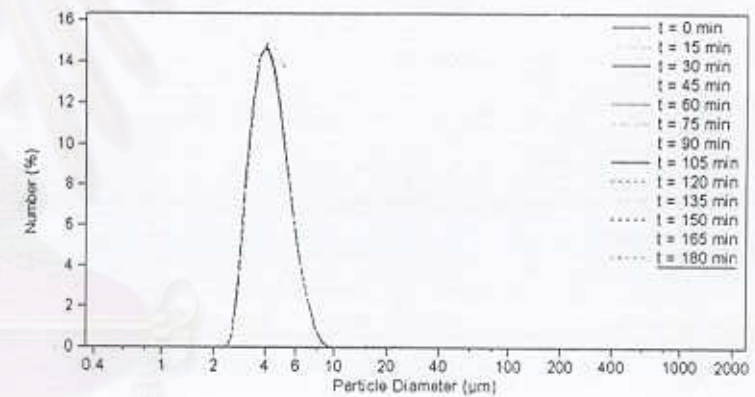
(a) 500 rpm



(b) 1500 rpm



(c) 2000 rpm



(d) 3000 rpm

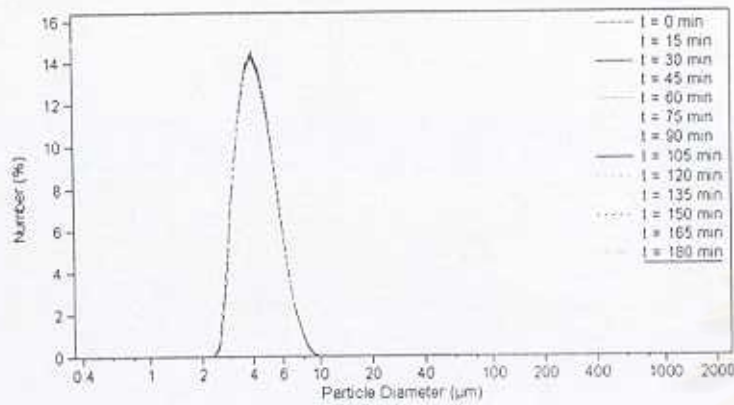
Figure 6-24. Yeast cell size distribution at various impeller speed in fluidized bed with draft tube measured by Beckman Coulter LS 230

$$U_i = 0 \text{ cm/min}$$

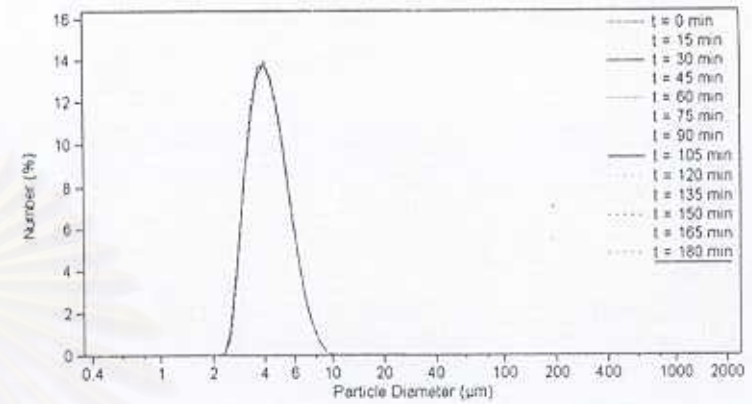
$$U_g = 10 \text{ cm/min}$$

$$N = 500, 1500, 2000 \text{ and } 3000 \text{ rpm}$$

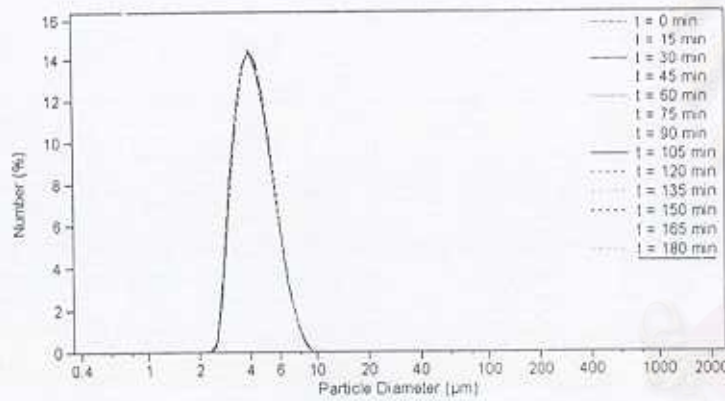
Absence of glass beads



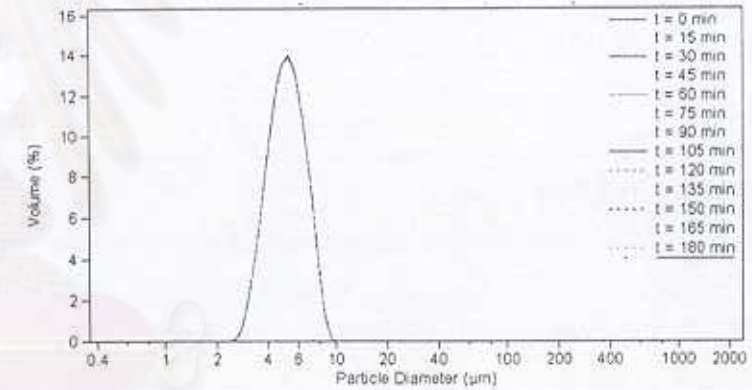
(a) 500 rpm



(b) 1500 rpm



(c) 2000 rpm



(d) 3000 rpm

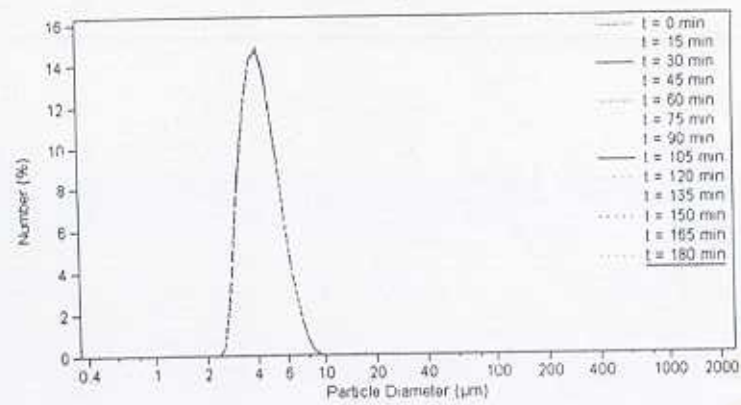
Figure 6-25. Yeast cell size distribution at various impeller speed in fluidized bed with draft tube measured by Beckman Coulter LS 230

$$U_i = 0 \text{ cm/min}$$

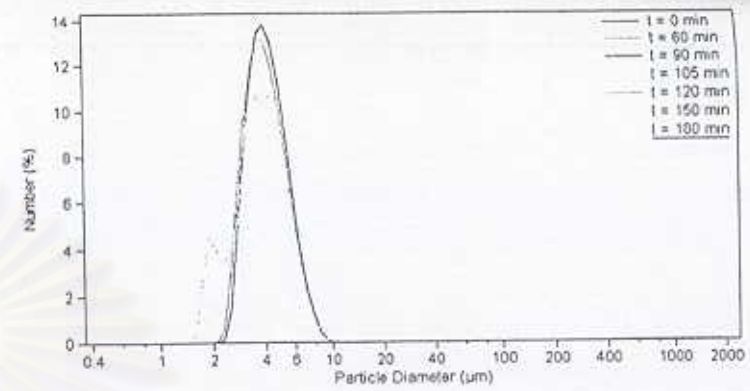
$$U_g = 40 \text{ cm/min}$$

$$N = 500, 1500, 2000 \text{ and } 3000 \text{ rpm}$$

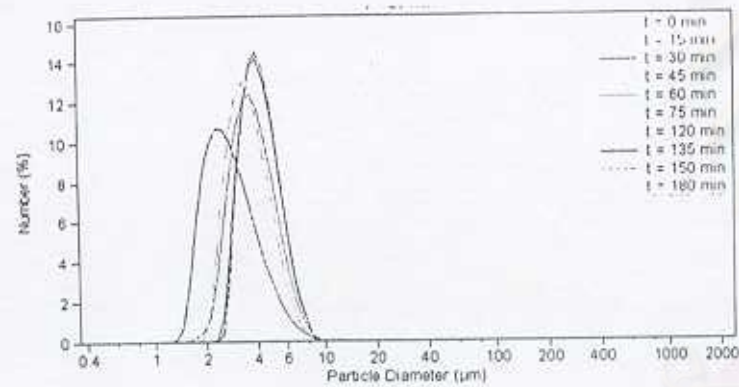
Absence of glass beads



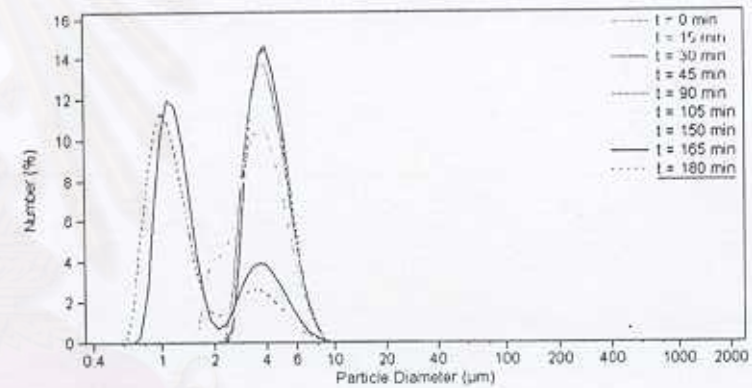
(a) 500 rpm



(b) 1500 rpm



(c) 2000 rpm



(d) 3000 rpm

Figure 6-26. Yeast cell size distribution at various impeller speed in the fluidized bed with draft tube (measured by Beckman Coulter LS 230)

$U_i = 0 \text{ cm/min}$

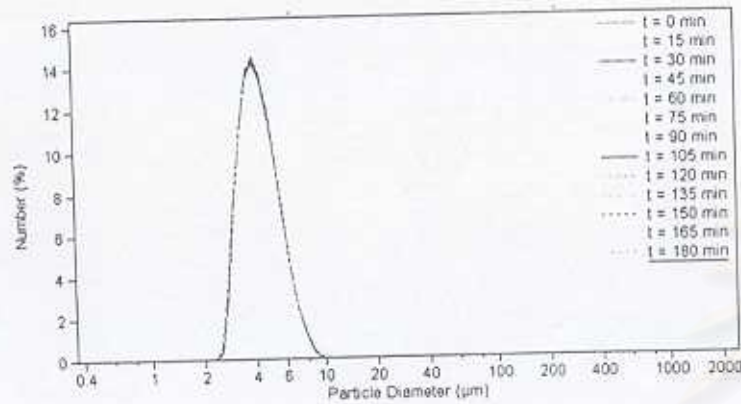
$U_g = 10 \text{ cm/min}$

$N = 500, 1500, 2000 \text{ and } 3000 \text{ rpm}$

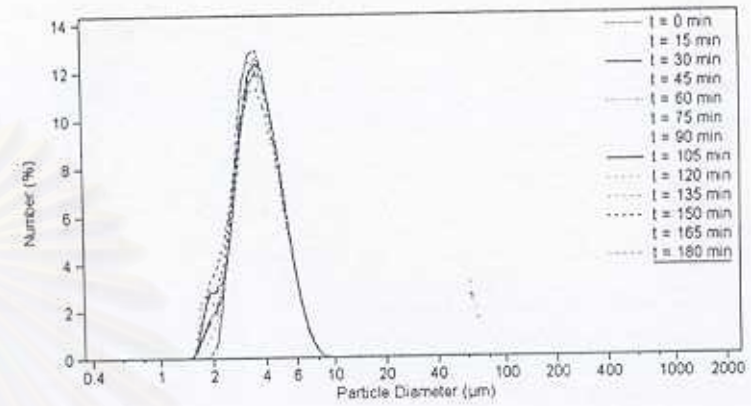
Bead size =  $1000 \mu\text{m}$

Bead loading =  $1/3$  volume of annular fluidized bed

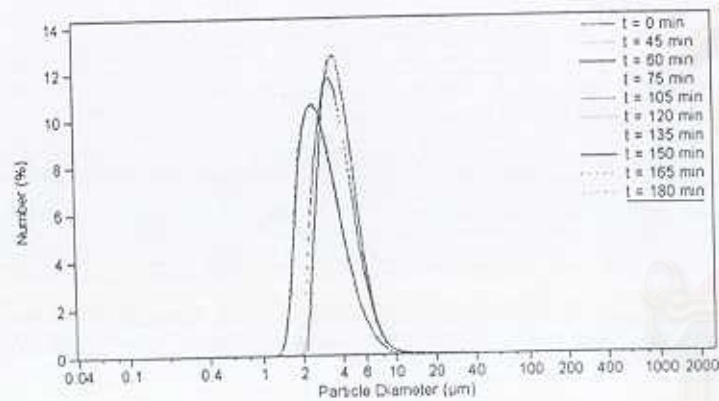




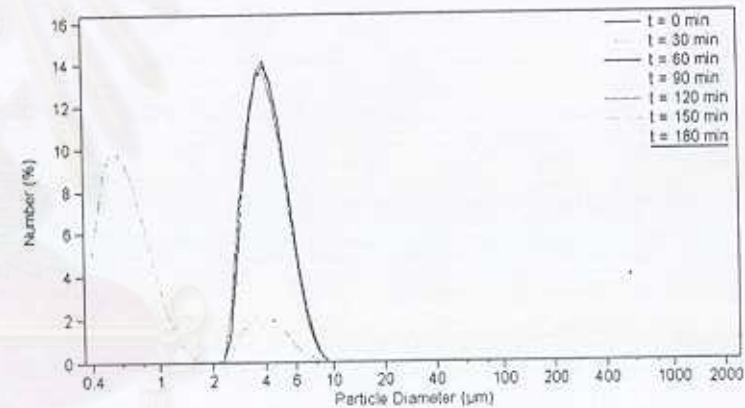
(a) 500 rpm



(b) 1500 rpm



(c) 2000 rpm



(d) 3000 rpm

Figure 6-27. Yeast cell size distribution at various impeller speed in the fluidized bed with draft tube (measured by Beckman Coulter LS 230)

$U_i = 0$  cm/min

$U_g = 40$  cm/min

$N = 500, 1500, 2000$  and  $3000$  rpm

Bead size =  $1000 \mu\text{m}$

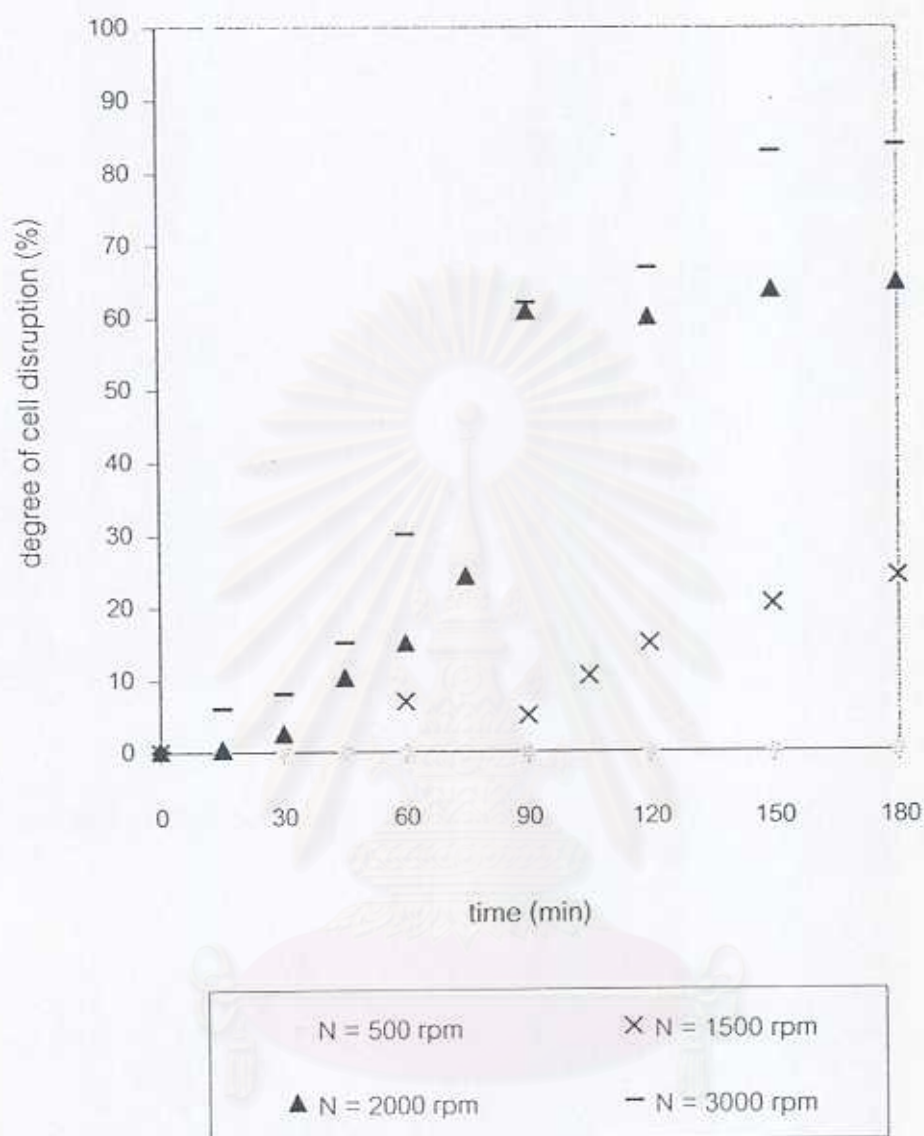


Figure 6-28. Influence of impeller speed on yeast cell disruption in the fluidized bed with draft tube

$$U_i = 0 \text{ cm/min}$$

$$U_g = 10 \text{ cm/min}$$

$$N = 500, 1500, 2000 \text{ and } 3000 \text{ rpm}$$

$$\text{Bead size} = 1000 \mu\text{m}$$

$$\text{Bead loading} = 1/3 \text{ volume of annular fluidized bed}$$



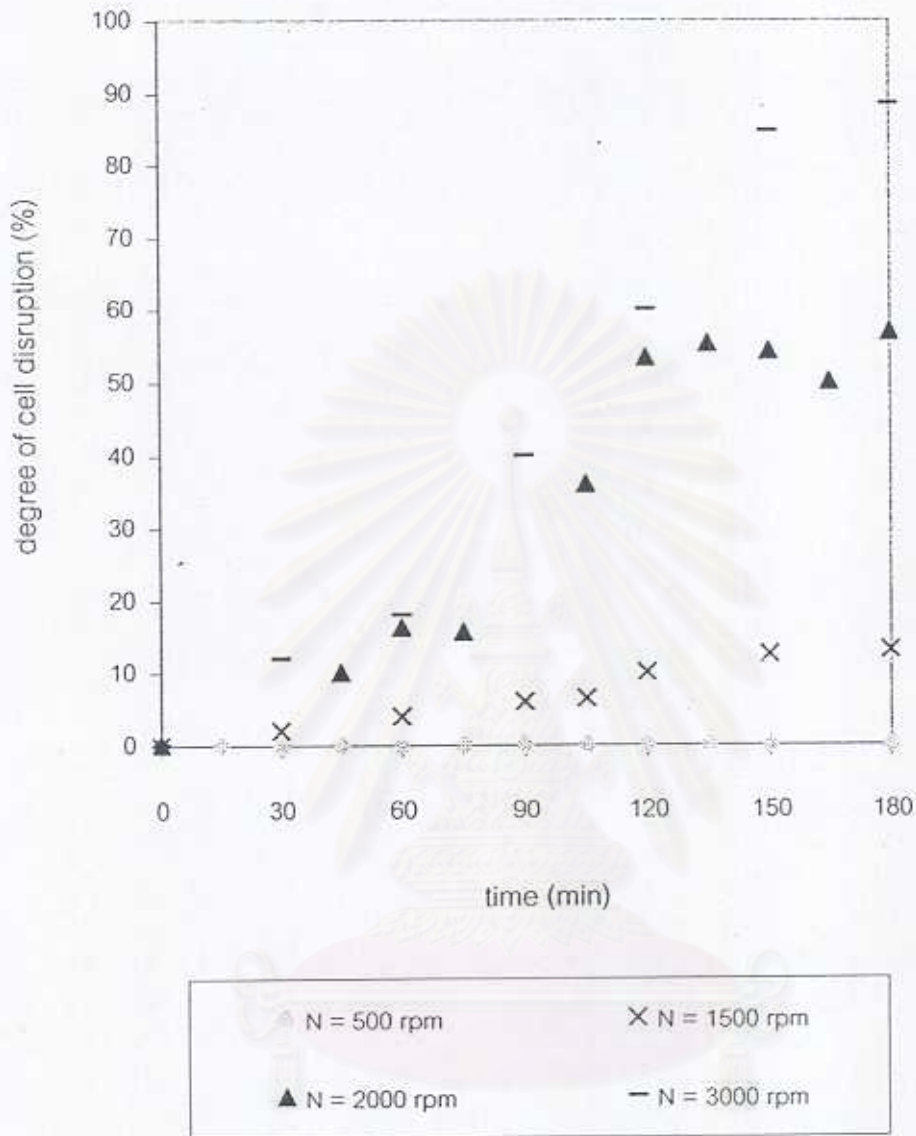


Figure 6-29. Influence of impeller speed on yeast cell disruption

in the fluidized bed with draft tube

$$U_l = 0 \text{ cm/min}$$

$$U_g = 40 \text{ cm/min}$$

$N = 500, 1500, 2000$  and  $3000$  rpm

Bead size =  $1000 \mu\text{m}$

Bead loading =  $1/3$  volume of annular fluidized bed

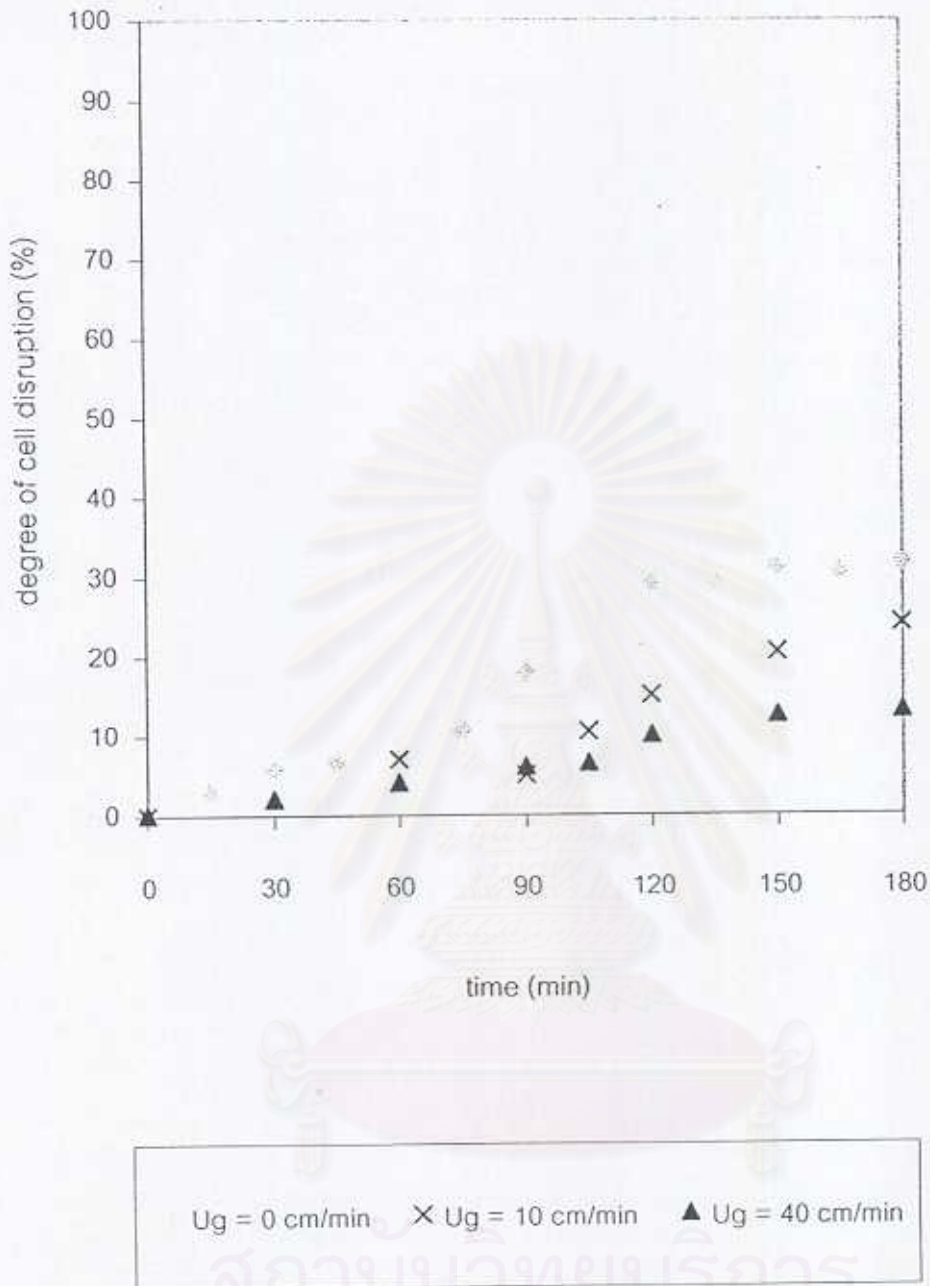


Figure 6-30. Influence of superficial gas velocity on yeast cell disruption in fluidized bed with draft tube

U<sub>I</sub> = 0 cm/min

U<sub>g</sub> = 0, 10 and 40 cm/min

N = 1500 rpm

Bead size = 1000 μm

Bead loading = 1/3 volume of annular fluidized bed

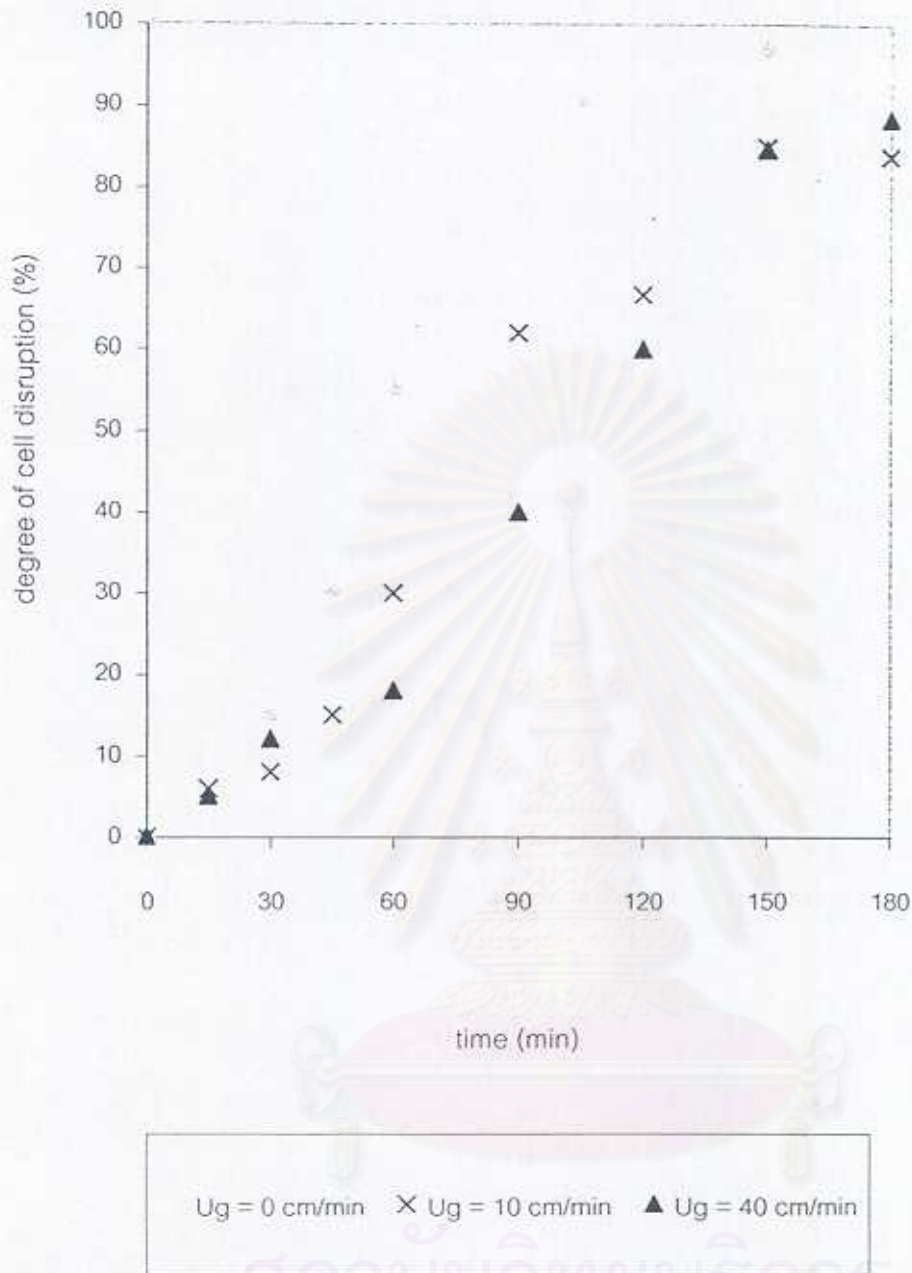


Figure 6-31. Influence of superficial gas velocity on yeast cell disruption

in the fluidized bed with draft tube

$U_l = 0$  cm/min

$U_g = 0, 10$  and  $40$  cm/min

$N = 3000$  rpm

Bead size =  $1000 \mu\text{m}$

Bead loading =  $1/3$  volume of annular fluidized bed

## 6.6 Influence of Superficial Gas Velocity on the Yeast Cell Disruption in Three-Phase Fluidized Bed System

The objective of this experiment is to investigate the effect of the superficial gas velocity on the yeast cell disruption in the continuously operated processes, which is accompanied with agitation and loaded with glass beads.

The effect of the gas superficial velocity on the degree of yeast cell disruption in the three-phase system operated continuously is shown in Figure 6-32. It could be seen that introduction of the air bubble into the system could hinder the yeast cell disruption. For confirmation, the content of protein released in the supernatant taken from the system was also examined (Figure 6-33). It was found that at the higher gas superficial velocity, the protein found in the suspension was less than that of no gas feed. This could be used to confirmed the concept that the air bubbles introduced into the system either in two-phase or three-phase condition would retard the yeast cell disruption due to their role as the contact barrier among the yeast cells and other obstacle in the system.

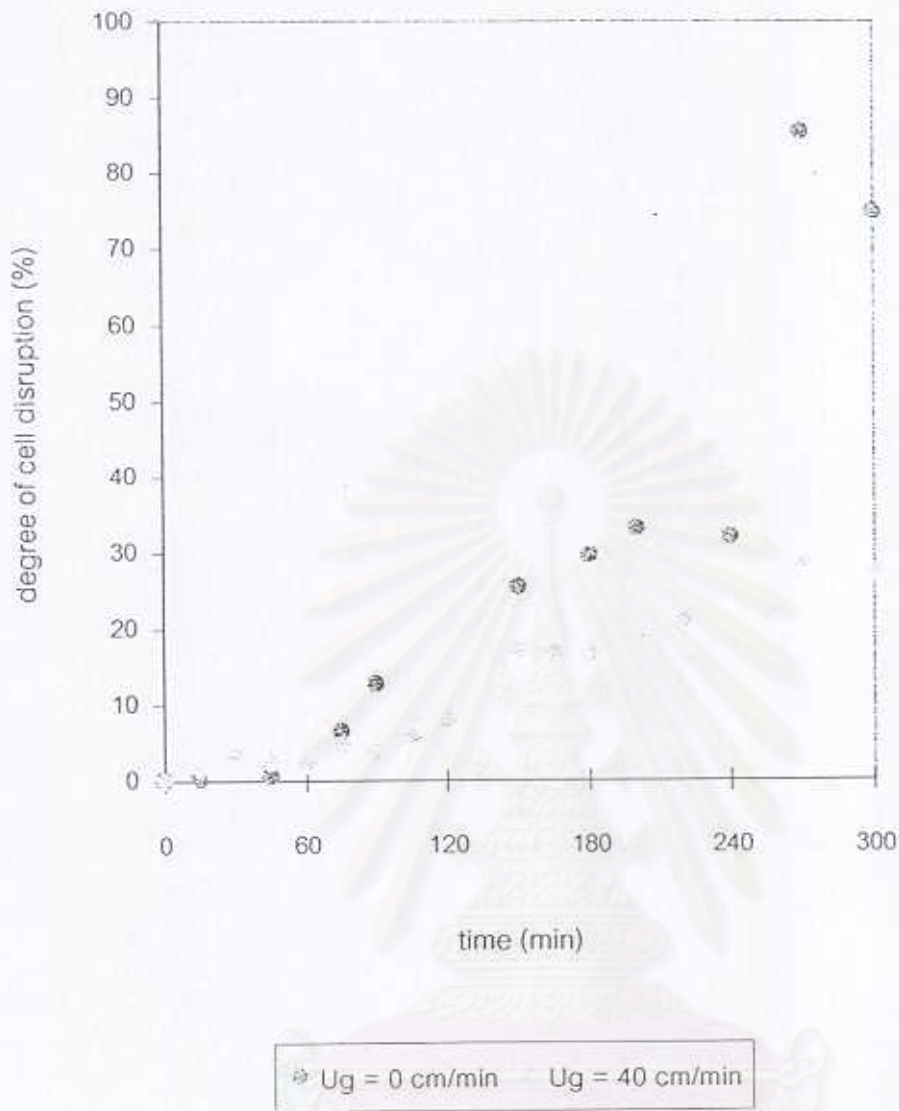


Figure 6-32. Influence of superficial gas velocity on yeast cell disruption in the fluidized bed with draft tube

$$U_i = 10 \text{ cm/min}$$

$$U_g = 0 \text{ and } 40 \text{ cm/min}$$

$$N = 3000 \text{ rpm}$$

$$\text{Bead size} = 1000 \mu\text{m}$$

$$\text{Bead loading} = 1/3 \text{ volume of annular fluidized bed}$$



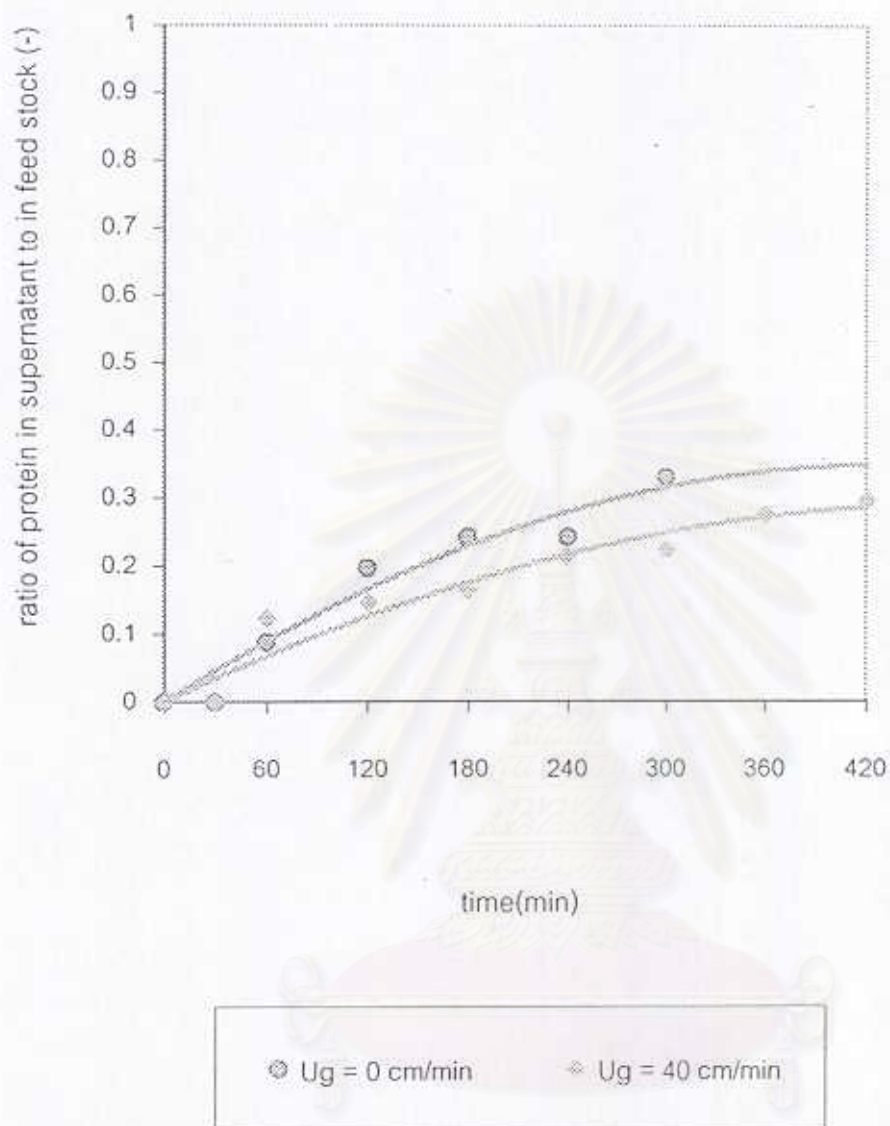


Figure 6-33. Content of protein released at various superficial gas velocity in the fluidized bed with draft tube (measured by Kjeldahl method (Tecator Kjeltec KD-02))

$$U_i = 10 \text{ cm/min}$$

$$U_g = 0 \text{ and } 40 \text{ cm/min}$$

$$N = 3000 \text{ rpm}$$

$$\text{Bead size} = 1000 \mu\text{m}$$

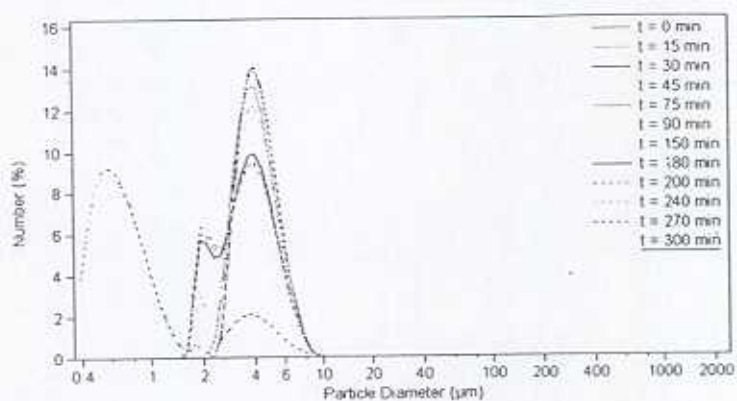
$$\text{Bead loading} = 1/3 \text{ volume of annular fluidized bed}$$



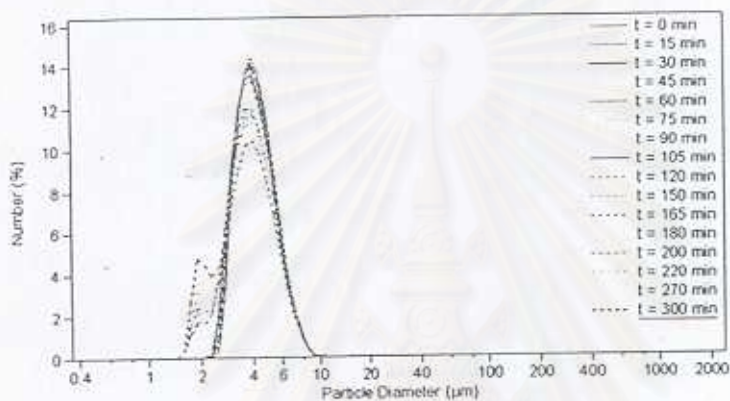
## 6.7 Influence of Superficial Liquid Velocity on the Yeast Cell Disruption in Three-Phase Fluidized Bed System

Similarly, the purpose of this experiment is to study the effect of superficial liquid velocity on the yeast cell disruption in the three-phase fluidized bed system. The disruption processes was carried out at the superficial gas velocity and the impeller speed of 10 cm/min and 3000 rpm, respectively in the fluidized bed column filled with glass beads.

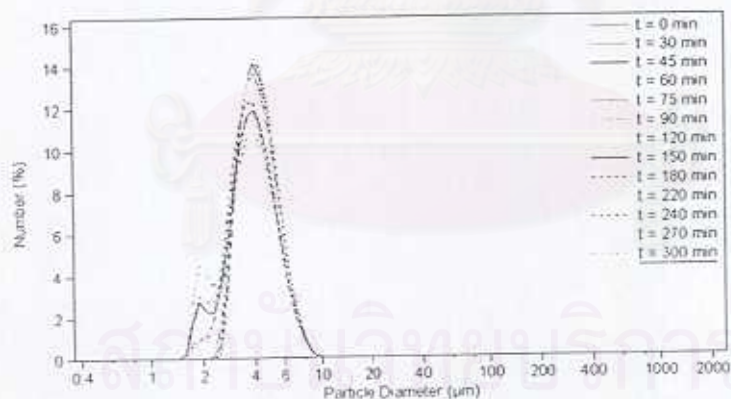
Figures 6-34 and 6-35 show the cell size distribution and the degree of cell disruption at superficial liquid velocity of 10 cm/min and 20 cm/min, respectively. The increase in the superficial gas velocity from 10 to 20 cm/min led to the decrease in the degree of cell disruption at the end of the operation time approximately from 80% to 30%. Similarly, the protein content in supernatant obtained from the condition of applying higher superficial liquid velocity became less than that of lower liquid flow rate. This might be implied that the increase in the liquid flow rate would decrease the resident time of the yeast cell suspension inside the system, in turn decreasing the probability of cells to be disrupted even though the shear rate in the system would become more rigorous (Figure 6-36). It could be concluded that the degree of cell disruption should approximately be inversely proportional to the liquid feed rate, which is also in fair agreement with the results reported by Kula and Schutte, 1987 and Middelberg A.P.J., 1995.



(a) 10 cm/min



(b) 20 cm/min



(c) 30 cm/min

Figure 6-34. Yeast cell size distribution at various superficial liquid velocity in the fluidized bed with draft tube

(measured by Beckman Coulter LS 230)

$U_l = 10, 20$  and  $30$  cm/min

$U_g = 10$  cm/min

$N = 3000$  rpm

Bead size =  $1000 \mu\text{m}$

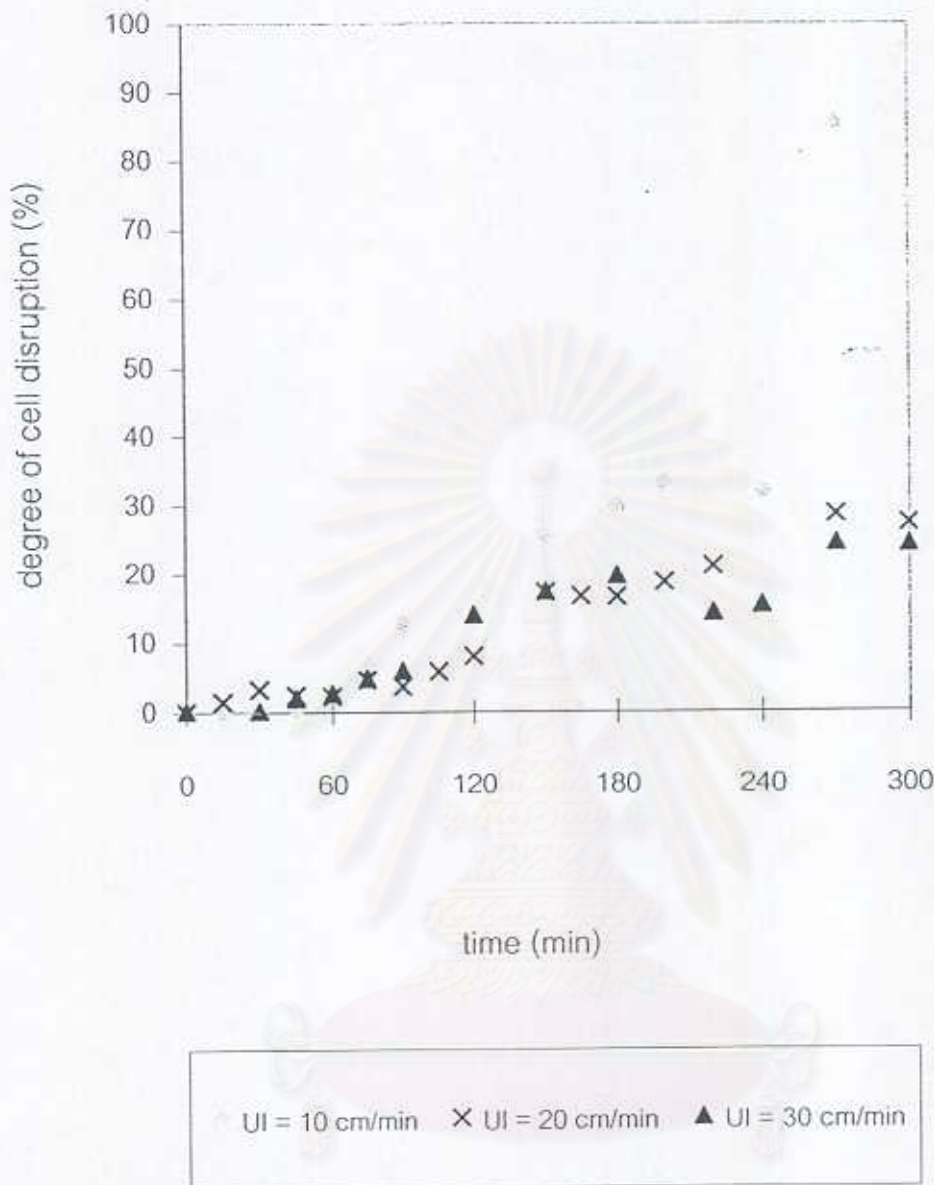


Figure 6-35. Influence of superficial liquid velocity on yeast cell disruption in the fluidized bed with draft tube

$$U_l = 10, 20 \text{ and } 30 \text{ cm/min}$$

$$U_g = 10 \text{ cm/min}$$

$$N = 3000 \text{ rpm}$$

$$\text{Bead size} = 1000 \mu\text{m}$$

$$\text{Bead loading} = 1/3 \text{ volume of annular fluidized bed}$$

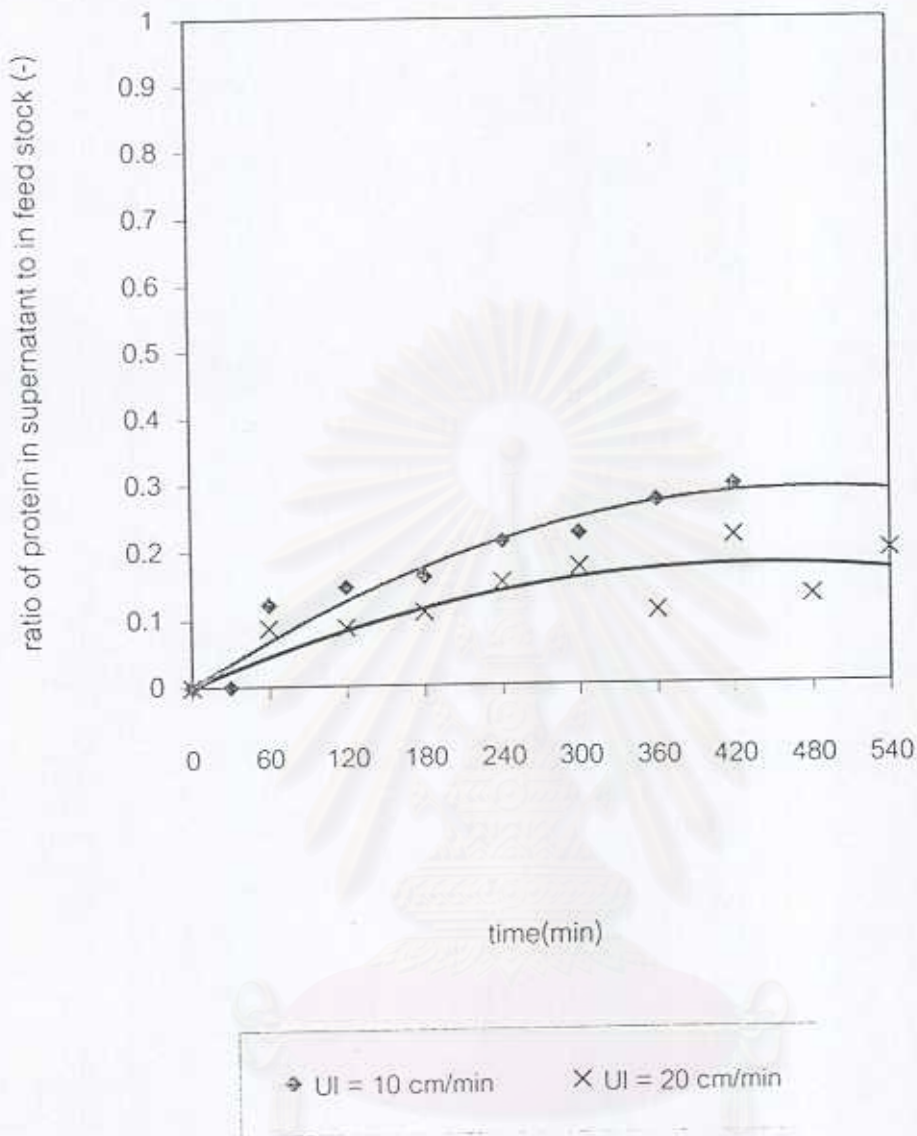


Figure 6-36. Content of protein released at various superficial liquid velocity in the fluidized bed with draft tube (measured by Kjeldahl method (Tecator Kjeltec KD-02))

$$U_i = 10, 20 \text{ and } 30 \text{ cm/min}$$

$$U_g = 10 \text{ cm/min}$$

$$N = 3000 \text{ rpm}$$

$$\text{Bead size} = 1000 \mu\text{m}$$

$$\text{Bead loading} = 1/3 \text{ volume of annular fluidized bed}$$

## 6.8 Influence of Bead Size on the Yeast Cell Disruption in Three-Phase Fluidized Bed System

Lead-free glass beads are the medium of choice for most biotechnology applications because of their inertness, abrasion resistance and low cost. In this experiment, lead-free glass beads are also employed as grinding media for disrupting yeast cells in the three-phase fluidized bed with agitator. The effect of bead size (1000  $\mu\text{m}$  and 2000  $\mu\text{m}$  in diameter) is investigated at the superficial gas velocity, superficial liquid velocity and impeller speed of 10 cm/min, 10 cm/min, and 3000 rpm, respectively. The results of cell size distribution and degree of cell disruption are illustrated in Figures 6-37 and 6-38, respectively. The cell size distributions obtained from the condition of employing 1000  $\mu\text{m}$  glass beads shifted toward to smaller size, while the degree of cell disruption was found to become detectable. No change in the yeast cell size distribution was observed when 2000  $\mu\text{m}$  glass beads were employed.

In addition, the microscopic evidences (Figure 6-39) clearly indicate that the 1000  $\mu\text{m}$  bead size could help break down the yeast cell. On the other hand, using 2000  $\mu\text{m}$  glass beads resulted in the insignificant change of the yeast cell morphology. No cell debris was found under the condition using the coarse glass beads.

It could be concluded that the smaller beads (1000  $\mu\text{m}$ ) were applicable for disruption the yeast suspension in the three-phase fluidized bed. For the same volume of filling, the number of beads as well as the specific surface area increases considerably with the decrease in the bead size, therefore increasing the probability of collision and grinding of the yeast cell by the glass beads (Millis J.R., 1997).



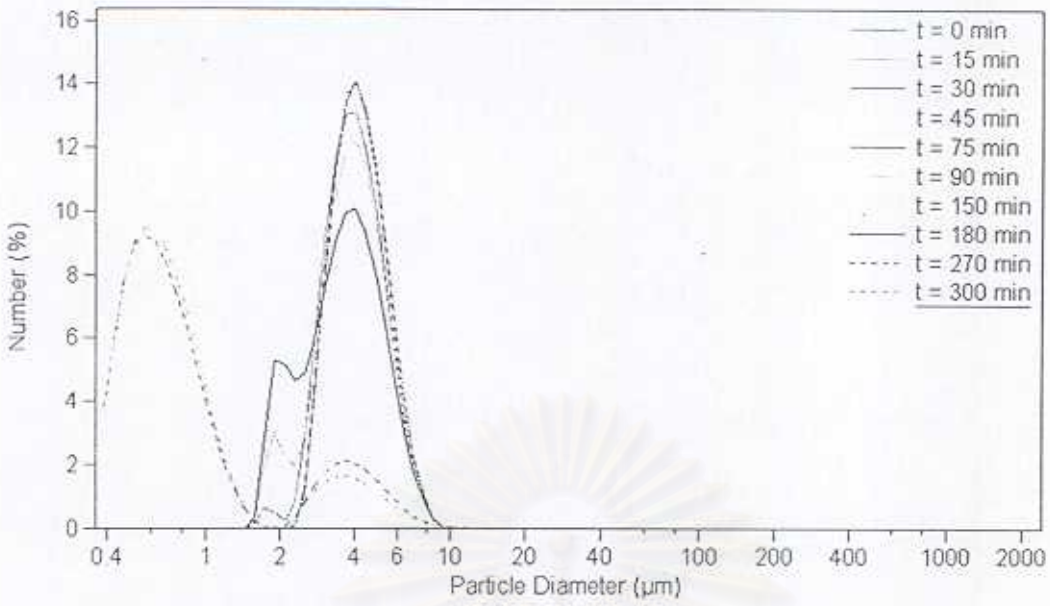
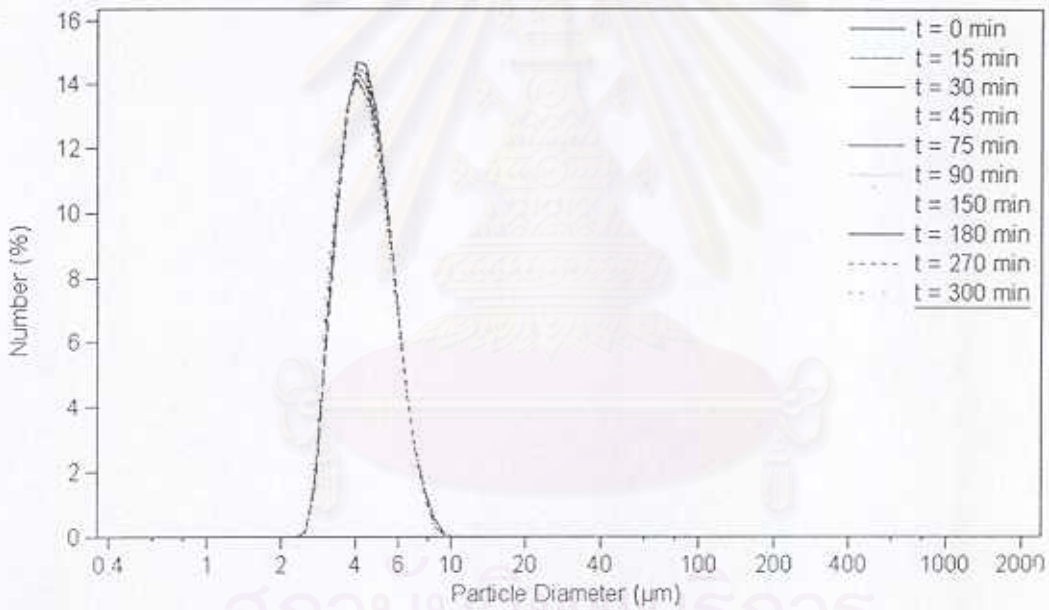
(a) 1000  $\mu\text{m}$ (b) 2000  $\mu\text{m}$ 

Figure 6-37. Yeast cell size distribution at different bead size in the fluidized bed with draft tube (measured by Beckman Coulter LS 230)

$$U_i = 10 \text{ cm/min}$$

$$U_g = 10 \text{ cm/min}$$

$$N = 3000 \text{ rpm}$$

$$\text{Bead size} = 1000 \text{ and } 2000 \mu\text{m}$$

$$\text{Bead loading} = 1/3 \text{ volume of annular fluidized bed}$$



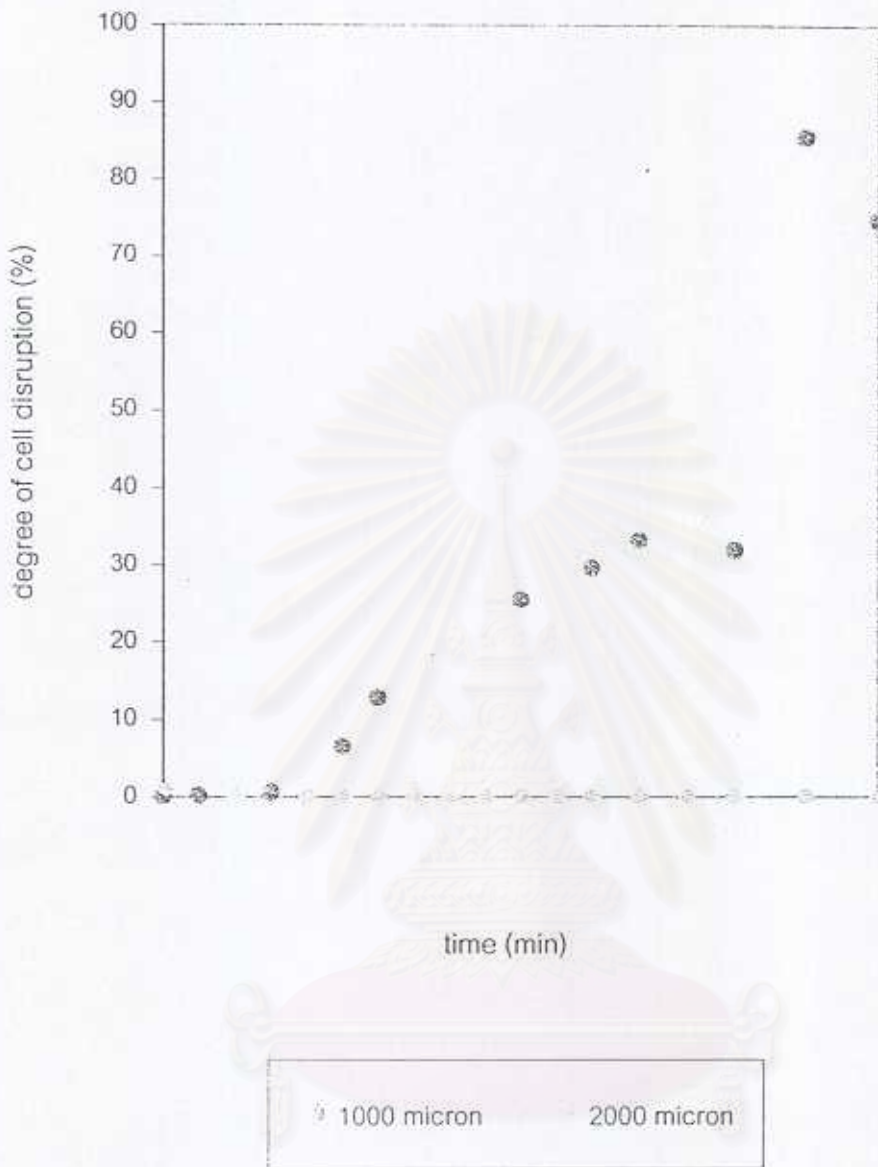


Figure 6-38. Influence of bead size on yeast cell disruption in the fluidized bed with draft tube

$$U_l = 10 \text{ cm/min}$$

$$U_g = 10 \text{ cm/min}$$

$$N = 3000 \text{ rpm}$$

Bead size = 1000 and 2000  $\mu\text{m}$

Bead loading = 1/3 volume of annular fluidized bed

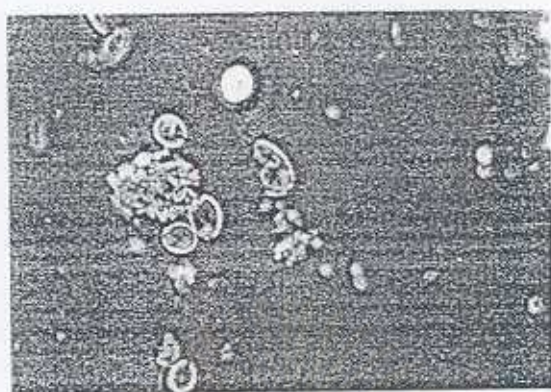
(a) 1000  $\mu\text{m}$ (b) 2000  $\mu\text{m}$ 

Figure 6-39. Yeast cell morphology at different bead size in the fluidized bed with draft tube after operated for 300 min (observed by Olympus Microscopoe B071)

$$U_i = 10 \text{ cm/min}$$

$$U_g = 10 \text{ cm/min}$$

$$N = 3000 \text{ rpm}$$

$$\text{Bead size} = 1000 \text{ and } 2000 \mu\text{m}$$

$$\text{Bead loading} = 1/3 \text{ volume of annular fluidized bed}$$

## 6.9 Influence of Low Impeller Speed in Three-Phase Fluidized Bed System without Draft Tube on the Yeast Cell Disruption

This experiment was carried out to examine the performance of disruption processes using three-phase fluidized bed unit in two different conditions. First, the disruption process was carried out in the fluidized bed column in which the coaxial draft tube was installed. One-third volume of the annular of fluidized bed column was filled up with glass beads. This disruption process was operated at the superficial gas velocity, superficial liquid velocity and speed of impeller of 10 cm/min, 10 cm/min, and 3000 rpm, respectively. Second, the disruption process was again operated in the fluidized bed column using low speed of impeller to avoid the erosion of glass beads but no draft tube was installed. This disruption process was operated at the superficial gas velocity, superficial liquid velocity and speed of impeller as 10 cm/min, 10 cm/min, and 25 rpm, respectively.

Figures 6-40 and 6-41 show the cell size distribution and the degree of cell disruption of two different systems. In the case of higher impeller speed with existing of draft tube, there was a shift of cell size distribution toward smaller size range and the degree of cell disruption became higher as the disruption time was extended. For lower impeller speed without using the draft tube, no change of the cell size distribution and the degree of cell disruption with respect to the disruption time were observed.

The protein content in supernatant, sampled from the condition of using lower impeller speed in the system without the draft tube, indicates that no cell disruption took place in the system.

The another evidence to conclude that under the mild condition of low impeller speed there was no significant disruption of the yeast cell is the microscopic observation of yeast illustrated in Figure 6-42. It can be seen that there is no change of cell shape and cell size after processing at low impeller speed without using draft tube. While the cell debris and the intracellular material released were observed at higher impeller speed and with using draft tube, there was no change of the yeast cell observed at the condition of lower impeller speed.

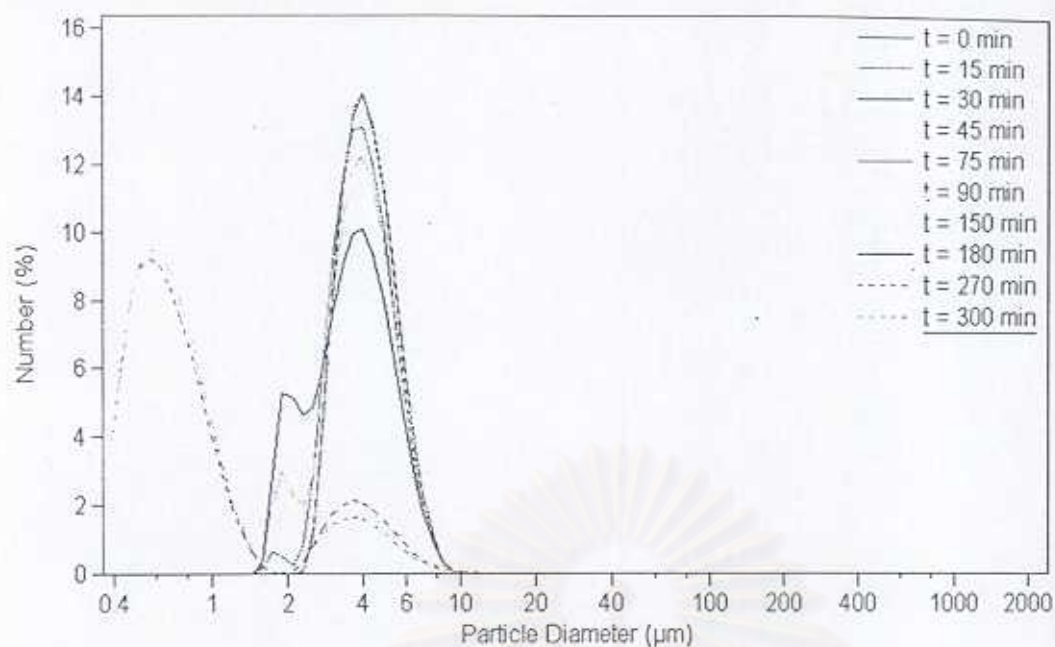
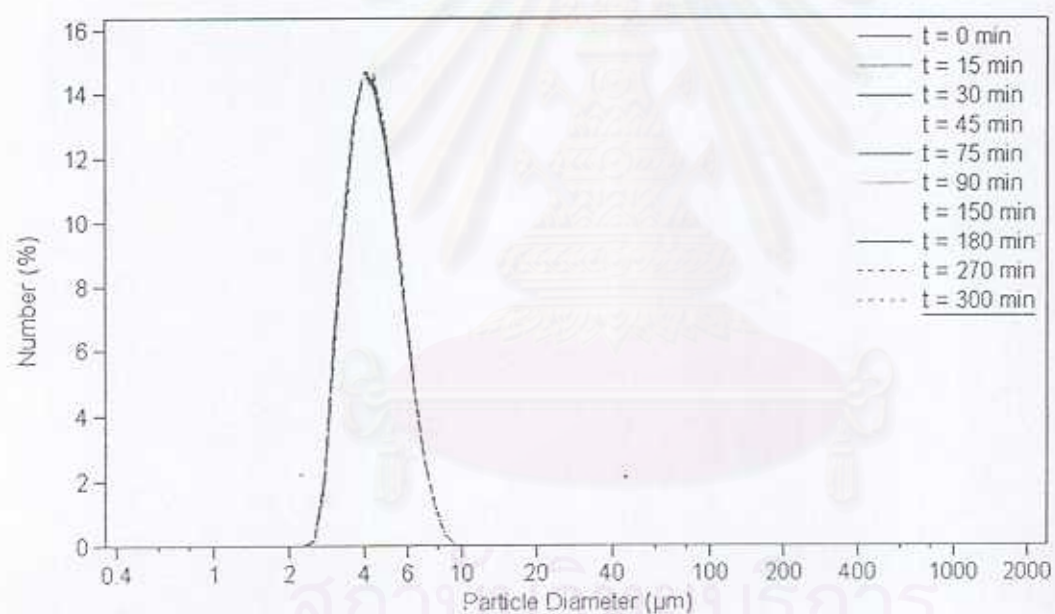
(a)  $N = 3000$  rpm, fluidized bed with draft tube(b)  $N = 25$  rpm, fluidized bed without draft tube

Figure 6-40. Yeast cell size distribution comparison between low impeller speed in the fluidized bed without draft tube and high impeller speed in the fluidized bed with draft tube

(measured by Beckman Coulter LS 230)

$$U_i = 10 \text{ cm/min}$$

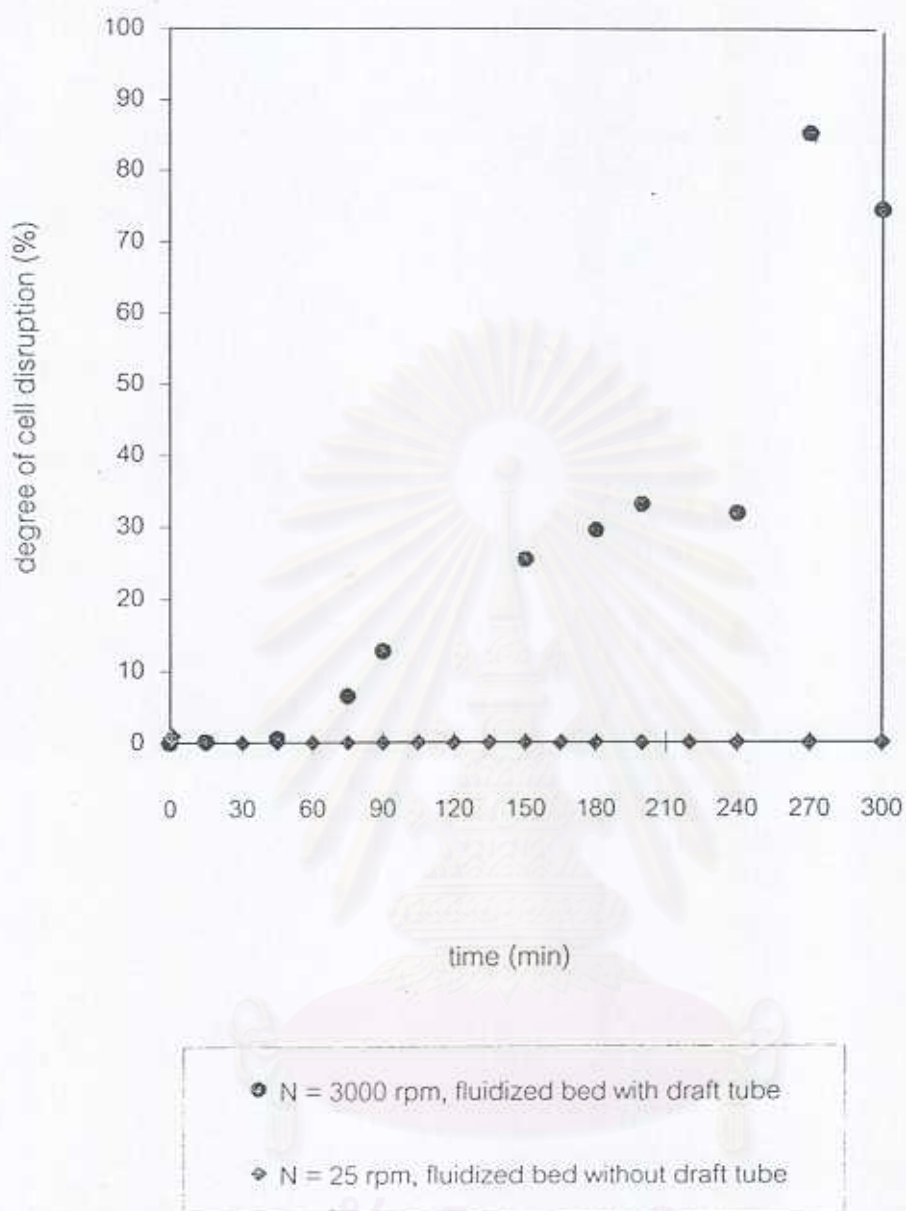
$$U_g = 10 \text{ cm/min}$$

$$N = 25 \text{ and } 3000 \text{ rpm}$$

$$\text{Bead size} = 1000 \text{ } \mu\text{m}$$

$$\text{Bead loading} = 1/3 \text{ volume of annular fluidized bed}$$





6-41. Comparison of degree of cell disruption examined under the conditions of between low impeller in the fluidized bed without draft tube and high impeller speed in the fluidized bed with draft tube

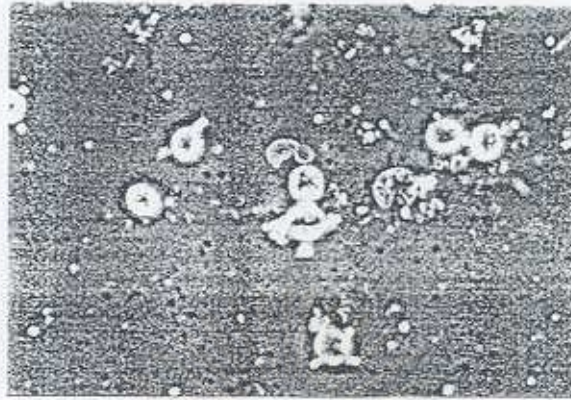
$$U_i = 10 \text{ cm/min}$$

$$U_g = 10 \text{ cm/min}$$

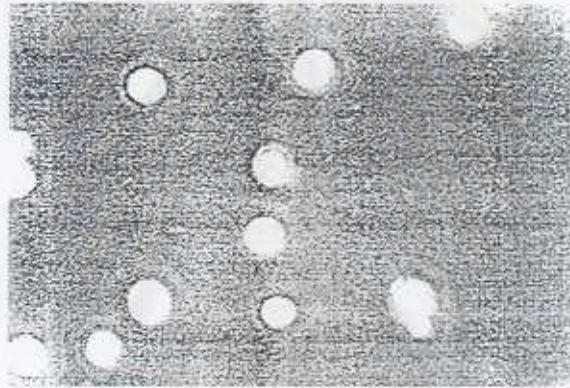
$$N = 25 \text{ and } 3000 \text{ rpm}$$

$$\text{Bead size} = 1000 \mu\text{m}$$

$$\text{Bead loading} = 1/3 \text{ volume of annular fluidized bed}$$



(a)  $N = 3000$  rpm, fluidized bed with draft tube



(b)  $N = 25$  rpm, fluidized bed without draft tube

Figure 6-42. Comparison of the yeast cell morphology investigated under the conditions of low impeller speed in the fluidized bed without draft tube and high impeller speed in the fluidized bed with draft tube at 300 min (observed by Olympus Microscope B071)

$$U_i = 10 \text{ cm/min}$$

$$U_g = 10 \text{ cm/min}$$

$$N = 25 \text{ and } 3000 \text{ rpm}$$

$$\text{Bead size} = 1000 \mu\text{m}$$

$$\text{Bead loading} = 1/3 \text{ volume of annular fluidized bed}$$



## CHAPTER 7

### CONCLUSIONS AND RECOMMENDATIONS

This chapter will be focused on conclusions of all experimental details on operating parameters of gas-liquid-solid fluidized bed with agitation. In section 7.2, the recommendations for further study will be extended.

#### 7.1 Conclusions

##### 7.1.1 In the case of absence of glass beads

1. Increasing the impeller speed between in the range of 500 rpm and 3000 rpm does not affect on yeast cells disruption whether or not the air bubbles are present in the system.
2. The installation of the coaxial draft tube in the fluidized bed column does not increase the yeast cell disruption at any impeller speed compared with the system without the draft tube.
3. Introduction of bubbles into the column does not affect the yeast cell disruption whether the agitation is employed or not.
4. The circulation of yeast suspension using the centrifugal pump at the feed rate between 10 cm/min and 30 cm/min provides insignificant influence on the yeast cell disruption.

### 7.1.2 In the case of presence of glass beads

1. The degree of yeast cell disruption increases with the increase in the impeller speed in the range of 500 rpm and 3000 rpm regardless of the absence or presence of the air bubbles in the system.
2. Introduction of the air bubbles into the system without agitation and circulation of yeast suspension does not affect yeast cell disruption.
3. The increase in the superficial gas velocity between 10 cm/min and 40 cm/min in the fluidized bed with draft tube and presence of glass beads lead to the decrease in the degree of yeast cell disruption because the bubbles is acting as barrier between the glass beads and yeast cells. In addition, the bubbles can absorb the energy from the agitator employed in the system.
4. Only circulation of yeast suspension through the three-phase fluidized bed column without agitation provides insignificant influence on the yeast cell disruption.
5. The increase the superficial liquid velocity retards the degree of yeast cell disruption in the three-phase fluidized bed system due to the decrease in the mean residence time.
6. Glass beads with a diameter as 1000  $\mu\text{m}$  contribute to the degree of yeast cell disruption higher than that of 2000  $\mu\text{m}$ . The reason is that the smaller beads have larger surface area than the larger bead.
7. The yeast cell rupture becomes inefficient at low impeller speed (25 rpm) although the direct contact between glass beads and impeller blades is employed.

Finally, it can be concluded that the three-phase fluidized bed with agitator has potential to be applied as the disrupting equipment for yeast cells.

## 7.2 Recommendation for further study

1. The influence of the bead loading should be studied to maximize the grinding elements.
2. An increase in the concentration of yeast suspension to cover the range employed in the commercial scale.
3. Modify the reactor design such as increasing the number of impellers and the pinhole around the draft tube as well as changing the design of impeller.
4. Develop the more efficient cooling system to control the disruption temperature and prevent the denaturation of protein.



สถาบันวิทยบริการ  
จุฬาลงกรณ์มหาวิทยาลัย

## REFERENCES

- Agerkvist, I.; and Enfors, S. O. *Biotechnol. Bioeng.* 36(1990): 1083 – 1089.
- Andrews, B. A.; and Asenjo, J. A. *Biotechnol. Bioeng.* 28(1986): 1366 – 1375.
- Asenjo, J. A.; and Dunnill, P. *Biotechnol. Bioeng.* 23(1981): 1045 – 1056.
- Bierau, H; Zhang, Z; and Lydditt, A. *J. Chem. Technol. Biotechnol.* 74(199): 208-212.
- Bowen, W. R.; Sabuni, H. A. M.; and Ventham, T. J. *Biotechnol. Bioeng.* 40(1992):  
1309 – 1318.
- Brookman, J.S.G. *Biotechnol. Bioeng.* 14(1974): 371-383.
- Brookman, J.S.G. *Biotechnol. Bioeng.* 18(1975): 465-479.
- Bunge, F.; Pietzsch, M.; Muller, R.; and Syldalk, C. *Chem. Eng. Sci.* 47(1992): 225 – 232.
- Carlson, A.; Signs, M.; Liermann, L.; Boor, R.; and Jem, K. J. *Biotechnol. Bioeng.* 48(1995):  
303 – 315.
- Clarkson, A. I.; Lefevre, P.; and Titchener – Hooker, N. J. *Biotechnol. Prog.* 9(1993):  
462 – 467.
- Chalmers, J. J. *Cytotechnol.* 15(1994): 311 – 320.
- Chisti, Y.; and Moo – Young, M. *Enzyme Microb. Technol.* 8(1986): 194 – 204.
- Choi, H.; Laleye, L.; Amantea, G.F.; and Simard, R.E. *Biotechnol. Techniq.* 11(1997):  
451-453.
- Cumming, R. H.; Tuffnell, J.; and Street, G. *Biotechnol. Bioeng.* 27(1985): 887 –889.
- Cunningham, S. D.; Cater, C. M.; and Mattil, K. F. *J. Food Sci.* 40(1975): 732 – 735.
- Currie, J. A.; Dunnill, P.; and Lilly, M.D. *Biotechnol. Bioeng.* 14(1972): 725 – 736.
- David, J. M.; Alen, J. M.; and Jame, C. P. *Biochem. J.* 135(1973): 19 – 30.
- Doulah, M.S.; Hammond, T.H.; and Brookman, J.S.G. *Biotechnol. Bioeng.* 17(1975):  
845-858.
- Engler, C. R.; and Robinson, C. W. *Biotechnol. Bioeng.* 21(1979): 1861 - 1869.
- Follows, M.; Hetherington, P. J.; Dunnill, P.; and Lilly, M. D. *Biotechnol. Bioeng.* 13(1971):  
549 – 560.
- Gianfreda, L.; Modefferi, M.; and Guido, G. J. *Enzyme Microb. Technol.* 7(1976): 78 – 82.

- Hedenskog, G.; and Mogren, H. **Biotechnol. Bioeng.** 15(1973): 129-142.
- Heim, A; and Solecki, M. **Powder Technol.** 105(1999): 389-395.
- Hunter, J. B.; and Asenjo, J. A. **Biotechnol. Bioeng.** 30(1987): 481 – 490.
- Keleman, M. V.; and Sharpe, J. E. E. **J. Cell Sci.** 35(1979): 431 – 441.
- Keshavarz, M. E.; Hoare, M.; and Dunnill, P. **Enzyme Microb. Technol.** 12(1990): 764 – 770.
- Kleinig, A. R.; and Middelberg, A. P. J. **Chem. Eng. Sci.** 53(1998): 891 – 898.
- Lander, R.; Manger, W.; Scouloudis, M.; Ku, A.; Davis, C.; and Lee, A. **Biotechnol. Prog.** 16(2000): 80 – 85.
- Limon-Lasom, J.; Hoare, M; Orsborn, C. B.; Doyle, D.J.; and Dunnill, P. **Biotechnol. Bioeng.** 21(1979): 745-774.
- Marffy, F.; and Kula, M.R. **Biotechnol. Bioeng.** 16(1974): 623-634.
- Middelberge, A. P. J. **Biotechnol. Adv.** 13(1995): 491 – 551.
- Millburn, P. T.; and Dunnill, P. **Biotechnol. Bioeng.** 44(1994): 736 – 744.
- Morohashi, S.; Okada, S.; Hataya, T.; Sasaki, T.; Hoshino, K.; and Sasakura, T. **J. Chem. Eng. Jap.** 3(1997): 182 – 186.
- Mosqueira, F. G.; Higgins, J. J.; Dunnill, P.; and Lilly, M. D. **Biotechnol. Bioeng.** 23(1981): 335 – 343.
- Rechacek; J.; and Schaefer; J. **Biotechnol. Bioeng.** 19(1977): 1523-1534.
- Ricci-Silva, M. E.; Vitolo, M.; and Abrahao-Neto, J. **Proc. Biochem.** 35(2000): 831-835.
- Sauer, T.; Robinson, C. W.; and Gilk, B. R. **Biotechnol. Bioeng.** 33(1989): 1330 –1342.
- Schutte, H.; and Kula, M. **Biotechnol. App. Biochem.** 12(1990): 599 – 620.
- Scully, D.B.; and Wimpenny. J.W.T. **Biotechnol. Bioeng.** 16(1974): 675-687.
- Shamlou, P. A.; Makagiansar, A. P. I.; and Lilly, M. D. **Chem. Eng. Sci.** 49(1994): 2621 – 2631.
- Shamlou, P. A.; Siddiqi, S. F.; and Titchener – Hooker, N. J. **Chem. Eng. Sci.** 50(1995): 1383 – 1391.
- Shirgaondar, I. Z.; Lothe, R. R.; and Pandit, A. B. **Biotechnol. Prog.** 14(1998): 657 - 660.
- Shimizu, M.; Matsuyama, T.; and Yamamoto, H. Proceeding by 6<sup>th</sup> Asian Conference on Fluidized-Bed and Three-Phase Reactor, Edt. By Hai-Soo Chun and Sang-Done Kim, 1998.

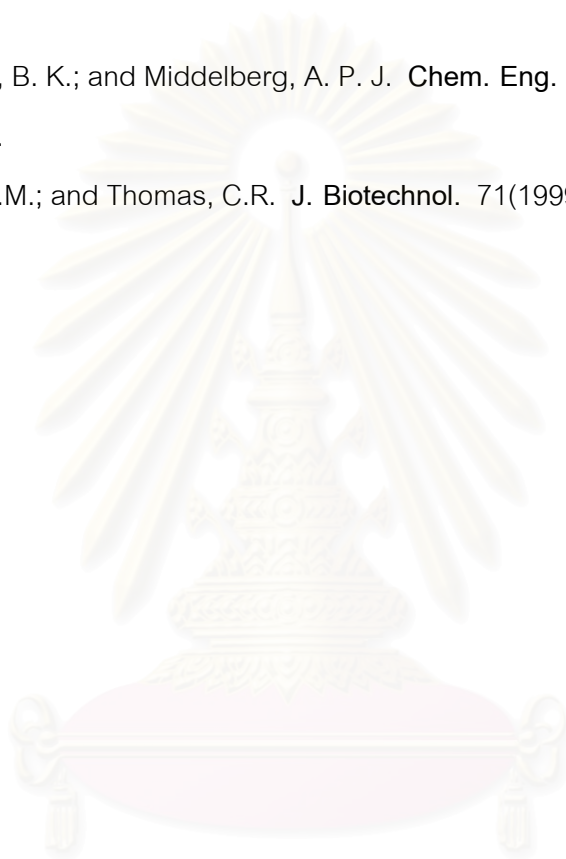
Siddiqi, S. F.; Titchener – Hooker, N. J.; and Shamlou, P. A. *Biotechnol. Bioeng.* 50(1995): 145 – 150.

Siddiqi, S. F.; Titchener – Hooker, N. J.; and Shamlou, P. A. *Biotechnol. Bioeng.* 55(1997): 642 – 649.

Smith, A. E.; Moxham, K. E.; and Middelberg, A. P. J. *Chem. Eng. Sci.* 55(2000): 2043-2053.

Wong, H. H.; O'Neill, B. K.; and Middelberg, A. P. J. *Chem. Eng. Sci.* 52(1997): 2883 – 2890.

Zhang, Z; Blewett, J.M.; and Thomas, C.R. *J. Biotechnol.* 71(1999): 17-24.



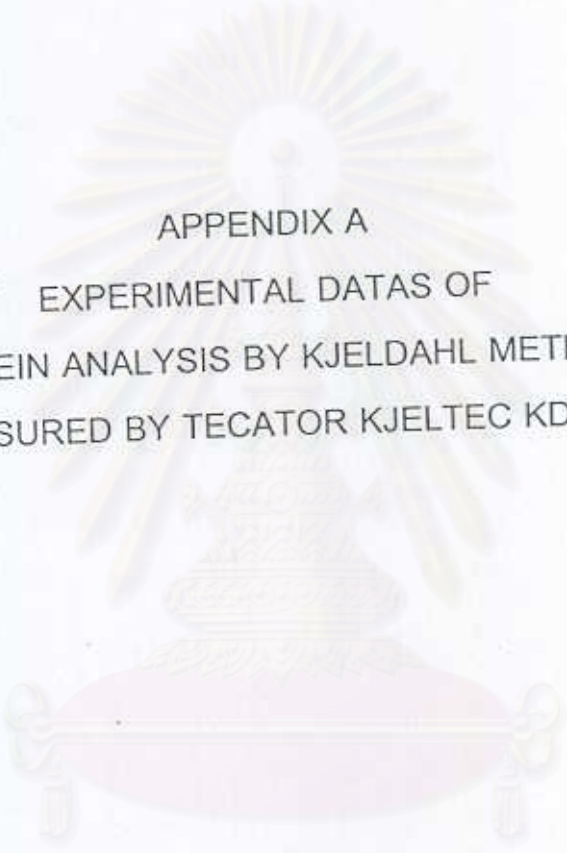
สถาบันวิทยบริการ  
จุฬาลงกรณ์มหาวิทยาลัย





## APPENDIX

สถาบันวิทยบริการ  
จุฬาลงกรณ์มหาวิทยาลัย



APPENDIX A  
EXPERIMENTAL DATAS OF  
PROTEIN ANALYSIS BY KJELDAHL METHOD  
MEASURED BY TECATOR KJELTEC KD-02

สถาบันวิทยบริการ  
จุฬาลงกรณ์มหาวิทยาลัย

## Protein assay by Kjeldahl method

Analyzer Tecator Kjeltec (KD-02)

Sample 1 g of yeast

no.	% nitrogen	% protein
1	7.980	49.880

Sample 1% (w/v) of yeast suspension after preparation

no.	% nitrogen	% protein
1	0.130	0.740
2	0.110	0.630
3	0.100	0.570
Average	0.113	0.647

Sample Supernatant of 1% (w/v) of yeast suspension after passing through the fluidized bed column

Condition  $U_l = 0$  cm/min $U_g = 0$  cm/min $N = 500$  rpm

Without glass beads

With draft tube

time (min)	% nitrogen	% protein	X	Y
0	0.020	0.125	0.000	0.000
30	0.020	0.125	0.000	0.000
60	0.020	0.125	0.000	0.000
120	0.020	0.125	0.000	0.000
180	0.020	0.125	0.000	0.000

Condition  $U_l = 0$  cm/min $U_g = 0$  cm/min $N = 3000$  rpm

Without glass beads

With draft tube

time (min)	% nitrogen	% protein	X	Y
0	0.019	0.120	0.000	0.000
30	0.019	0.120	0.000	0.000
60	0.019	0.120	0.000	0.000
120	0.019	0.120	0.000	0.000
180	0.019	0.120	0.000	0.000

\* X = protein in supernatant at any time - protein in supernatant at initial time

Y = (protein in supernatant at any time - protein in supernatant at initial time)/protein in feed stock

## Protein assay by Kjeldahl method

Analyzer Tecator Kjeltec (KD-02)

Sample Supernatant of 1% (w/v) of yeast suspension after passing through the fluidized bed column

Condition  $U_l = 0$  cm/min $U_g = 0$  cm/min $N = 500$  rpm

With glass beads Bead size = 1 mm

Bead loading = 1/3 volume of annular fluidized bed

With draft tube

time (min)	% nitrogen	% protein	X	Y
0	0.018	0.113	0.000	0.000
30	0.018	0.113	0.000	0.000
60	0.018	0.113	0.000	0.000
120	0.018	0.113	0.000	0.000
180	0.018	0.113	0.000	0.000

Condition  $U_l = 0$  cm/min $U_g = 0$  cm/min $N = 3000$  rpm

With glass beads Bead size = 1 mm

Bead loading = 1/3 volume of annular fluidized bed

With draft tube

time (min)	% nitrogen	% protein	X	Y
0	0.016	0.100	0.000	0.000
30	0.038	0.238	0.138	0.213
60	0.051	0.319	0.219	0.338
120	0.051	0.319	0.219	0.338
180	0.059	0.369	0.269	0.416

Condition  $U_l = 0$  cm/min $U_g = 10$  cm/min $N = 0$  rpm

Without glass beads

With draft tube

time (min)	% nitrogen	% protein	X	Y
0	0.014	0.088	0.000	0.000
30	0.014	0.088	0.000	0.000
60	0.014	0.088	0.000	0.000
120	0.014	0.088	0.000	0.000
180	0.014	0.088	0.000	0.000

\* X = protein in supernatant at any time - protein in supernatant at initial time

Y = (protein in supernatant at any time - protein in supernatant at initial time)/protein in feed stock

## Protein assay by Kjeldahl method

Analyzer Tecator Kjeltec (KD-02)

Sample Supernatant of 1% (w/v) of yeast suspension after passing through the fluidized bed column

Condition  $U_l = 0$  cm/min $U_g = 40$  cm/min $N = 0$  rpm

Without glass beads.

With draft tube

time (min)	% nitrogen	% protein	X	Y
0	0.010	0.063	0.000	0.000
30	0.010	0.063	0.000	0.000
60	0.010	0.063	0.000	0.000
120	0.010	0.063	0.000	0.000
180	0.010	0.063	0.000	0.000

Condition  $U_l = 0$  cm/min $U_g = 10$  cm/min $N = 0$  rpm

With glass beads

Bead size = 1 mm

Bead loading = 1/3 volume of annular fluidized bed

With draft tube

time (min)	% nitrogen	% protein	X	Y
0	0.014	0.088	0.000	0.000
30	0.014	0.088	0.000	0.000
60	0.014	0.088	0.000	0.000
120	0.014	0.088	0.000	0.000
180	0.014	0.088	0.000	0.000

Condition  $U_l = 0$  cm/min $U_g = 40$  cm/min $N = 0$  rpm

With glass beads

Bead size = 1 mm

Bead loading = 1/3 volume of annular fluidized bed

With draft tube

time (min)	% nitrogen	% protein	X	Y
0	0.012	0.075	0.000	0.000
30	0.012	0.075	0.000	0.000
60	0.012	0.075	0.000	0.000
120	0.012	0.075	0.000	0.000
180	0.012	0.075	0.000	0.000

\* X = protein in supernatant at any time - protein in supernatant at initial time

Y = (protein in supernatant at any time - protein in supernatant at initial time)/protein in feed stock



## Protein assay by Kjeldahl method

Analyzer Tecator Kjeltac (KD-02)

Sample Supernatant of 1% (w/v) of yeast suspension after passing through the fluidized bed column

Condition  $Uf = 10 \text{ cm/min}$  $Ug = 0 \text{ cm/min}$  $N = 0 \text{ rpm}$ 

Without glass beads

With draft tube

time (min)	% nitrogen	% protein	X	Y
0	0.016	0.100	0.000	0.000
30	0.016	0.100	0.000	0.000
60	0.016	0.100	0.000	0.000
120	0.016	0.100	0.000	0.000
180	0.016	0.100	0.000	0.000

Condition  $Uf = 30 \text{ cm/min}$  $Ug = 0 \text{ cm/min}$  $N = 0 \text{ rpm}$ 

Without glass beads

With draft tube

time (min)	% nitrogen	% protein	X	Y
0	0.010	0.063	0.000	0.000
30	0.010	0.063	0.000	0.000
60	0.010	0.063	0.000	0.000
120	0.010	0.063	0.000	0.000
180	0.010	0.063	0.000	0.000

Condition  $Uf = 10 \text{ cm/min}$  $Ug = 0 \text{ cm/min}$  $N = 0 \text{ rpm}$ 

With glass beads

Bead size = 1 mm

Bead loading = 1/3 volume of annular fluidized bed

With draft tube

time (min)	% nitrogen	% protein	X	Y
0	0.012	0.075	0.000	0.000
30	0.012	0.075	0.000	0.000
60	0.012	0.075	0.000	0.000
120	0.012	0.075	0.000	0.000
180	0.012	0.075	0.000	0.000

\*  $X = \text{protein in supernatant at any time} - \text{protein in supernatant at initial time}$  $Y = (\text{protein in supernatant at any time} - \text{protein in supernatant at initial time}) / \text{protein in feed stock}$



## Protein assay by Kjeldahl method

Analyzer: Tecator Kjeltéc (KD-02)

Sample: Supernatant of 1% (w/v) of yeast suspension after passing through the fluidized bed column

Condition:  $U_l = 30 \text{ cm/min}$  $U_g = 0 \text{ cm/min}$  $N = 0 \text{ rpm}$ 

With glass beads: Bead size = 1 mm

Bead loading = 1/3 volume of annular fluidized bed

With draft tube:

time (min)	% nitrogen	% protein	X	Y
0	0.014	0.088	0.000	0.000
30	0.014	0.088	0.000	0.000
60	0.014	0.088	0.000	0.000
120	0.014	0.088	0.000	0.000
180	0.014	0.088	0.000	0.000

Condition:  $U_l = 10 \text{ cm/min}$  $U_g = 40 \text{ cm/min}$  $N = 3000 \text{ rpm}$ 

with glass beads: Bead size = 1 mm

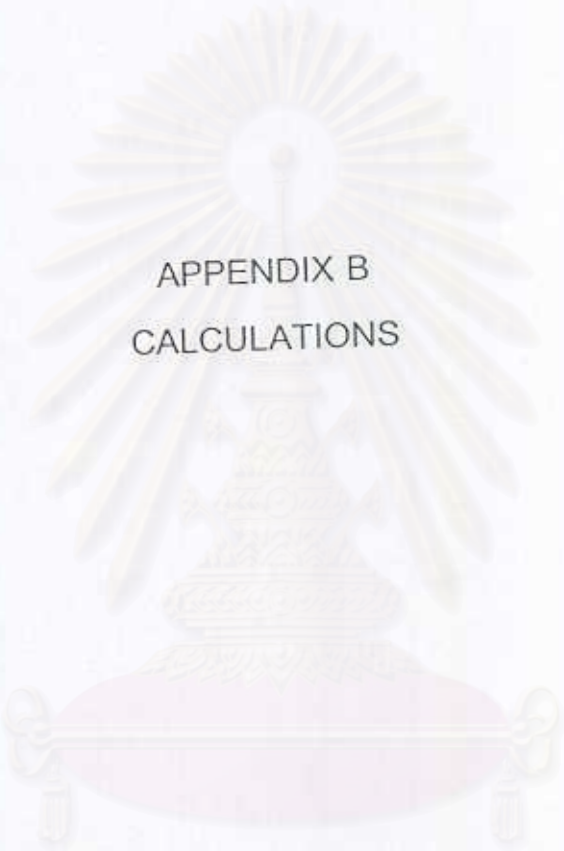
Bead loading = 1/3 volume of annular fluidized bed

Withdraft tube:

time (min)	% nitrogen	% protein	X	Y
0	0.014	0.085	0.000	0.000
60	0.023	0.141	0.056	0.087
120	0.025	0.155	0.070	0.108
180	0.029	0.183	0.098	0.151
240	0.032	0.197	0.112	0.173
300	0.029	0.155	0.070	0.108
360	0.036	0.226	0.141	0.218
420	0.027	0.169	0.084	0.130
480	0.034	0.212	0.127	0.196

\* X = protein in supernatant at any time - protein in supernatant at initial time

Y = (protein in supernatant at any time - protein in supernatant at initial time)/protein in feed stock



APPENDIX B  
CALCULATIONS

สถาบันวิทยบริการ  
จุฬาลงกรณ์มหาวิทยาลัย

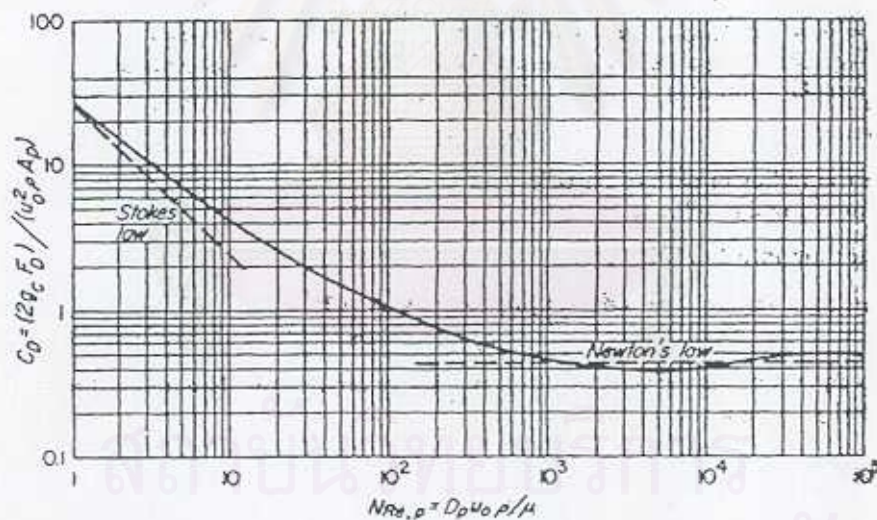
Calculation of terminal velocity,  $u_t$

$$u_t = (4g(\rho_p - \rho)D_p / 3C_D \rho)^{1/2}$$

For sphere particle, the terminal velocity can be found by trial and error after guessing  $N_{re,p}$  to get an initial estimate of Drag coefficient,  $C_D$ , dimensionless (where the relationship between  $C_D$  and Reynolds' number for spheres is showed in Figure 4.6 p 51 )

$D_p$ (m)	$u_0$ (m/s)	$\rho_p$ (kg/m <sup>3</sup> )	$\rho$ (kg/m <sup>3</sup> )	$(\rho_p - \rho)$ (kg/m <sup>3</sup> )	$\mu$ (kg/m s)	$g$ (m/s <sup>2</sup> )	$N_{re,p} = D_p u_0 \rho / \mu$	$C_D$	$u_t = (4g(\rho_p - \rho)D_p / 3C_D \rho)^{1/2}$ (m/s)
0.001	0.0017	2500	992	1500	0.001	9.800	1.68640	24	0.029
0.001	0.029	2500	992	1500	0.001	9.800	28.46284	2.1	0.097
0.001	0.097	2500	992	1500	0.001	9.800	96.22197	1.1	0.134
0.001	0.134	2500	992	1500	0.001	9.800	132.94975	0.9	0.148
0.001	0.148	2500	992	1500	0.001	9.800	146.98148	0.85	0.152
0.001	0.152	2500	992	1500	0.001	9.800	151.24270	0.86	0.152

So that, terminal velocity of glass beads is 0.152 m/s or 912 cm/min, which is higher than superficial gas velocity and superficial liquid velocity range in our experiment.



Relationship between the Reynolds number,  $N_{re}$  and Drag coefficient,  $C_D$

(Redrawn from McCabe W.L., Smith J.C., and Harriott P. *Unit operations of chemical engineering*, 1993, p.158.)

### Calculation of Minimum fluidized bed velocity for gas-liquid-solid fluidized bed system

Song et al. (1987) developed a general empirical correlation equation (in SI units) for calculation of minimum fluidized bed velocity in gas-liquid-solid fluidized bed system as given below:

$$U_{mf}/U_{mfo} = 1.376 u_g^{0.327} \mu_l^{0.227} d_e^{0.213} (\rho_s - \rho_l)^{-0.423}$$

When $U_{mf}$	=	minimum fluidized bed velocity for gas-liquid-solid system
$U_{mfo}$	=	minimum fluidized bed velocity for liquid-solid system
$u_g$	=	gas velocity
$\mu_l$	=	liquid viscosity
$d_e$	=	equivalent particle diameter
$\rho_s$	=	solid density
$\rho_l$	=	liquid density

This equation has the widest range of applicability among correlation for  $U_{mf}$  proposed to data, i.e.,

$$0 \leq u_g \leq 17 \text{ cm/s}$$

$$0.9 \text{ (or } 9 \times 10^{-3}) \leq \mu_l \leq 11.4 \text{ (or } 0.114) \text{ cP (or g/cm.s)}$$

$$0.046 \leq d_e \leq 0.63 \text{ cm}$$

$$1.8 \leq \rho_l \leq 2.5 \text{ g/cm}^3$$

สถาบันวิทยบริการ  
จุฬาลงกรณ์มหาวิทยาลัย



Minimum fluidized bed velocity for liquid-solid system,  $U_{mf}$

when  $N_{mf} < 1$

$$U_{mf} = \frac{g(\rho_s - \rho)}{150\mu} \frac{\epsilon_M^3}{1 - \epsilon_M} \phi_s^2 D_p^2$$

$g(m/s^2)$	$(\rho_s - \rho)(kg/m^3)$	$\epsilon_M(-)$	$\epsilon_M^3(-)$	$\phi_s^2(-)$	$D_p(m)$	$D_p^2(m^2)$	$\mu(kg/m\ s)$	$U_{mf}(m/s)$	$U_{mf}(cm/min)$
9.80	1508	0.380	0.0549	1.0000	0.001000	0.0000010	0.0010	0.004974	29.8423

Minimum fluidized bed velocity for gas-liquid-solid system,  $U_{mf}$

$$U_{mf}/U_{mf0} = 1 - 376 u_0^{0.227} \mu^{0.227} D_p^{0.213} (\rho_s - \rho)^{-0.422}$$

$U_0(cm/min)$	$U_0(m/s)$	$U_0^{0.227}$	$\mu(kg/m\ s)$	$\mu^{0.227}$	$D_p(m)$	$D_p^{0.213}$	$(\rho_s - \rho)(kg/m^3)$	$(\rho_s - \rho)^{-0.422}$	$U_{mf}/U_{mf0}$	$U_{mf}(m/s)$	$U_{mf}(cm/min)$
40	0.0067	0.1943	0.0010	0.2084	0.0010	0.2296	1508	0.0452	0.8418	0.0042	25.2547
20	0.0033	0.1549	0.0010	0.2084	0.0010	0.2296	1508	0.0452	0.8739	0.0044	26.2171
10	0.0017	0.1235	0.0010	0.2084	0.0010	0.2296	1508	0.0452	0.8995	0.0045	26.9843
0	0.0000	0.0000	0.0010	0.2084	0.0010	0.2296	1508	0.0452	1.0000	0.004974	29.8423

Calculation of the degree of cell disruption at any time

The distribution of yeast cell diameter at 0 min at any condition shows that initial size distribution of yeast whole cells has a modal size of approximately 4.047  $\mu\text{m}$ . The frequency of the peak at 4.047  $\mu\text{m}$  decreases with increasing the disruption time. There is a shift toward smaller sizes as cell disruption progresses. It is suggested that the peak at 4.047  $\mu\text{m}$  correspond to the size of whole cell remained in the sample. And the standardized frequency of 4.047  $\mu\text{m}$  is defined as the ratio of non-disrupted cell at certain time to the frequency at 0 min (Shimizu et al, 1998)

$$\begin{aligned} \text{Ratio of non-disrupted cell (-)} \\ &= \frac{\text{average of \% number of yeast whole cell at any time}}{\text{average of \% number of yeast whole cell at 0 min.}} \end{aligned}$$

And then,

$$\begin{aligned} \text{Degree of cell disruption (\%)} \\ &= (1 - \text{ratio of non-disrupted cell}) \times 100 \end{aligned}$$

Condition  $U_i = 0$  cm/min,  $U_g = 0$  cm/min,  $N = 3000$  rpm in fluidized bed with draft tube and with presence of glass beads. From the particle size distribution of yeast at 0 min, the plot showed that the yeast whole cell was 4.047  $\mu\text{m}$  in diameter

$$\text{Ratio of non-disrupted cell (-) at 180 min} = 0.90/14.27 = 0.06$$

Where average of % number of yeast whole cell at 180 min = 0.90 %

average of % number of yeast whole cell at 0 min = 14.27 %

So that

$$\text{Degree of cell disruption (\%)} = (1 - 0.06) \times 100 = 94 \%$$



## Particle size analysis by Laser Diffraction

Analyze Beckman Coulter LS 230 Particle Size Analyzer

Sample 1% (w/v) of yeast suspension after passing the fluidized bed with draft tube

Condition UI = 0 cm/min

 $U_g = 0$  cm/min

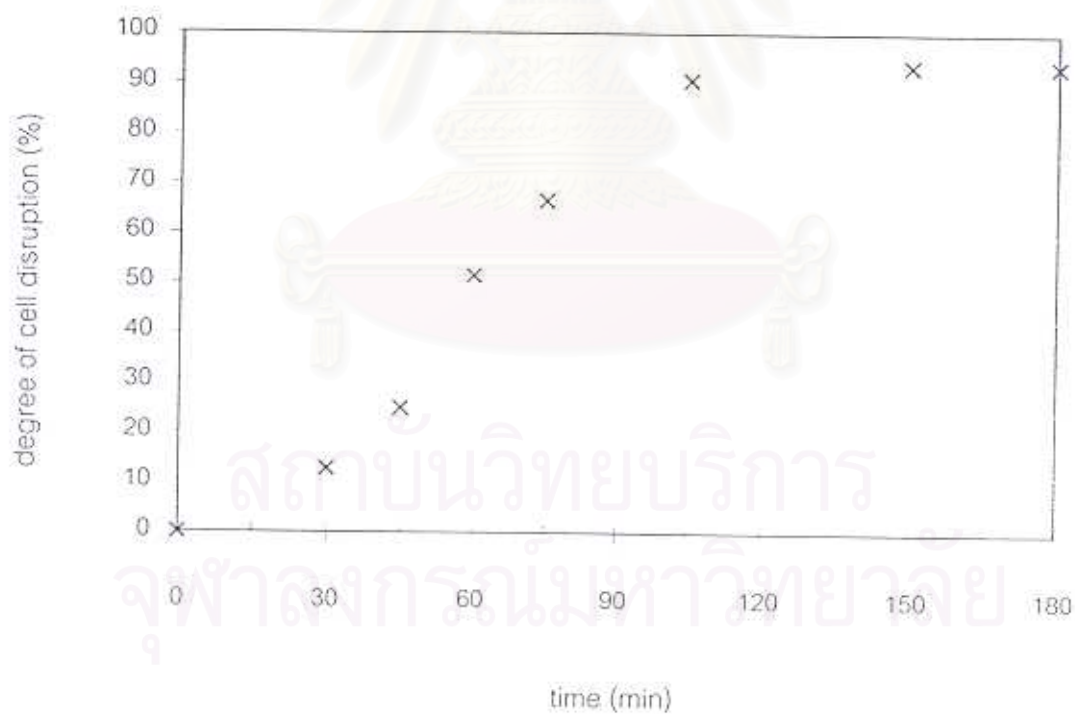
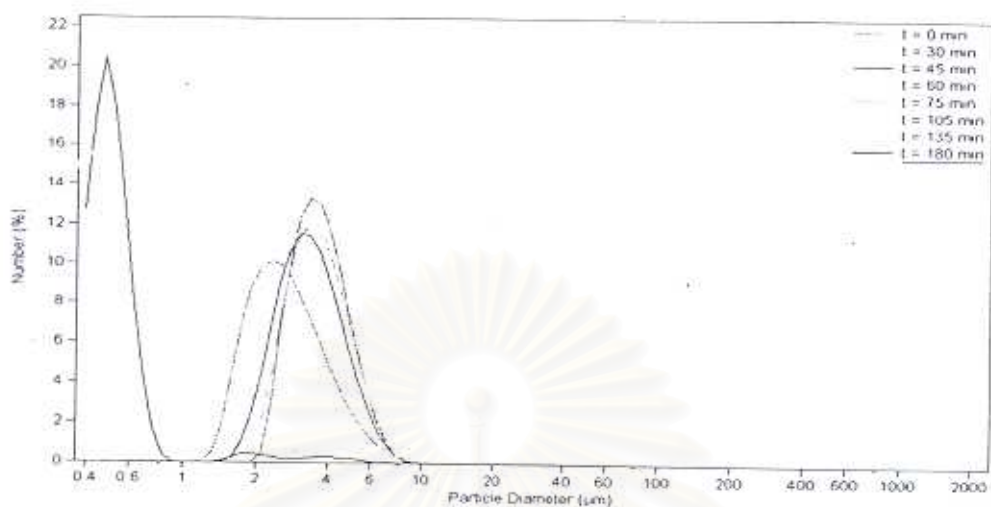
N = 3000 rpm

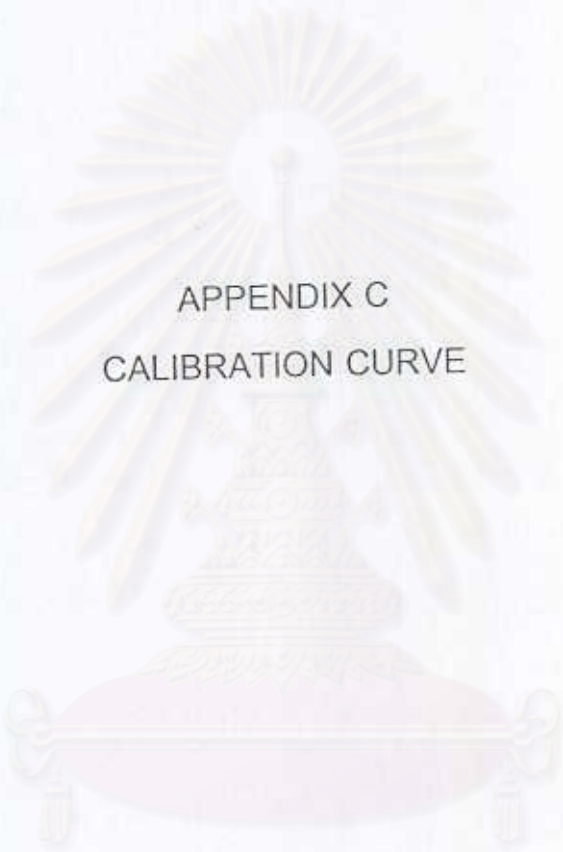
Bead size = 1000  $\mu$ m

Bead loading = 1/3 volume of annular fluidized bed

time (min)	% number of yeast whole cells(%)			ave. % number of yeast whole cells(%)	ratio of non-disrupted cells(-)	degree of cell disruption (%)
0	14.28	14.27	14.27	14.27	1.00	0
30	12.24	13.09	12.03	12.45	0.87	13
45	11.35	10.29	10.52	10.72	0.75	25
60	7.45	6.98	6.34	6.92	0.49	51
75	5.31	4.22	4.76	4.76	0.33	67
105	1.03	0.94	1.98	1.32	0.09	91
150	1.00	1.02	0.71	0.91	0.06	94
180	0.88	1.10	0.72	0.90	0.06	94

สถาบันวิทยบริการ  
จุฬาลงกรณ์มหาวิทยาลัย



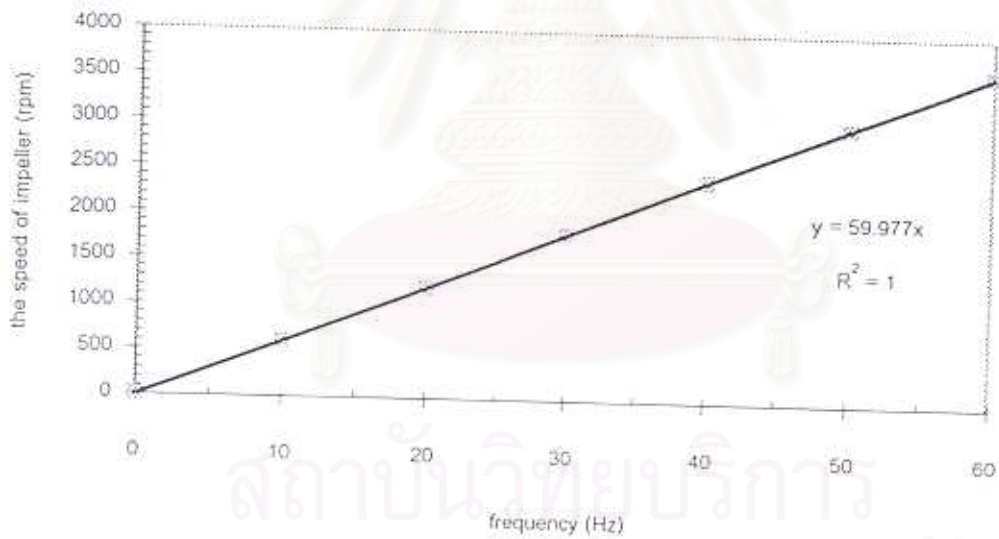


APPENDIX C  
CALIBRATION CURVE

สถาบันวิทยบริการ  
จุฬาลงกรณ์มหาวิทยาลัย

Calibration curve of speed of impeller

frequency (Hz)	the speed of impeller (rpm)										sum(rpm)	average(rpm)
10	600.4	600.3	554	600	600.2	599.8	600.4	600.2	600	600	5955.3	595.53
20	1200	1199	1199	1198	1199	1198	1200	1199	1200	1200	11992	1199.2
30	1802	1803	1801	1800	1803	1801	1802	1802	1801	1802	18017	1801.7
40	2402	2402	2405	2401	2402	2402	2403	2400	2401	2402	24020	2402
50	2998	2998	2997	2999	2997	2997	2998	2997	2997	3000	29976	2997.8
60	3596	3597	3596	3596	3597	3598	3600	3597	3596	3598	35972	3597.2



Calibration curve of the speed of impeller.

Calibration of Reynold's number of impeller tank at any speed of impeller

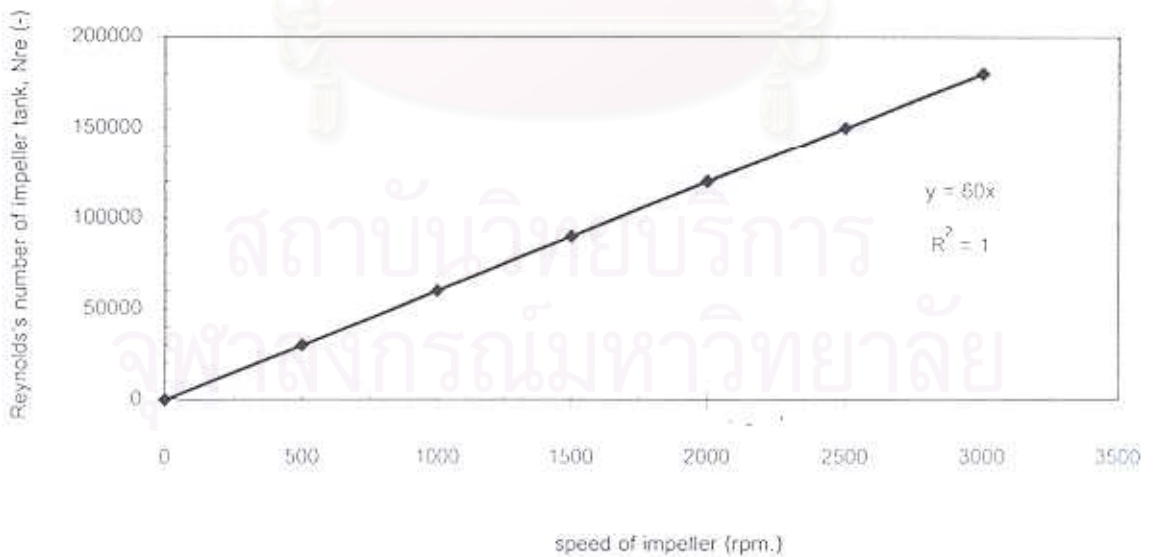
$N(\text{min}^{-1})$	$N(\text{s}^{-1})$	$D_a(\text{m})$	$D_a^2(\text{m}^2)$	$\rho(\text{kg/m}^3)$	$\mu(\text{kg/m s})$	$N_{re}$
500	8.33	0.06	0.0036	992	0.001	29760
1000	16.67	0.06	0.0036	992	0.001	59520
1500	25.00	0.06	0.0036	992	0.001	89280
2000	33.33	0.06	0.0036	992	0.001	119040
2500	41.67	0.06	0.0036	992	0.001	148800
3000	50.00	0.06	0.0036	992	0.001	178560

Reynold's number of impeller tank,  $N_{re} = D_a^2 N \rho / \mu$

$N_{re} < 10$  : flow is a laminar range

$N_{re} = 10 - 10000$  : flow is a transition range

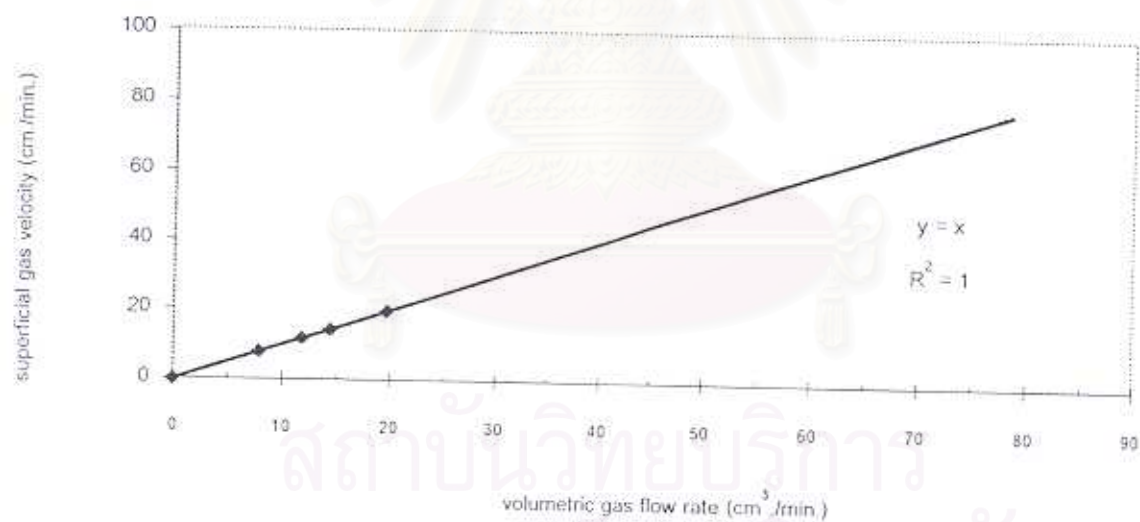
$N_{re} > 10000$  : flow is a turbulent range



Calibration of Reynold's number of impeller tank at any speed of impeller

Calibration curve of superficial gas velocity

Volumetric Gas Flow rate.(cc./min.)	Data (cc./min.)		Ave.(cc./min )	Superficial Gas Velocity (cm./min.)
1000	937.5	1000	968.75	7.6
1500	1375	1500	1437.5	11.3
2000	1867	2000	1833	14.5
2500	2500	2500	2500	19.7
5000	5000	5000	5000	39.5
10000	9900	10000	9950	78.5

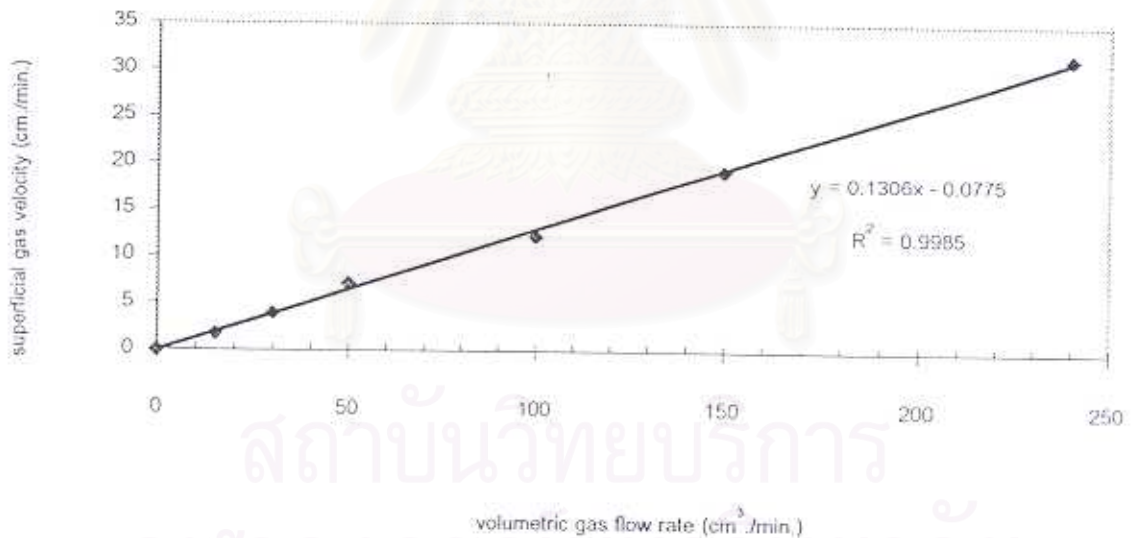


Calibration curve of superficial gas velocity, without packing.



Calibration curve of superficial liquid velocity

Volumetric Liquid Flow rate.(cc./min.)	Data (cc./min.)		Ave.(cc./min.)	Superficial Liquid Velocity (cm./min.)
15	230	200	215	2
30	500	500	500	4
50	1000	800	900	7
100	1600	1500	1550	12
150	2500	2400	2450	19
240	4000	4000	4000	32



สถาบันวิทยบริการ  
จุฬาลงกรณ์มหาวิทยาลัย

Calibration curve of superficial liquid velocity

## BIOGRAPHY

Miss Narisara Suksamai was born on 14<sup>th</sup> April 1976 in Bangkok, Thailand. She finished her secondary school from Suksanaree school in 1993. After that, she studied in the major of Food Science and Technology in Faculty of Science and Technology at Thammasat University. She continued her further study for Master's degree in Chemical Engineering at Chulalongkorn University. She proudly participated in the Particle Technology and Material Processing group and achieved her Master's degree in April 2001.



สถาบันวิทยบริการ  
จุฬาลงกรณ์มหาวิทยาลัย